The Preparation, Characterization and Phenylacetylene Polymerization of Novel Palladacycles

by
Moegamat Cassiem Joseph

Thesis presented in fulfilment of the requirements for the degree of Masters of Science in the Faculty of Chemistry and Polymer Science at Stellenbosch University

Supervisor: Prof Selwyn Frank Mapolie

March 2016

Declaration

By submitting this thesis electronically, I declare that the entirety of the work contained therein is my own, original work, that I am the sole author thereof (save to the extent explicitly otherwise stated), that reproduction and publication thereof by Stellenbosch University will not infringe any third party rights and that I have not previously in its entirety or in part submitted it for obtaining any qualification.

.....

Cassiem Joseph

March 2016

Abstract

This thesis describes the synthesis and characterization of novel cationic palladacycles derived from various *N*-benzylidene-2,6-diisopropylaniline ligands and their use as catalysts in the polymerization of phenylacetylene.

A series of *N*-benzylidene-2,6-diisopropylaniline ligands of general formula (2-R-C_6H_3)CH=N-(2,6-^{i}Pr$_2$-C_6H_3), (R = H (**L1**); R = Cl (**L2**); R = Br (**L3**); R = F (**L4**); R = OMe (**L5**)) were prepared by the Schiff-base condensation reaction of 2,6-diisopropylaniline with the respective mono-substituted aldehyde in a 1:1 molar ratio. Reactions of ligands **L1-L5** with $(MeCN)_2PdCl_2$ in a 1:1 molar ratio in the presence of NaOAc generated the dinuclear μ-Cl palladacycles (**C1-C5**) of the type [PdCl(R-C_6H_3)CH=N-{2,6-(^{i}Pr)$_2$-C_6H_3}]$_2$ (R = H (**C1**), Cl (**C2**), Br (**C3**), F (**C4**), OMe (**C5**)). The complexes were characterized by FT-IR-, ^{1}H- and ^{13}C{^{1}H} NMR spectroscopy.

The mononuclear neutral palladacycles of the type [Pd(PR'$_3$)Cl(R-C_6H_3)CH=N{2,6-^{i}Pr$_2$-C_6H_3}Cl] (PR'$_3$ = PTA (**C6-C10**); PR'$_3$ = PCy_3 (**C16-C20**); PR'$_3$ = PPh_3 (**C26-30**)) were prepared by the cleavage of the μ-Cl palladacycles **C1-C5** with two molar equivalents of the respective phosphine ligand. These complexes were fully characterized by FT-IR-, ^{1}H-, ^{13}C{^{1}H}- and ^{31}P{^{1}H} NMR spectroscopy, ESI-MS spectrometry as well as elemental analysis. Single crystal X-ray diffraction analysis of complexes **C8**, **C9**, **C18** and **C30** confirmed that the geometry around the metal centre is slightly distorted square planar and that the coordination of the phosphine ligand is *trans* relative to the imine moiety.

To generate the novel mononuclear cationic palladacycles, complexes **C6-C10**, **C16-C20** and **C26-C30** were subjected to chloride abstraction by $NaBAr_4$ (Ar_4 = 3,5-*bis*(trifluoromethyl)phenyl) in the presence of MeCN as coordinating solvent resulting in the cationic analogues with general formula [Pd(MeCN)(PR'$_3$)(R-C_6H_3)CH=N-{2,6-(^{i}Pr)$_2$-C_6H_3}]$^+$ [B(Ar)$_4$]$^-$ (PR'$_3$ = PTA (**C11-C15**); PR'$_3$ = PCy_3 (**C21-C25**); PR'$_3$ = PPh_3 (**C31-35**)) being isolated as air- and moisture-stable solids. These complexes

were characterized by FT-IR-, ^{1}H-, $^{13}C\{^{1}H\}$- and $^{31}P\{^{1}H\}$ NMR spectroscopy, ESI-MS spectrometry, elemental analysis and in the case of complexes **C15** and **C25** by single crystal X-ray diffraction. Spectroscopy data reveals that the coordination of the phosphine ligand to the metal centre remains *trans* relative to the imine moiety after coordination of the acetonitrile ligand. From the crystal structures of **C15** and **C25** it was observed that both complexes have a slightly distorted square planar geometry around the metal centre with the plane of the 2,6-diisopropylaniline moiety almost perpendicular to the plane of the *endocycle* ring.

The reactivity of the novel cationic palladacycle complexes (**C11-C15**, **C21-C25**, **C31-C35**) towards phenylacetylene was evaluated. All complexes evaluated showed some degree of activity in phenylacetylene polymerization, with conversions ranging from 56 % to 95 %. A mixture of both *cis*-transoidal and *trans*-cisoidal polyphenylacetylene (PPA) were produced at room temperature with moderate molecular weights while the *trans*-cisoidal PPA can selectively be produced when the reactions are performed at slightly higher temperatures (60 °C). The nature of the ortho-substituent on the cyclometallated-ring had a marked effect on the efficiency of the catalysts with the highest conversion of 95 % being obtained for the complex with the most electron withdrawing substituent (**C14**). Increasing the steric bulk of the auxiliary phosphine ligand leads to higher molecular weight polyphenylacetylene being produced.

Opsomming

Hierdie tesis beskryf die sintese, karakterisering en katalitiese aktiwiteit van nuwe kationiese palladasikliese komplekse afgelei vanaf verskillende *N*-bensilideen-2,6-diisopropielanilien ligande en die gebruik daarvan as katalisators in die polimerisering van fenielasetileen.

'n Reeks *N*-bensilideen-2,6-diisopropielfenielamien ligande met die algemene formule (2-R-C_6H_3)CH=N-(2,6-^{i}Pr$_2$-C_6H_3), (R = H (**L1**); R = Cl (**L2**); R = Br (**L3**); R = F (**L4**); R = OMe (**L5**)) is deur middel van 'n Schiff-basis kondensasie reaksie van 2,6-diisopropielanilien met onderskeie monogesubstitueerde aldehiede in 'n 1:1 molêre verhouding berei. Reaksies van ligande **L1-L5** met $(MeCN)_2PdCl_2$ in 'n 1:1 molêre verhouding in die teenwoordigheid van NaOAc genereer die μ-Cl tweekernige palladasikliese komplekse (**C1-C5**) van die tipe [PdCl(R-C_6H_3)CH=N-{2,6-(^{i}Pr)$_2$-C_6H_3}]$_2$ (R = H (**C1**), Cl (**C2**), Br (**C3**), F (**C4**), OMe (**C5**)). Die komplekse is met FT-IR-, ^{1}H- en ^{13}C KMR spektroskopie gekarakteriseer.

Die eenkernige neutrale palladasikliese komplekse van die tipe [Pd(PR'$_3$)Cl(R-C_6H_3)CH=N{2,6-^{i}Pr$_2$-C_6H_3}Cl] (PR'$_3$ = PTA (**C6-C10**); PR'$_3$ = PCy_3 (**C16-C20**); PR'$_3$ = PPh_3 (**C26-30**)) is deur middel van die splitsing van die μ-Cl tweekernige palladasikliese komplekse **C1-C5** met twee mol ekwivalent van die onderskeie fosfien ligande berei. Hierdie komplekse is volledig deur FT-IR-, ^{1}H-, ^{13}C{^{1}H}- en ^{31}P{^{1}H} KMR spektroskopie, ESI-massa spektrometrie sowel as mikroanalise gekarakteriseer. Enkelkristal X-straal diffraksie analise van komplekse **C8**, **C9**, **C18** en **C30** bevestig dat die geometrie rondom the metaal effens verwronge vierkantvlakkig is en dat die koordinasie van die fosfien ligand *trans* relatief tot die imien gedeelte is.

Ten einde nuwe eenkernige kationiese palladasikliese komplekse te vorm, is komplekse **C6-C10**, **C16-C20** en **C26-C30** met die chloried-abstraksiemiddel, $NaBAr_4$ (Ar_4 = 3,5-*bis*(trifluoormetiel)feniel) in die teenwoordigheid van MeCN as stabiliserende ligand, gereageer wat

lei tot die kationiese analoë met algemene formule [Pd(MeCN)(PR'$_3$)(R-C_6H_3)CH=N-{2,6-(^{i}Pr)$_2$-C_6H_3}]$^+$ [B(Ar)$_4$]$^-$ (PR'$_3$ = PTA (**C11-C15**); PR'$_3$ = PCy$_3$ (**C21-C25**); PR'$_3$ = PPh$_3$ (**C31-35**)) wat as stabiele vastestowwe geïsoleer is. Hierdie komplekse is deur FT-IR-, ^{1}H-, ^{13}C{^{1}H}- en ^{31}P{^{1}H} KMR spektroskopie, ESI-massa spektrometrie, mikroanalise en in die geval van komplekse **C15** en **C25**, deur enkelkristal X-straal diffraksie analise gekarakteriseer. Spektroskopie data bevestig dat die koordinasie van die fosfien ligand aan die metaal *trans* relatief tot die imien gedeelte bly na koordinasie van die asetonitriel ligand. Die kristal strukture van **C15** en **C25** toon aan dat beide komplekse 'n effens verwronge vierkantvlak geometrie rondom die metaal het met die vlak van die 2,6-diisopropielanilien gedeelte wat amper loodreg tot die vlak van die *endo*sikliese ring is.

Die reaktiwiteit van die nuwe kationiese palladasikliese komplekse (**C11-C15**, **C21-C25**, **C31-C35**) teenoor fenielasetileen was geëvalueer. Alle komplekse wat in fenielasetileen polimerisasie geëvalueer was, het tot 'n mate aktiwiteit vertoon met omsettings tussen 56 % en 95 %. 'n Mengsel van beide *cis*-transoïed en *trans*-cisoïed polifenielasetileen was geproduseer by kamertemperatuur met matige molekulêre massas terwyl die *trans*-cisoïed polifenielasetileen selektief geproduseer word wanneer reaksies by 60 °C uitgevoer was. Die aard van die orto-substituent aan die siklometallerende-ring het 'n merkbare uitwerking op die doeltreffendheid van die katalisators met 'n omsetting van 95 % wat bereik is vir die kompleks wat die mees elektron-onttreking substituent het (**C14**). 'n Verhoging in die steriese groote van die fosfien ligand het gelei tot die produksie van hoër molekulêre massa polifenielasetileen.

Dedication

This Master's thesis is dedicated to my mother

Murieda Joseph

For your love, support and motivation throughout my studies

and

to the loving memory of my late father

Moegamat Noeroedin Almansoor Joseph

Your legacy remains a source of inspiration to me

Acknowledgements

I would like to express my sincere gratitude to following people for their support and contribution during the course of my MSc studies:

My supervisor, Professor Selwyn F. Mapolie for his valuable advice and continuous support during this project. This project would not have been possible without your guidance and encouragement. I could not have imagined having a better advisor for my MSc study. Your extensive knowledge and passion for chemistry has been inspiring.

To the Inorganic/Organometallic Research Group at Stellenbosch University; Drs. Rehana Malgas-Enus, Andrew Swarts and Hennie Kotze, Manana Moletsane, Corli Joubert, Derik Wilbers, Angelique Blanckenberg, Ené Slazus, Annick van Niekerk and Laura Leckie. Thank you for your research input, fruitful discussion and making the lab a more pleasurable experience, I would not have survived without it. The experience I have gained with the group has been absolutely invaluable. A special word of thanks has to be directed to Jacquin October who is not only a good friend I have grown fond of but also someone who I can have a good laugh to end the day. Thanks buddy!

I would like to thank Dr. Jaco Brand and Elsa Malherbe for their assistance with NMR analysis; Dr. Marietjie Stander and Fletcher Hiten for MS analysis, Dr. Nadine Makan, for GPC analysis and Dr. Vincent Smith, for SCD analysis.

Life as a student would have been very difficult without the love and support from my family: Mariam, Latiefa, Grizelda, Louis, Janeline, Lameecé, Ruqyah, Tara, Carah-lee and Nathier. Thank you for your endless support and encouragement. A special thanks to my mother Murieda Joseph, who always put the extra into ordinary and taught me that even the largest task can be accomplished if it is done one step at a time.

To all my friends, thank you for your support, inputs, good times and navigation throughout my academic journey. You guys rock!!!

Of course, nothing would have been possible without the technical staff that keep the well-oiled machine that is research running. Therefore, a big thank you to Sylette, Malcolm Taylor, Malcolm McLean, Johnny, Moebarick, Chalon, Jabu and Peta for all your assistance whenever I needed it.

Lastly, I would like to extend my thanks to the National Research Foundation (NRF) and the c*change Centre of Excellence in Catalysis, the Department of Science and Technology (DST) for their financial support throughout my MSc studies.

Conference Contributions

Poster Presentations

Cassiem Joseph and Selwyn Mapolie

Synthesis and Characterization of Cationic Palladacycle Complexes and Their Application as Olefin Transformation Catalysts. Catalysis Society of South Africa (CATSA) annual conference, Port Edward (Wild Coast Sun Hotel), South Africa, 2013.

Cassiem Joseph and Selwyn Mapolie

Synthesis and Reactivity of Neutral- and Cationic Palladium Complexes as Catalyst Precursors for Catalytic Transformations of Unsaturated Hydrocarbons. Catalysis Society of South Africa (CATSA) annual conference, Pretoria (St Georges Hotel and Conference Centre), South Africa, 2014.

Cassiem Joseph and Selwyn Mapolie

Synthesis and Reactivity of Cationic Palladacycles as Catalyst Precursors for Phenylacetylene Polymerization. Catalysis Society of South Africa (CATSA) annual conference, Kleinmond (Arabella Hotel and Spa Conference Centre), Cape Town, South Africa, 2015.

Table of Contents

List of Figures

Chapter 1: ***Palladacycles – Synthetic Methodologies and Versatile Catalysts for Carbon-Carbon Coupling Reactions***

Chapter 2: ***The Synthesis and Characterization of Neutral Palladacycles Derived from Schiff Base Imine ligands***

Chapter 3: ***The Synthesis and Characterization of Cationic Palladacycles Derived from Neutral Mononuclear Palladacycles***

Chapter 4: ***Reactivity of Cationic Palladacycle Complexes in the Oligomerization and Polymerization of Phenylacetylene***

List of Schemes

Chapter 2: ***The Synthesis and Characterization of Neutral Palladacycles Derived from Schiff Base Imine ligands***

Chapter 3: ***The Synthesis and Characterization of Cationic Palladacycles Derived from Neutral Mononuclear Palladacycles***

Chapter 4: ***Reactivity of Cationic Palladacycle Complexes in the Oligomerization and Polymerization of Phenylacetylene***

List of Tables

Chapter 3: ***The Synthesis and Characterization of Cationic Palladacycles Derived from Neutral Mononuclear Palladacycles***

Chapter 4: ***Reactivity of Cationic Palladacycle Complexes in the Oligomerization and Polymerization of Phenylacetylene***

List of Abbreviations and Symbols

δ	chemical shift
η^2	eta two
+.ve	positive mode
-.ve	negative mode
υ	Tolman electronic parameter
θ_T	Tolman steric parameter
Å	angstrom
AcOH	acetic acid
Anal. Found	analytical found
Ar	aromatic
ATR	attenuated total reflectance
br	broad
BPIB	bis(2-pyridylmethylidene)-o-diiminobenezene
BPIC	bis(2-pyridylmethylidene)- 1,2-diiminocyclohexane
Calc.	calculated
cm^{-1}	inverse centimetre
comp.	complex (denotes complex pattern of overlapping proton resonances)
Da	dalton
DFT	density functional theory
dba	dibenzylideneacetone
DMF	dimethylformamide
DCM	dichloromethane
d	doublet

dd	doublet of doublets
Et_2O	diethyl ether
ESI-MS	electrospray ionization mass spectrometry
EtOH	ethanol
et. al.	and others
Eq	equivalent(s)
Et_3N	triethylamine
FT-IR	fourier-transform infrared spectroscopy
GPC	gel permeation chromatography
h	hour
hrs	hours
^{i}Pr	isopropyl
J	coupling constant
K	temperature in Kelvin
MS	mass spectroscopy
m/z	mass to charge ratio
MHz	megahertz
M.p	melting point
MeOH	methanol
MeCN	acetonitrile
mL	millilitres
mM	millimolar

mmol	millimoles
mmol	moles
m	multiplet (denotes complex pattern for a single proton)
M_n	number average molecular weight
M_w	weight average molecular weight
nm	nanometre
NMR	nuclear magnetic resonances
OAc	acetate
ORTEP	oak ridge thermal ellipsoid plot
pKa	acid dissociation constant
ppm	parts per million
PTA	phosphatriazaadamantane
PDI	polydispersity
PEG	polyethyleneglycol
PPA	polyphenylacetylene
q	quartet
qq	quartet of quartets
r.t	room temperature
s	singlet
sept.	septet
THF	tetrahydrofuran
^{t}Bu	tertiary butyl

tfb	tetrafluorobenzobarrelene
t	triplet
td	triplet of doublets
TOF	turnover frequency
TON	turnover number
UV-Vis	ultraviolet-visible spectroscopy
µmol	micromole
XRD	x-ray diffraction

Chapter 1

Palladacycles – Synthetic Methodologies and Versatile Catalysts for Carbon-Carbon Coupling Reactions

1.1 Introduction

The last three decades have witnessed tremendous growth in palladacycle chemistry largely due to a change in perception that these compounds were no longer being viewed as being deactivated compounds but rather highly active catalysts for C-C and C-heteroatom bond formation. Palladacycles are defined as organopalladium compounds which contain a palladium centre, intramolecularly stabilized by at least one $2e^-$ donor group (**Figure 1.1**). They have a very rich chemistry and are amongst the most readily available transition metal complexes. Their synthesis is facile which make it possible to modulate their steric and electronic properties by simply changing (i) the nature of the metallated carbon atom, (ii) the donor group and its substituents, (iii) the size of the metallacyclic ring or (vi) the nature of the anionic ligand X. [1]

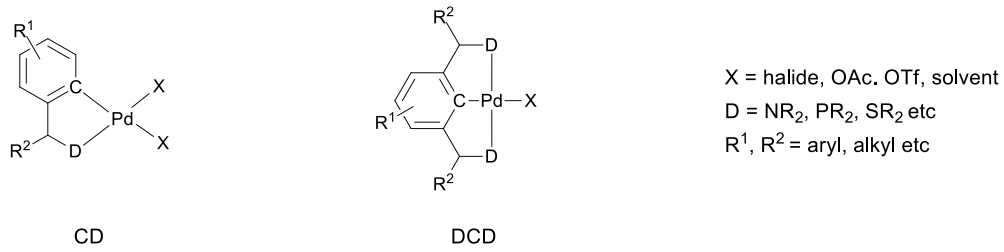

Figure 1.1: Palladacycle templates. Anionic four-electron donor (CD) and anionic six-electron donor palladacycles.

This brief overview will concentrate palladacycles as catalyst precursors in common coupling reactions.

1.1.1 A brief historical overview

Palladacycles date back to the mid 1960's when Cope *et al.* [2,3] carried out analogous reactions of *N*,*N*-dimethylbenzylamines and azobenzene using palladium(II) dichloride or lithiumtetrachloropalladate(II) metal precursors which initially afforded the first isolated and well characterized palladacycle (**1.1**) shown in **Figure 1.2**. In 1963, Dubeck *et al.* [4] obtained a cyclopentadienyl nickel compound (**1.2**) with a similar azobenzene ligand, however the structure originally proposed was incorrectly assigned in that the N=N double bond was considered to be coordinated to the nickel centre in a η^2 fashion.

Nevertheless, these types of compounds exhibit high thermal stability in the solid state and gained more prominence in the 1990's when Herrmann and co-workers highlighted the true potential of a cyclopalladated tris(*o*-tolyl)-phosphine palladacycle (**1.3**) as a structurally defined catalyst for the Heck olefination of chloro- and bromoarenes,[5] and as mediators in other aryl coupling reactions.[6] Since then, palladacycles have become more pervasive in catalytic transformations as catalyst precursors and numerous reviews have been dedicated to their structural aspects and applications in organometallic chemistry. [1,7–9]

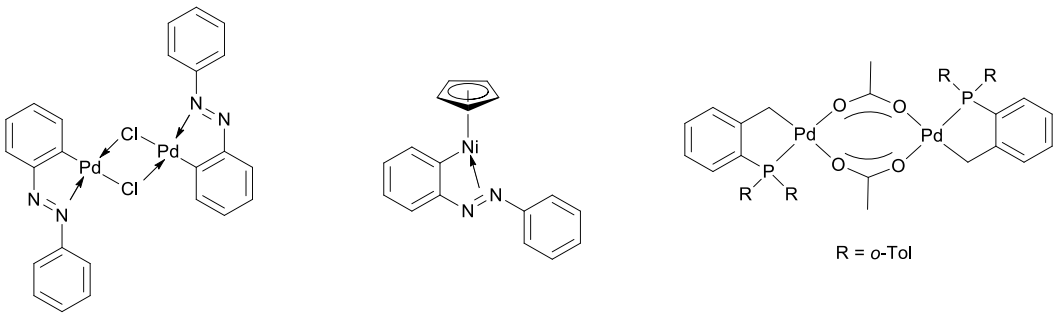

1.1 **1.2** **1.3**

Figure 1.2: (**1.1**) First reported cyclopalladated complex,[2,3] (**1.2**) Cyclopentadienyl azobenzene nickel complex of Dubeck *et al.*[4] and (**1.3**) Herrmann's palladacycle.[5]

1.1.2 Types of palladacycles

There are two distinct types of palladacycles based on their basic structural features: CD (bidentate) (**I**) or DCD (tridentate) (**II**) system (where D denotes a $2e^-$ donor atom shown in **Figure 1.3**) with five membered nitrogen-containing rings being the most common. The former most commonly exists as acetate- or halogen-bridge dimers which can exist as one of two geometric isomers: the *cisoid* isomers (**III**) in which the donor atoms are *cis* relative to one another and the *transoid* isomers (**IV**) in which the donor atoms are *trans* to one another.

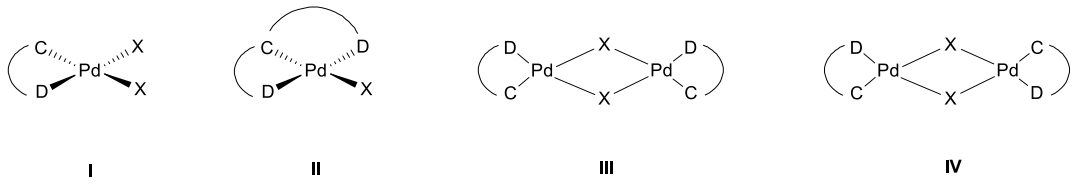

Figure 1.3: General cyclopalladated complex structures (with D = donor group and X = halide, triflate or solvent). Bidentate complex (**I**), tridentate complex (**II**), *cisoid*-cyclopalladated complex (**III**) and *transoid*-cyclopalladated complex (**IV**).

Species **I** may be isolated as a neutral dimer (**1.4, Figure 1.4**),[10] neutral monomer (**1.5**),[11] cationic (**1.6**) [12] or anionic (**1.7**) [13] complex depending on the nature of the ligands occupying the coordination sphere of the metal-centre. In general, the metallated carbon of the complexes is usually an aromatic sp^2 – hybridised carbon however cyclopalladation via the less common aliphatic sp^3 and vinylic sp^2 carbon is also possible.[14]

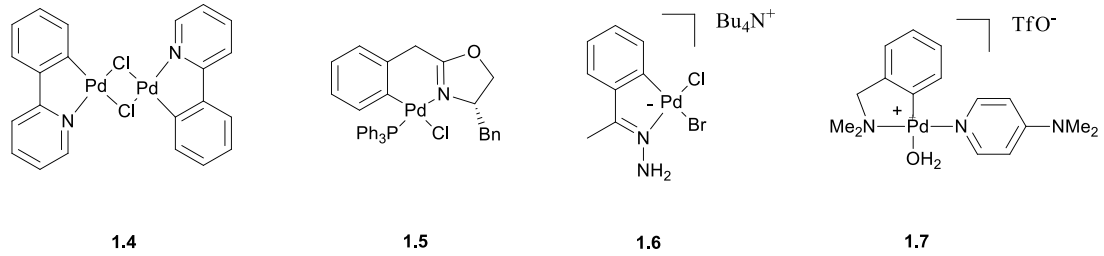

Figure 1.4: Examples of different types of bidentate palladacycles. Neutral dimeric palladacycle (**1.4**),[10] neutral monomeric palladacycle (**1.5**),[11] cationic monomeric palladacycle (**1.6**) [12] and anionic palladacycle (**1.7**). [13]

The tridentate palladacycle, also known as a pincer-type palladacycle, is usually symmetrical with two equivalent five-membered rings (**1.8**, **Figure 1.5**).[15] The unsymmetrical, mixed six membered-ring (**1.9**)[16] and the less commonly encountered pincer-type complexes **1.10** [17] containing both five and six membered-ring with a vinylic sp^2 metallated carbon have also been isolated and characterized.

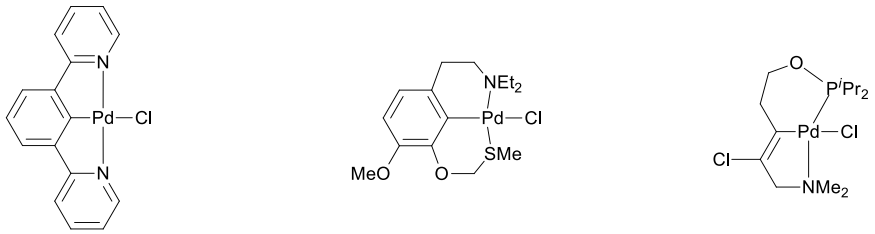

1.8 **1.9** **1.10**

Figure 1.5: Examples of different types of pincer-type palladacycles. Symmetrical NCN (**1.8**), [15] unsymmetrical mixed NCS (**1.9**) [16] and NCP (**1.10**) pincer type palladacycles. [17]

1.2 Common methodologies for palladacycle synthesis

There exist several known methods in literature for the synthesis of palladacycles, a process also known as cyclopalladation. The most common methods include the formation of palladacycles via electrophilic C-H bond activation, oxidative-addition and transmetallation reactions which often yield stable five- or six membered chelates with a Pd-C bond.[18] The following sections contain a brief discussion of the above-mentioned methods employed in cyclopalladation reactions.

1.2.1 Cyclopalladation via electrophilic C-H bond activation

The most efficient and direct method for generating palladacycles is via direct chelation assisted palladation of C-H bonds which allows the use of simple and inexpensive organometallic precursors. [18] Palladation agents commonly used include palladium acetate or palladium chloride salts ($(MeCN)_2PdCl_2$, K_2PdCl_4, Na_2PdCl_4 and Li_2PdCl_4) as shown in **Scheme 1.1**.

The formation of new palladacycles can also be achieved by another method, known as transcyclopalladation, which involves a ligand exchange process using another palladacycle as a palladation agent (**Scheme 1.2**). This method for example has been employed in the synthesis of species **1.13** in greater than 85% yield as opposed to the low yield afforded when the 1,3-*bis*(methylthiomethyl)benzene ligand was reacted directly with palladium acetate. In general, palladation reactions are usually performed in polar solvents such as methanol, ethanol, acetone, acetic acid, dichloromethane and chloroform.[19,20]

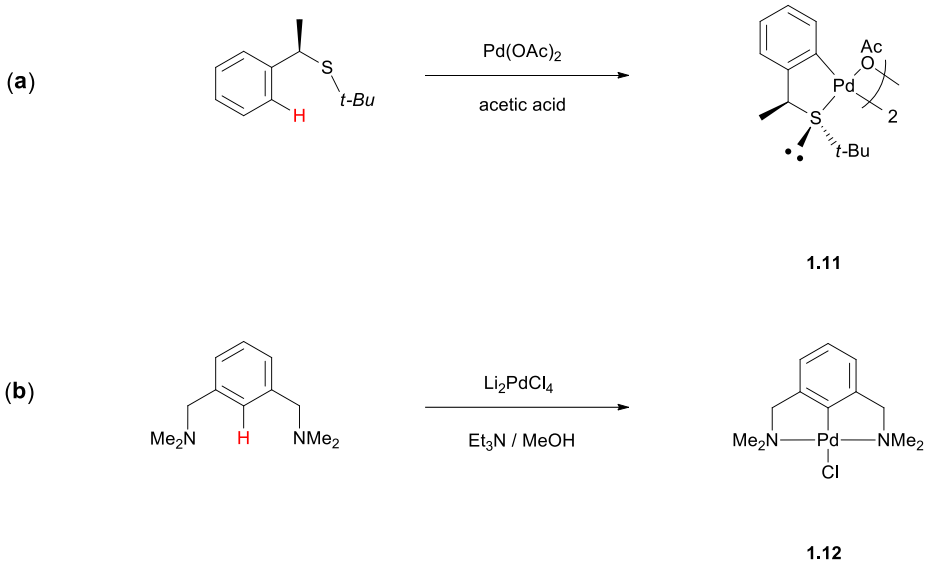

Scheme 1.1: Examples of cyclopalladation via electrophilic C-H activation using (**a**) $Pd(OAc)_2$ and (**b**) Li_2PdCl_4 as palladating agents. [21,22] The activated H-atom is indicated in red.

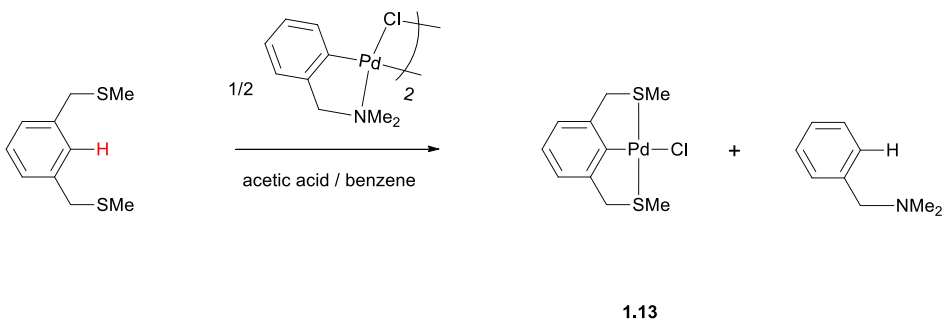

Scheme 1.2: Palladacycle employed as a palladating agent for transcyclopalladation. [22]

The nature of the donor atom is pivotal in initiating electrophilic C-H bond activation as well as determining the regioselectivity of the cyclopalladation process. The formation of the stable coordination complex species **C** (**Scheme 1.3**) is common and has been previously observed and isolated.[23] The formation of the unsaturated 14e$^-$ species **B** is generally assumed to occur only upon the dissociation of one donor ligand from species **C**.[24] Depending on the strength of the Pd-donor bond, it can either promote the formation of species **C** if the ligand coordination is strong, while weak ligand coordination disfavours complex formation, hence no coordination of species **A** to the metal precursor. The ability of the ligand to coordinate to the metal precursor can be modulated by changing the heteroatom as well as the steric bulk of the other ligands. For instance, amines and imines are common ligands in cyclopalladation since their bonding to palladium is neither too strong nor too weak. [24] The steric shielding of the nitrogen lone pair by the substituents on this donor atom is a crucial parameter in the bonding ability of amines (NR_2; R = alkyl) with greater steric shielding promoting cyclopalladation. Sterically demanding groups such as cyclic alkyl groups only coordinate to palladium if their rotational degree of freedom is restricted. In the case of imines, the steric effects are less significant since the nitrogen atom is sp^2 hybridized. For phosphine and sulphide donors, incorporating steric bulk around these donor atoms ensures that the Pd-P and Pd-S bonds do not become too strong. For instance, the Pd-P bond in palladium complexes comprised of phosphines with large cone angles are weaker due to the steric repulsion of the phosphine ligand.

The species **B** can undergo C-H activation via electrophilic aromatic substitution to form the cyclopalladated species **F**. The electrophilic aromatic substitution involves two crucial intermediates: the formation of a π-complex (species **D**) followed by the formation of a σ-complex which is an arenium intermediate (species **E**, **Scheme 1.3**). Analogues of species **E** have been prepared and fully characterized in platinum-mediated C-C and C-H bond formation and bond breaking processes for a NCN pincer type scaffold.[25] However, up till now, no evidence for the existence of species **D** as the preceding intermediate has been obtained. Nevertheless, species **E** undergoes proton abstraction to form the cyclopalladated species **F**. Macgregor *et.al.* refined the C-H activation mechanism with the

use of DFT calculations which predict agostic interactions during the initial stage of the bond activation process. This was shown in studies of cyclopalladation of dimethylbenzylamines with $Pd(OAc)_2$.[26] The results showed that the hydrogen-bonded complex (species **G**) initiates the C-H activation process and the displacement of one acetate molecule from the palladium centre by the C-H bond appeared to be the rate-determining step (ΔE = 13 kcalmol^{-1}) in the mechanism, which subsequently leads to the agostic species **H**. It has been postulated that this species is predominatly stabilized via AcO••••H-C_{aryl} hydrogen bonding involving the ortho-hydrogen and the oxygen donor of the displaced acetate ligand.[24] An analogous agostic complex has previously been structurally characterized in a rhodium PCP pincer complex.[27] The last step which involves the C-H bond cleavage and subsequent cyclopalladation has been modelled and found to proceed with virtually no activation barrier (0.1 kcalmol^{-1}).

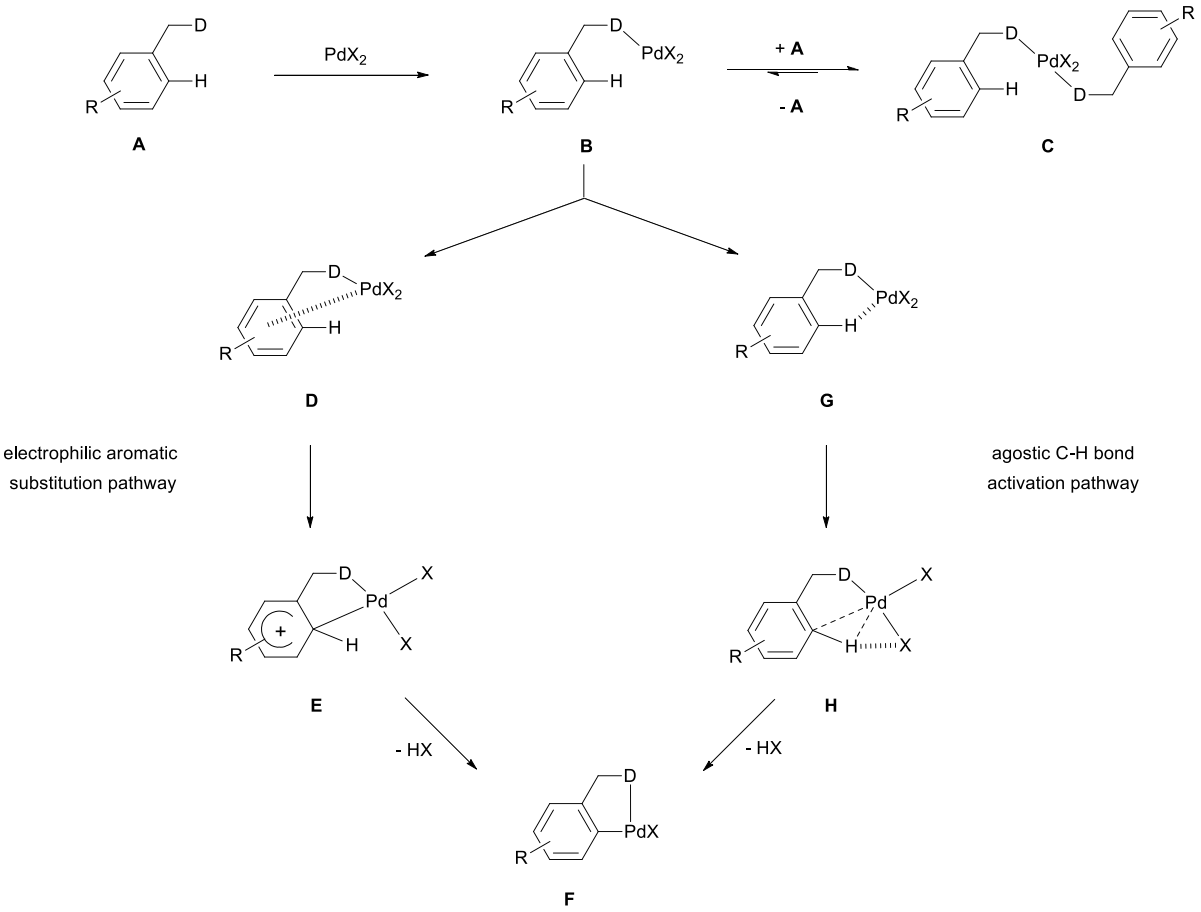

Scheme 1.3: Proposed C-H activation mechanism for the cyclopalladation of aromatic ligands via electrophilic aromatic substitution (**D**-**E**) or agostic C-H bond activation (**G**-**H**).[24]

The characteristic differences between the two mechanistic pathways are related to the distinct geometric parameters of the arenium species **E** in comparison to the agostic species **H**. In the arenium complex, the Pd•••H contact is large and the Pd-C-H angle is expected to be wide. In the agostic complex, the Pd•••H contact is shorter and the Pd-C-H angle elongated due to hydrogen bonding.[25] By correlating the rate-dependence of the cyclometallation with the electron donor ability of the aromatic substituents, it is also possible to distinguish between the two pathways. A strong correlation which gives a large Hammett plot would suggest that the C-H activation proceeds via an arenium intermediate while a weak correlation would suggest C-H activation via the agostic intermediate.

The nature of the cyclometallated carbon can influence the regioselectivity in cyclopalladation. Albert *et.al.* [28] studied the cyclopalladation of *N*-mesitylideneamines using $Pd(OAc)_2$ as palladating agent (**Scheme 1.4**). Not only were they able to isolate both *endo*- (imine bond situated inside of the metallacycle) and *exo* palladacycles (imine bond situated outside of the metallacycle) but they also gained insight into factors governing this process i.e. preferential activation of aromatic over aliphatic C-H bond and the ring size of the palladacycle formed. It was found that six membered *endo*-species such as **1.15** were formed containing an aliphatic Pd-C bond in preference to the common four-, five- and six-membered *exo*-species (**1.16**) containing an aromatic Pd-C bond when the *N*-mesitylideneamine ligands and $Pd(OAc)_2$ were refluxed in acetic acid. Employing milder conditions, the five membered *exo*-species (**1.16**) was isolated which can either isomerize to the six-membered *endo*-species (**1.15**) when refluxed in acetic acid or isomerize to the Z-form *exo*-species **1.17**. It is believed that the thermodynamic driving force for the former reaction is the formation of the *endo*-palladacycle, although it results in the formation of a six membered ring. Steric effects were also found to have a marked effect on the regioselectivity. Incorporating a methyl-group and blocking the 5-position of the ligand resulted in the selective formation of the six-membered *endo*-species (**1.15**) with an aliphatic Pd-C bond.

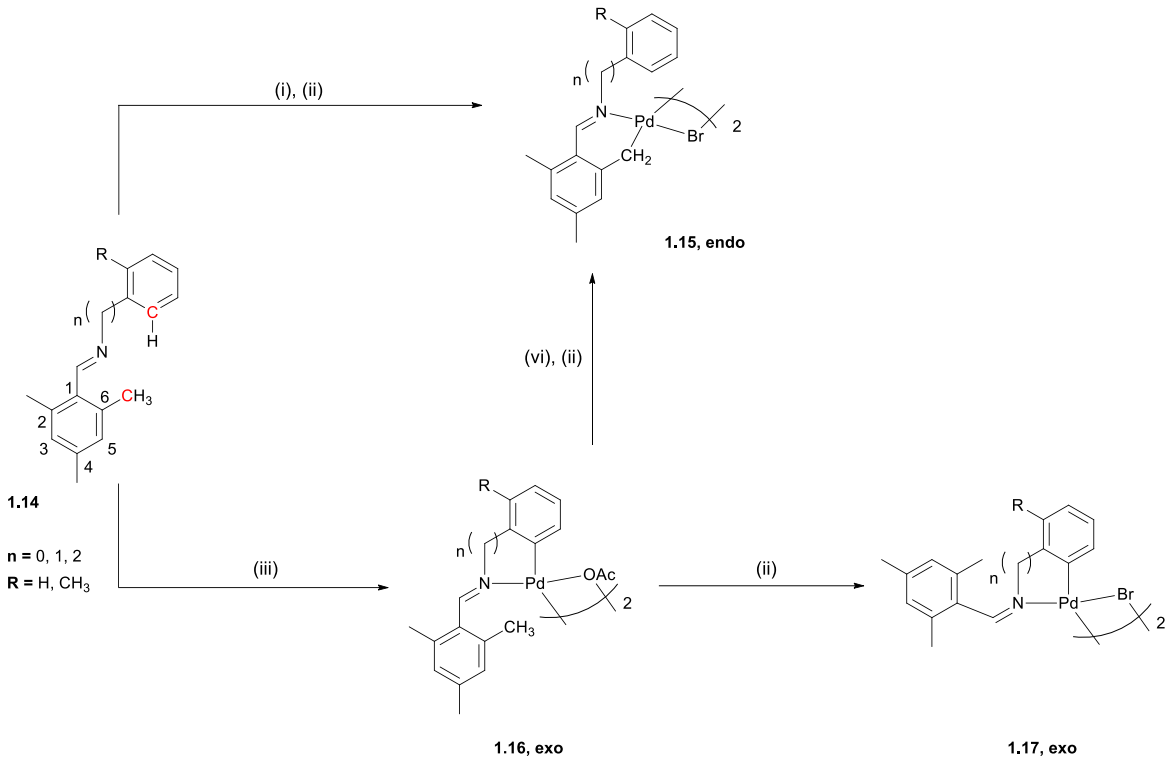

Reaction conditions: (**i**) $Pd(OAc)_2$, AcOH, reflux, 45 min; (**ii**) LiBr, EtOH; (**iii**) $Pd(OAc)_2$, AcOH, 40-60 °C, 2h; (vi) AcOH, reflux, 45 min.

Scheme 1.4: Synthetic pathway for the regioselective synthesis of cyclopalladated mesitylbenzylideneamines. [28] Red carbons indicate the position where cyclopalladation occurs.

1.2.2 Cyclopalladation *via* oxidative-addition

It is clear that the electrophilic C-H activation pathway provides one of the most elegant ways to form palladacycles. However, the oxidative-addition of aryl halides and although the latter is less commonly alkyl halides, which consist of a 2é donor group, is also an important pathway to prepare various palladacycles that cannot be accessed by the electrophilic C-H activation methodology, i.e. preparation of three- and four-membered ring palladacycles (**Scheme 1.5**). Common palladating agents includes $Pd(PPh_3)_4$, $Pd_2(dba)_3$ or $Pd(dba)_2$ which generate either dimeric palladacycles bridged by halogens, neutral pincer-type palladacycles or triphenylphosphine bound monomers.[18]

Oxidative-addition is important in generating palladacycles with reactive functionalities with the intention of using the palladated product for further transformations such as the synthesis of carbocycles (species **1.19**, **Scheme 1.5**) or carbene insertion in the Pd-C bond to form a five-membered palladacycle with an aliphatic Pd-C bond (species **1.22**). Solé *et.al.* isolated the first four-membered azapalladacycles such as **1.18** as intermediates for the intramolecular carbocyclization of aryl halides and ketones to form carbocycles.[29] Changing the substituent on the nitrogen donor atom does not prevent palladacycle formation (**1.20**), however it greatly alters the carbocyclization pathway. The reaction of *N*,*N*-dialkyl-2-iodoaniline with $Pd(PPh_3)_4$ afforded the four-membered species **1.21** which reacts easily to relieve steric strain to form a stable five-membered species **1.22**.[30]

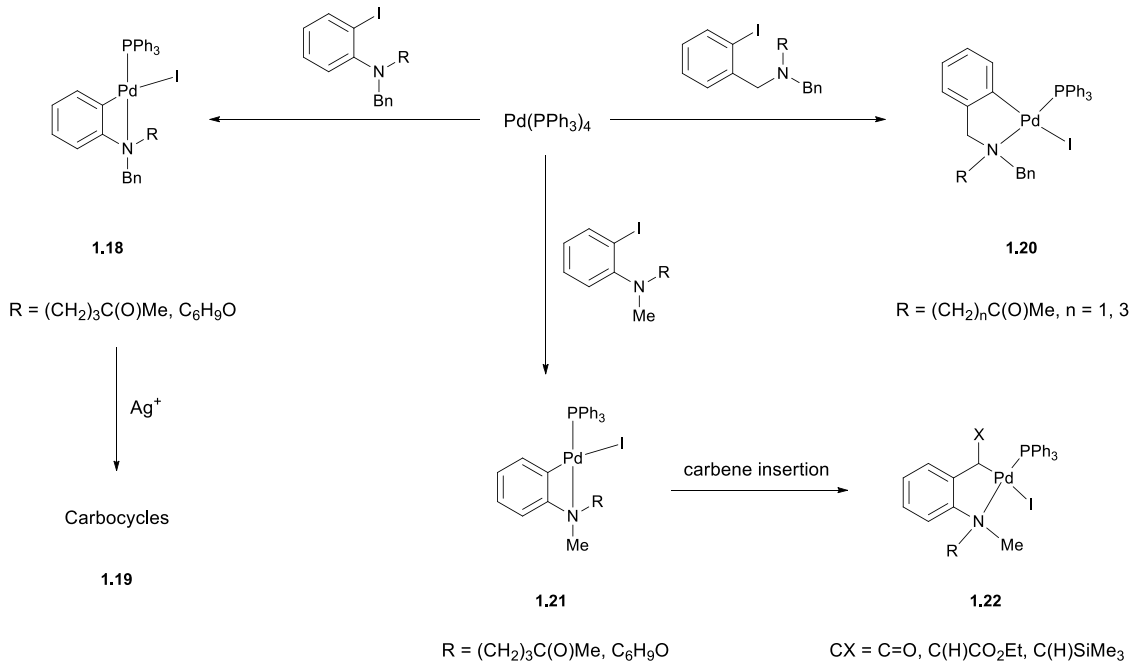

Scheme 1.5: Oxidative-addition employed for the synthesis of carbocycles and five-membered palladacycles via unfavourable four-membered palladacycle intermediates. [29-30]

The major constraint using the oxidative-addition methodology is the availability of the starting halide ligand which often requires a multistep procedure to prepare.

1.2.3 Cyclopalladation *via* transmetallation reaction

Another interesting and versatile method for the preparation of palladacycles is the transmetallation reaction. Similar to the oxidative-addition approach, this method can be utilized to generate palladacycles which cannot be synthesized employing the electrophilic C-H bond activation methodology. Transmetallating agents such as organolithium and organomercurial reagents are often used. van Koten *et. al.* [31] have reported the preparation of cyclopalladated naphthalene complexes in the 1- or 3-position (species **1.25** and **1.29**) selectively under controlled reaction conditions as shown in **Scheme 1.6a** and **b**.

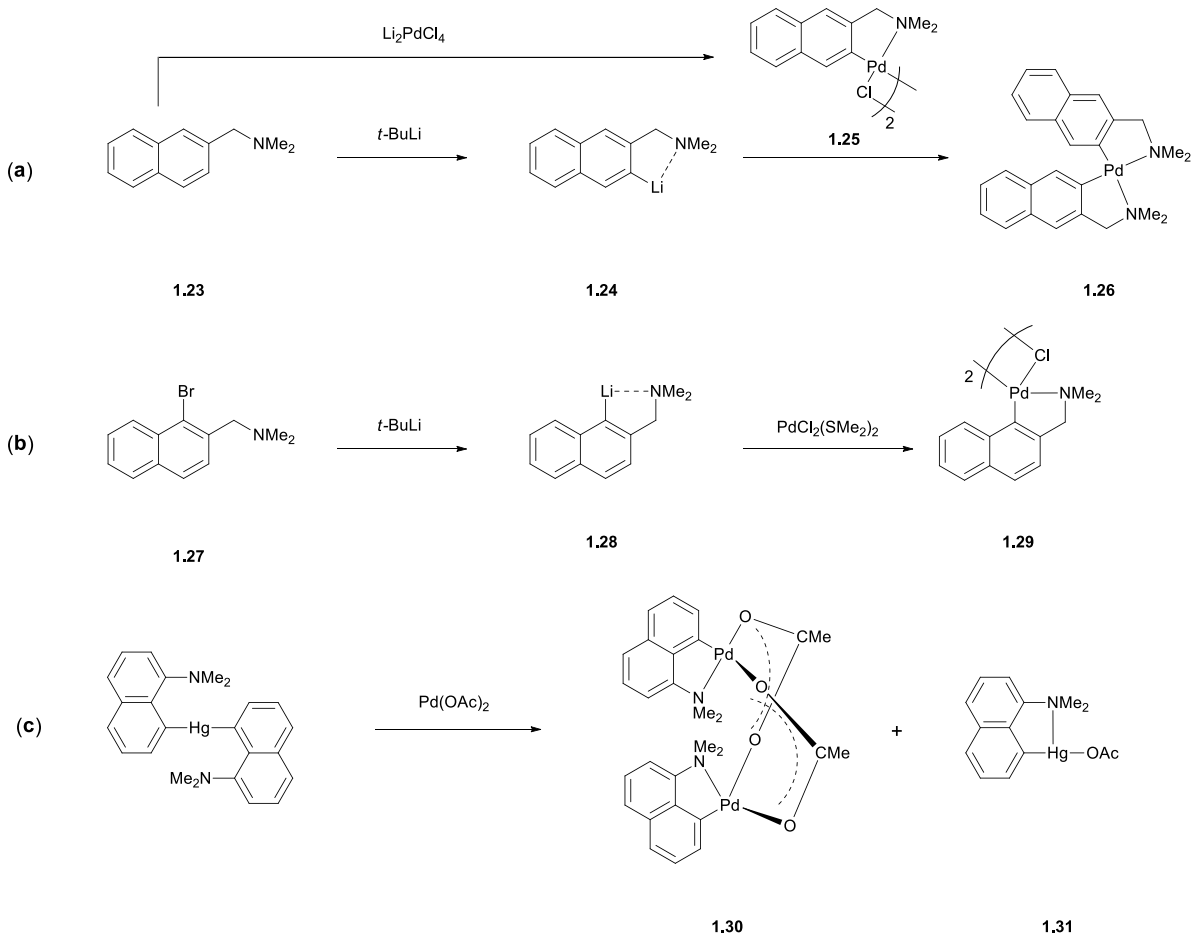

Scheme 1.6: Cyclopalladation via transmetallation reaction of (**a** and **b**) 2-(dimethylamino)methyl naphthalene ligands using an organolithium reagent and (**c**) *bis*-(8-dimethylaminonaphthyl)mecury using $Pd(OAc)_2$ palladating agent. [31]

Electrophilic C-H activation of naphthalene ligand **1.23** with Li_2PdCl_4 afforded the palladacycle **1.25** in the 3-position, however the lithiation of naphthalene ligand **1.27** which contains the bromide substituent allows the selective formation of palladacycle **1.29** in the 1-position. The reaction of the lithiated species **1.24** with palladacycle **1.25** afforded the *bis*-cyclopalladated complex **1.26**, a feature well known for transmetallated reactions. Organomercurial transmetalling reagents are also widely used due to their stability and reaction performance under mild conditions, although this class of reagents are considered to be highly toxic. This reagent also offers a useful route for the generation of bridged dimers (species **1.30**) which are either not accessible via electrophilic C-H activation, oxidative-addition or transmetallation using organolithium compounds. [32]

1.3 Application of palladacycles in catalysis

Palladacycles have become more prominent since their discovery in the middle 1960's and have become the subject of academic research as well as application in industry. There are excellent specialized review articles dedicated to the application of palladacycles in organometallic catalysis,[1,7,8] organic synthesis[18,24,33] and medicinal and biological chemistry.[34] The following sections will highlight important examples of palladacycles in C-C coupling reactions.

1.3.1 Mizoroki-Heck coupling reaction

The Mizoroki-Heck reaction is broadly defined as a Pd(0)-mediated coupling of an aryl- or vinyl halide with olefinic substrates under basic conditions (**Scheme 1.7**) which was independently discovered by Mizoroki [35] and Heck [36] in the early 1970's. Almost all palladium catalysts are able to facilitate the coupling of reactive substrates such as aryl iodides and activated aryl bromides, however the oxidative-addition of unactivated substrates such as alkyl halides and aryl chlorides requires highly active palladium catalysts.[37,38]

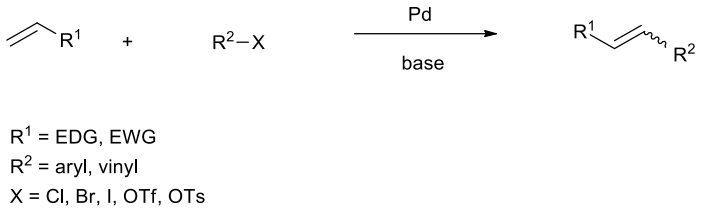

Scheme 1.7: General representation of Mizoroki-Heck coupling reaction.

Palladacycles have attracted increasing attention especially in C-C coupling reactions. As mentioned earlier, the true potential of palladacycles as catalysts in C-C coupling reactions was only discovered in 1995 when Herrmann and Beller employed a cyclopalladated tris(*o*-tolyl)-phosphine palladacycle (**1.3**, **Figure 1.6**) using unreactive aryl bromides as well as activated aryl chlorides.[5,6] The catalyst shows high thermal stability and exhibits high activities with turnover numbers (TONs) greater than 100 000. This discovery has led to the design of a wide variety of nitrogen-, oxygen-, phosphorous- and sulphur-containing palladacycles which also show extremely high activities in different coupling reactions.

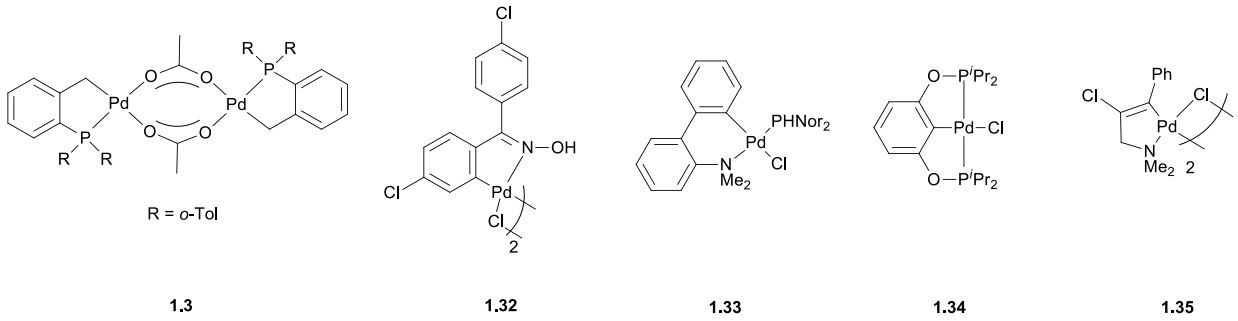

Figure 1.6: (**1.3**) Herrmann-Beller's phosphine-derived palladacycle, (**1.32**) Nájera's oxime-derived palladacycle,[39] (**1.33**) phosphine adduct of C-N palladacycle,[40] (**1.34**) pincer phosphinito palladacycle[41] and (**1.35**) bridge C-N palladacycle.[42]

The potential of oxime-derived palladacycles as catalyst precursors in C-C coupling reactions was highlighted by Nájera *et.al.* who reported catalyst systems which exhibit high thermal stability and are not air- or moisture sensitive.[39] Of all the oxime-derived catalysts tested, complex **1.32**

(**Figure 1.6**) was found to be the most efficient catalyst for the Mizoroki-Heck vinylation of aryl halides with various olefinic substrates. At high temperatures (130-160 °C), the catalyst was active under aerobic reaction conditions for the Heck vinylation of activated aryl chlorides and deactivated aryl bromides with different olefinic substrates although the yields were low in the case of the deactivated substrates. The oxime-derived complex was also highly efficient in the multiple vinylation of polybromo tribenzotriquinacenes (**1.36**) with either styrene or methyl acrylate affording species **1.37** under typical reaction conditions in Heck coupling of aryl bromides as shown in **Scheme 1.8**. Commercially available palladium catalysts such as $PdCl_2$, $Pd(OAc)_2$ and $Pd(PPh_3)_4$ employed in the polyvinylation of **1.36** did not provide satisfactory results.[43]

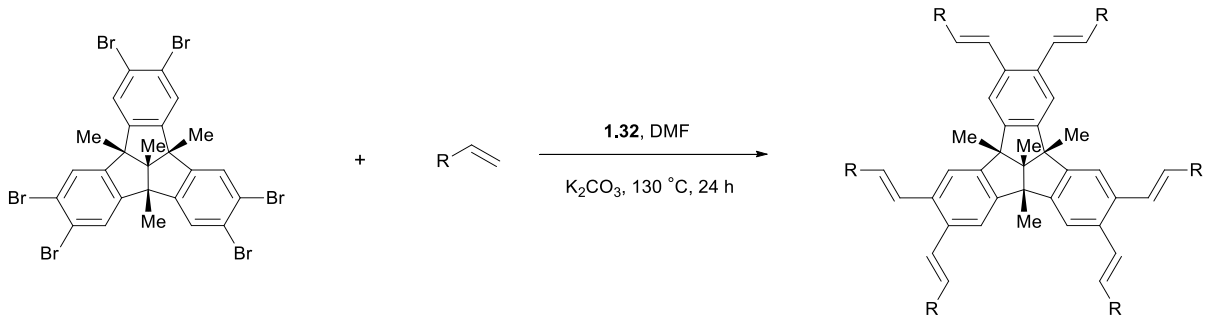

Scheme 1.8: Polyvinylation of tribenzotriquinacene catalyzed by Nájera's oxime-derived palladacycle **1.32**.

In general, the Heck reactions involving chloroarenes promoted by palladacycles remain a challenge due to their low reactivity. Reactions often require high temperatures which exceed 150 °C with no significant improvement in terms of yield or TON. Apart from the oxime-derived palladacycle (**1.32**), the CN-palladacycles containing bulky and electron-rich phosphines (**1.33**) [40] and PCP pincer palladacycles (**1.34**) [41] also showed remarkable catalytic activities in high temperature Heck reactions of aryl chlorides with styrene. In addition, palladacycle **1.35** is the only catalyst that promotes the Heck coupling of haloarenes with olefinic substrates at room temperature giving full conversion although with low TON. [42]

Although palladacycles are efficient catalyst precursors for C-C coupling reactions, separation of the catalyst from the product stream and the recyclability thereof remain challenging. Several palladacycles immobilized on either polymers or silica were studied in an attempt to circumvent these problems. [39] For example, Luo *et.al*. immobilized a phosphine-derived palladacycle onto a polystyrene support (**1.38**, **Figure 1.7**) and examined the Heck reaction of methyl acrylate with various aryl halides.[44] The supported catalyst exhibited high reactivity, similar to that of the Herrmann-Beller palladacycle (**1.3**, **Figure 1.6**) which is the unsupported analogue. This supported catalyst was found to be selective towards the *trans*-product. In addition to the high reactivity, catalyst **1.38** also displayed high recyclability with a product yield of 80 % observed after being recycled four times with ether as solvent of choice.

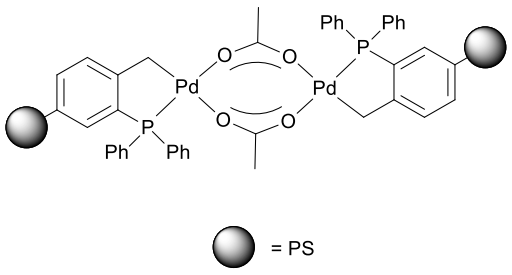

1.38

Figure 1.7: Polystyrene-supported palladacycle complex employed in Heck coupling of aryl halides with methyl acrylate. [44]

Evidence from experimental- and kinetic studies provides insight into the precise role of palladacycles in cross-coupling reactions. [45–47] Palladacycles in their own right are catalytically inactive species but are precursors of Pd(0) species in the reaction mixture into which they are released to be gradually incorporated into the catalytic cycle at a much slower rate than the overall catalytic reaction. It is believe that the Pd(0) species is generated after initial reaction of the palladacycle with the organic substrates and not via thermal decomposition as previously postulated.[39] This phenomenon prevents processes such as nucleation and growth of large palladium particles which could deactivate the catalyst. Although earlier studies suggested that Heck coupling catalysed

by palladacycles proceeds via a Pd(II)/Pd(IV) mechanism,[48] it is now accepted that the catalytically active species are based on Pd(0) and that the reaction proceeds via a Pd(0)/Pd(II) catalytic cycle.[49,50]

1.3.2 Suzuki-Miyaura coupling reactions

The Suzuki-Miyaura reaction, first reported in 1979, involves the palladium catalyzed coupling reaction of organohalides with organoboronic acids in the presence of a base as shown in **Scheme 1.9**.[51,52] This coupling reaction is an extremely powerful method for constructing new C-C bonds and is routinely used in fine chemical research and development as well as in pharmaceutical discovery laboratories. For example, the Suzuki-Miyaura reaction has been scaled to commercial operation for the production of Boscalid (**1.39**),[53] a fungicide for crop protection, and Valsartan (**1.40**),[54] an angiotensin II inhibitor for the treatment of hypertension and congestive heart failure (**Figure 1.8**). In general, this reaction offers the potential for high product yields, high functional group tolerance and non-toxic boronic acid by-products.

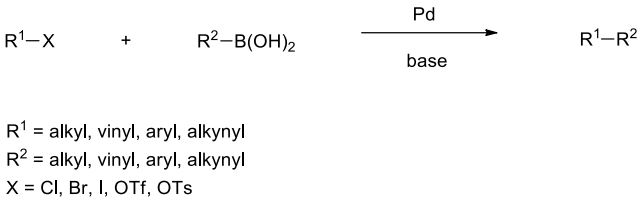

Scheme 1.9: General representation of Suzuki-Miyaura coupling reaction.

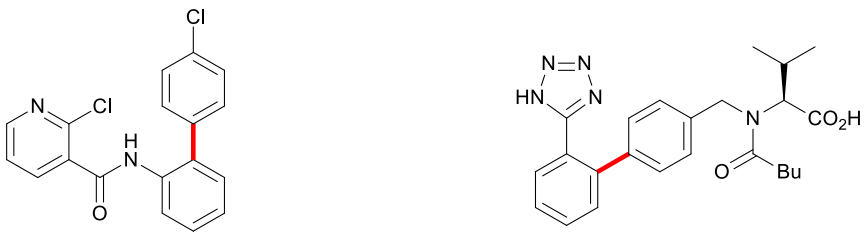

1.39 **1.40**

Figure 1.8: Examples of commercially available products produced *via* Suzuki-Miyaura coupling. The new C-C bond formed *via* the reaction is highlighted in red for Boscalid (**1.39**) [53] and Valsartan (**1.40**). [54]

Palladacycles are also efficient catalysts for Suzuki coupling of aryl boronic acids with aryl bromides and aryl iodides under mild conditions. For example, Bedford *et.al.* developed a phosphinito-derived palladacycle (**1.41**, **Figure 1.9**) which was found to be an extremely active catalyst giving high TON of up to 1 million for the coupling of 4-bromoacetophenone with phenylboronic acid in the presence of toluene using K_2CO_3 as base at 110 °C.[55] In contrast, the coupling of deactivated aryl chlorides substituted with electron-donating groups remains a challenge and many research efforts have been devoted in search of developing efficient catalyst systems which promote Suzuki coupling of these substrates.

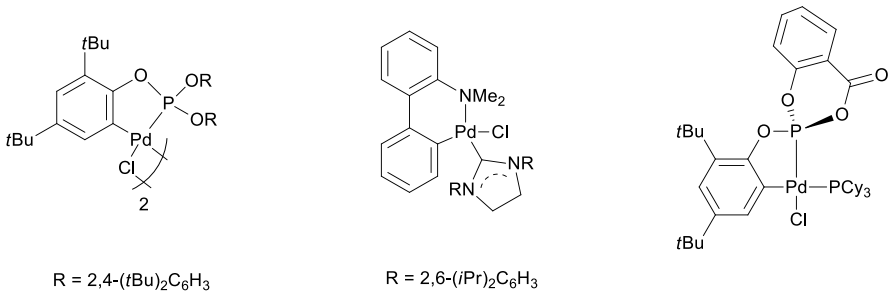

1.41 **1.42** **1.43**

Figure 1.9: Palladacycles that have been used in Suzuki coupling reactions. (**1.41**) Orthometallated triarylphosphite palladacycle, [55] (**1.42**) carbene-derived palladacycle, [56] (**1.43**) phosphine adduct of phosphite-based palladacycle. **.**[57]

Phosphapalladacycles and palladacycles modified with carbene or phosphorous containing ligands have so far been reported to produce the best results in Suzuki coupling of aryl chlorides with boronic acids due to the extra stability provided by the auxiliary ligand in stabilizing the low ligated catalytically active Pd(0) species involved in the catalytic cycle.[18] Of note is the coupling of 4-chloroanisole and 2-chlorotoluene with phenylboronic acid promoted by a phosphine palladacycle **1.33** [40] (**Figure 1.6**) and carbene-derived palladacycle **1.42** [56] (**Figure 1.9**) respectively. Although quantitative conversions were observed, low TON's were reported for these catalysts system. Bedford *et.al.*[57] demonstrated the ability of a phosphite-based palladacycle (**1.43**) with tricyclohexylphosphine (PCy_3) as auxiliary ligand, generated *in situ*, to catalyze Suzuki coupling of deactivated, activated and

sterically hindered aryl chloride substrates. Extremely high activities with TON's up to 128 000 and 116 000 were observed for the Suzuki coupling of deactivated 4-chloroanisole and sterically hindered 2-chloro-*m*-xylene with phenylboronic acid respectively in the presence 1,4-dioxane using Cs_2CO_3 as base at 100 °C.

The Suzuki coupling of sterically hindered coupling partners has always been a stumbling block in designing and developing new C-C coupling catalysts. Previous attempts at the sixfold alkenylation of hexabromobenzene (**1.44**, **Scheme 1.10**) with styrene and substituted styrenes have been reported, however the reaction was hampered by the competing 5-*exo*-*trig* cyclizations due to the consecutive alkenylation of the intermediate *o*-bromostyrene subunit on the central benzene ring.[58] This led to a variety of benzylideneinane and benzylindene by-products of which the separation of the sixfold alkenylation product and the by-products proved to be extremely difficult. In contrast, the sixfold Suzuki coupling catalyzed by Herrmann-Beller palladacycle **1.3**, gave the highly congested alkenylation product **1.45**, albeit in only 6 % conversion.[59]

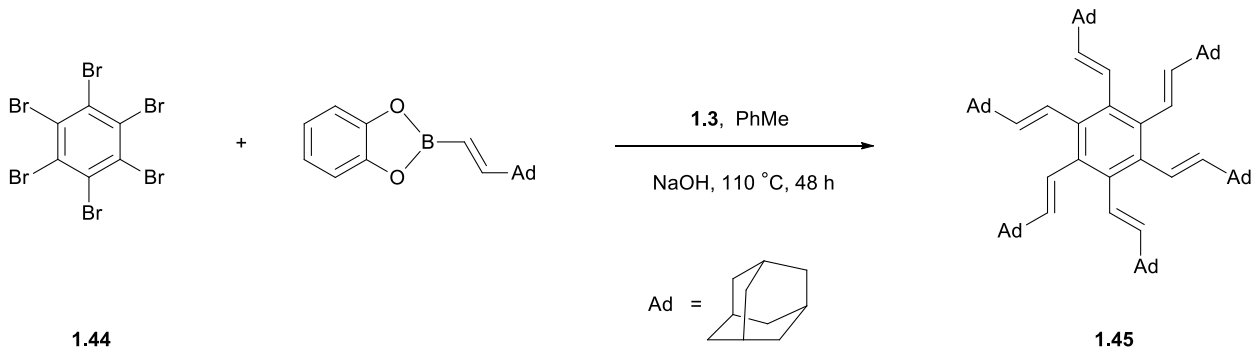

Scheme 1.10: Sixfold Suzuki alkenylation of hexabromobenzene (**1.45**) catalyzed by Herrmann-Beller palladacycle **1.3**. [59]

1.3.3 Sonogashira and other C-C coupling reactions

Palladacycles have also been shown to be efficient and versatile precatalysts for other important C-C coupling reactions such as Sonogashira,[60] Stille [61] and Negishi reactions.[62] García *et.al.* developed an oxime carbapalladacycle covalently anchored on a soluble polyethyleneglycol (PEG) scaffold with an average molecular weight of 6000 Da (**1.46**, **Figure 1.10**) for the copper-free Sonogashira coupling of 4-bromoacetophenone with phenylacetylene as shown in **Scheme 1.11**.[63] This catalytic system is among the most active and reusable phosphine-free palladium catalyst systems and displays high recyclability of up to 10 runs with complete substrate conversion. The original PEG-anchored catalyst largely decomposes during the first catalytic cycle, forming palladium nanoparticles (average particle size of 6 nm, σ ± 2). These resulting particles which are stabilized by the PEG ligand, are active catalysts in their own right. Stabilization by the polymeric carrier prevents palladium leaching from the PEG phase thus retaining the catalytic properties.

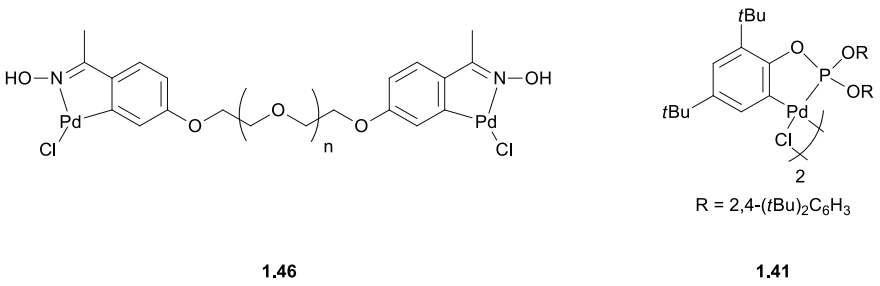

1.46 **1.41**

Figure 1.10: (**1.46**) PEG supported oxime-derived palladacycle, (**1.41**) orthometallated triarylphosphite palladacycle and (**1.47**) metallated triarylphosphine palladacycle.

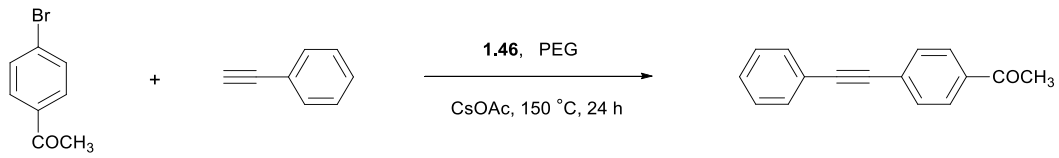

Scheme 1.11: Sonogashira coupling of 4-bromoacetophenone with phenylacetylene catalyzed by a PEG supported oxime-derived palladacycle (**1.46**). [63]

Encouraged by the results obtained in the Suzuki reaction catalyzed by the highly active palladacycle **1.41** discussed previously, Bedford and co-workers also evaluated the catalytic potential of **1.41** in the Stille coupling of aryl bromides with tributylphenyltin.[55] TON's of up to 840 000 were achieved within 18 hours at 120 °C with turnover frequencies (TOF) of nearly 830 000 when 4-bromoacetophenone was used as coupling partner.

The Herrmann-Beller palladacycle (**1.3, Figure 1.2**) employed was an efficient catalyst for the Negishi coupling of organozinc reagents with activated and non-activated aryl halides (**Scheme 1.12**) in quantitative yields, although early precipitation of palladium black occured.[7] The Negishi coupling in general tolerates functional groups such as amides, amines, cyano- and nitro groups, aldehydes, ketones and esters which provides a useful route to unsymmetrical biaryls and other fundamental building blocks in organic synthesis.

R^1 = H, NO_2, OCH_3, $COCH_3$
R^2 = Ph
X^1 = Cl, Br
X^2 = Br, Me

Scheme 1.12: Negishi coupling of aryl halides with zinc reagents catalyzed by Herrmann-Beller palladacycle (**1.3**).

1.4 Concluding remarks

Palladacycles have become very popular in C-C coupling reactions due to their exceptionally high activity and tolerance of almost all functional groups. In general, they are stable catalyst precursors and have been shown to even catalyse the transformation of unreactive substrates as discussed previously. Their electronic and steric properties can be modulated, which in turn could influence the selectivity towards certain substrates or products in catalysis. Recent developments in our research group have demonstrated palladacycles as active catalysts in phenylacetylene polymerization. To the best of our knowledge, there are no other reports in the literature which describe the polymerization of phenylacetylene catalyzed by palladacycles.

In light of the afore-mentioned, the objectives of this study are three-fold:

1. Preparation of novel cationic palladacycles with different ortho-substituents on the metallated ring ranging from electron-donating to electron withdrawing groups and auxiliary tertiary phosphine ligands with different basicities coordinating to the metal centre. These characteristics have the potential to fine tune the metal's electrophilicity, hence modulating the reactivity of the complexes.

2. The characterization of all novel palladacycle complexes using a range of analytical techniques including FT-IR- and NMR spectroscopy, mass spectrometry and X-ray diffraction analysis.

3. Evaluation of the cationic palladacycles as catalyst precursors in the polymerization of phenylacetylene. Reaction parameters such as solvent type, monomer to catalyst ratio, temperature and reaction time will be varied to study the behaviour of these complexes. Average molecular weight and polydispersity indices will be determined by gel permeation chromatography (GPC).

1.5 Overview of thesis content by chapter

Chapter 1 gives a brief overview and discusses the fundamental aspects of palladacycles. This includes a brief historical background, different types of palladacycles, synthetic methodologies that are employed for their preparation and their application as catalyst precursors in various C-C coupling reactions.

Chapter 2 details the synthesis and characterization of various μ-*Cl* binuclear palladacycles, via C-H electrophilic bond activation, derived from ortho-substituted benzylindene-2,6-diisopropylaniline ligands. The subsequent cleavage of the μ-*Cl* binuclear palladacycles with auxiliary tertiary phosphine ligands to form novel neutral palladacycle complexes are investigated and thoroughly discussed.

The synthesis and characterization of novel cationic palladacycle complexes prepared from their neutral analogues, discussed in **Chapter 2**, are presented in **Chapter 3**.

Chapter 4 describes the evaluation of cationic palladacycles as catalyst precursors in the polymerization of phenylacetylene. Reaction parameters such as the type of solvent, monomer to catalyst ratio, temperature and time are varied and catalytic activities of the different complexes are compared and discussed.

The last chapter, **Chapter 5**, summarizes the most important aspects of this study according to chapter. Conclusions are drawn from characterization data presented in **Chapter 2** and **Chapter 3** as well as the catalytic data presented in **Chapter 4**. This chapter concludes with some suggestions for future work which would complement and expand on the topics presented in this study.

1.6 Reference

1 J. Dupont, M. Pfeffer and J. Spencer, *Eur. J. Inorg. Chem.*, 2001, **2001**, 1917.

2 A. Cope and R. Siekman, *J. Am. Chem. Soc.*, 1965, **87**, 3272.

3 A. Cope and E. Friedrich, *J. Am. Chem. Soc.*, 1968, **90**, 909.

4 J. Kleinman and M. Dubeck, *J. Am. Chem. Soc.*, 1963, **85**, 1544.

5 W. Herrmann, C. Brossmer, K. Ofele, C. Reisinger, T. Priermeier, M. Beller and H. Fischer, *Angew. Chem. Int. Ed*, 1995, **34**, 1844.

6 M. Beller, H. Fischer, W. Herrmann, K. Ofele and C. Brossmer, *Angew. Chem. Int. Ed*, 1995, **34**, 1848.

7 W. Herrmann, V. Bohm and C. Reisinger, *J. Organomet. Chem.*, 1999, **576**, 23.

8 R. Bedford, *Chem. Commun.*, 2003, **15**, 1787.

9 R. Bedford, C. Cazin and D. Holder, *Coord. Chem. Rev.*, 2004, **248**, 2283.

10 M. Cargill, T. Leese and G. Reese, *Inorg. Chim. Acta*, 1991, **182**, 93.

11 R. Mawo, D. Johnson, J. Wood and I. Smoliakova, *J. Organomet. Chem.*, 2008, **693**, 33.

12 Z. Lu, X. Wang, B. Liu and R. Wang, *J. Organomet. Chem.*, 2010, **695**, 2191.

13 P. Braunstein, J. Dehand and M. Pfeffer, *Inorg. Nucl. Chem. Lett.*, 1974, **10**, 581.

14 J. Dupont, N. Basso, M. Meneghetti and R. Konrath, *Organometallics*, 1997, **16**, 2386.

15 C. Consorti, G. Ebeling, F. Rodembusch, V. Stefani, P. Livotto, F. Rominger, F. Quina, C. Yihwa and J. Dupont, *Inorg. Chem.*, 2004, **43**, 530.

16 R. Holton and R. Nelson, *J. Organomet. Chem.*, 1980, **201**, C35.

17 G. Rosa, G. Ebeling, J. Dupont and A. Monteiro, *Synthesis (Stuttg).*, 2003, 2897.

18 J. Dupont, C. Consorti and J. Spencer, *Chem. Rev.*, 2005, **105**, 2527.

19 J. Serrano, L. García, J. Pérez, E. Pérez, J. García, G. Sánchez, P. Sehnal, S. De Ornellas, T. Williams and I. Fairlamb, *Organometallics*, 2011, **30**, 5095.

20 N. Singh and A. Elias, *Dalton Trans.*, 2011, **40**, 4882.

21 J. Dupont, A. Gruber and G. Fonseca, *Organometallics*, 2001, **20**, 171.

22 J. Dupont, N. Beydoun and M. Pfeffer, *J. Chem. Soc., Dalt. Trans.*, 1989, 1715.

23 A. Ryabov, I. . Sakodinskaya and A. . Yatsimirsky, *J. Chem. Soc., Dalt. Trans.*, 1985, 2629.

24 J. Dupont and M. Pfeffer, *Palladacycles: Synthesis, Characterization and Applications*, Wiley-VCH Verlag GmbH & Co. KGaA, Weinheim, Germany, 2008.

25 M. Albrecht, A. Spek and G. Van Koten, *J. Am. Chem. Soc.*, 2001, **123**, 7233.

26 D. Davies, S. Donald and S. Macgregor, *J. Am. Chem. Soc.*, 2005, **127**, 13754.

27 A. Vigalok, O. Uzan, L. Shimon, Y. Ben-David, J. Martin and D. Milstein, *J. Am. Chem. Soc.*, 1998, **120**, 12539.

28 J. Albert, R. Ceder, M. Gómez, J. Granell and J. Sales, *Organometallics*, 1992, **11**, 1536.

29 D. Solé, L. Vallverdú, X. Solans, M. Font-Bardía and J. Bonjoch, *J. Am. Chem. Soc.*, 2003, **125**, 1587.

30 D. Solé, L. Vallverdú, X. Solans, M. Font-Bardía and J. Bonjoch, *Organometallics*, 2004, **23**, 1438.

31 J. Valk, F. Maassarani, P. van der Sluis, A. Spek, J. Boersma and G. van Koten, *Organometallics*, 1994, **13**, 2320.

32 E. Wehman, G. van Koten and J. Jastrzebski, *J. Chem. Soc. Dalt. Trans.*, 1988, 2975.

33 V. Dunina and O. Gorunova, *Russ. Chem. Rev.*, 2005, **74**, 871.

34 A. Kapdi and I. Fairlamb, *Chem. Soc. Rev.*, 2014, **43**, 4751.

35 T. Mizoroki, K. Mori and A. Ozaki, *Bull. Chem. Soc. Jpn.*, 1971, **44**, 581.

36 R. Heck and J. Nolley, *J. Org. Chem.*, 1972, **37**, 2320.

37 T. Luh, M. Leung and K. Wong, *Chem. Rev.*, 2000, **100**, 3187.

38 I. Beletskaya and A. Cheprakov, *J. Organomet. Chem.*, 2004, **689**, 4055.

39 D. Alonso and C. Nájera, *Chem. Soc. Rev.*, 2010, **39**, 2891.

40 A. Schnyder, A. Indolese, M. Studer and H. Blaser, *Angew. Chem. Int. Ed. Engl.*, 2002, **41**, 3668.

41 D. Morales-Morales, R. Redón, C. Yung and C. Jensen, *Chem. Commun.*, 2000, **3**, 1619.

42 C. Consorti, M. Zanini, S. Leal, G. Ebeling and J. Dupont, *Org. Lett.*, 2003, **5**, 983.

43 X. Cao, D. Barth and D. Kuck, *European J. Org. Chem.*, 2005, **2005**, 3482.

44 C. Lin and F. Luo, *Tetrahedron Lett.*, 2003, **44**, 7565.

45 J. Louie and J. Hartwig, *Angew. Chemie Int. Ed.*, 1996, **35**, 2359.

46 M. Nowotny, U. Hanefeld, H. Koningsveld and T. Maschmeyer, *Chem. Commun.*, 2000, 1877.

47 V. Böhm and W. Herrmann, *Chem. Eur. J*, 2001, **7**, 4191.

48 J. Brunel, M. Hirlemann, A. Heumann and G. Buono, *Chem. Commun.*, 2000, 1869.

49 M. Reetz and J. de Vries, *Chem. Commun.*, 2004, 1559.

50 A. de Vries, J. Mulders, J. Mommers, H. Henderickx and J. de Vries, *Org. Lett.*, 2003, **5**, 3285.

51 N. Miyaura and A. Suzuki, *J. Chem. Soc., Chem. Commun.*, 1979, 866.

52 N. Miyaura, K. Yamada and A. Suzuki, *Tetrahedron Lett.*, 1979, **20**, 3437.

53 H. Avenot and T. Michailides, *Crop Prot.*, 2010, **29**, 643.

54 H. Black, J. Bailey, D. Zappe and R. Samuel, *Drugs*, 2009, **69**, 2393.

55 D. A. Albisson, R. B. Bedford, P. Noelle Scully and S. E. Lawrence, *Chem. Commun.*, 1998, 2095.

56 O. Navarro, R. Kelly and S. Nolan, *J. Am. Chem. Soc.*, 2003, **125**, 16194.

57 R. Bedford, S. Hazelwood and M. Limmert, *Chem. Commun.*, 2002, 2610.

58 A. de Meijere and F. Meyer, *Angew. Chemie Int. Ed.*, 1994, **33**, 2379.

59 P. Prinz, A. Lansky, T. Haumann, R. Boese, M. Noltemeyer, B. Knieriem and A. Meijere, *Angew. Chemie Int. Ed.*, 1997, **36**, 1289.

60 D. Alonso, C. Nájera and M. Pacheco, *Tetrahedron Lett.*, 2002, **43**, 9365.

61 R. Bedford, C. Cazin and S. Hazelwood, *Chem. Commun.*, 2002, 2608.

62 A. Bruneau, M. Roche, M. Alami and S. Messaoudi, *ACS Catal*, 2015, **5**, 1386.

63 A. Corma, H. García and A. Leyva, *J. Catal.*, 2006, **240**, 87.

Chapter 2

The Synthesis and Characterization of Neutral Palladacycles Derived from Schiff Base Imine Ligands

2.1 Introduction

Schiff bases, also known as imines, are the nitrogen analogues (**c**) of a carbonyl group which form during the condensation reaction between a primary amine (**a**) and ketone or aldehyde (**b**) shown in **Scheme 2.1**. Schiff bases are represented by the general formula $R_1N{=}CR_2R_3$ and the reaction was discovered and named after the famous German chemist, Hugo Joseph Schiff. [1,2] Schiff bases derived from aliphatic aldehydes in general are relative unstable, while those containing aromatic aldehydes are more stable due to the inherent effective conjugation. [3,4]

Scheme 2.1: General Schiff base condensation reaction which involves the reaction between a primary amine and an aldehyde or ketone.

The past century has witnessed enormous growth of the application of Schiff-base ligands in coordination chemistry, both in research as well as in industry. Their synthesis is facile and the nucleophilic ability of the azomethine nitrogen atom allows them to coordinate to a wide range of metals

in different oxidation states, forming stable metal complexes. The design allows the incorporation of functional groups having various electronic and steric characteristics, hence promoting coordination of the ligand to the metal centre. Tetradentate *bis*-Schiff bases are well known ligands due to their ease of synthesis and the ability to incorporate structural rigidity into the backbone of the ligand. Oshima *et. al.*[5] developed *bis*-Schiff base ligands *cis*- (**2.1**) and *trans*- *N,N'*-bis(2-pyridylmethylidene)-1,2-diiminocyclohexane (**2.2**) and *N,N'*-bis(2-pyridylmethylidene)-o-diiminobenezene (**2.3**) (**Figure 2.1**) and investigated the effect of steric restriction around the donor atoms on complexation in the ion-pair extraction of divalent metal cations into nitrobenzene with picrate anion. Higher extractability was obtained for the BPIB-NaPic system (**2.3**) in comparison to those in *cis*- (**2.1**) and *trans*-BPIC (**2.2**) systems and this was attributed to an increase of steric distortion which originated from conformational restrictions.

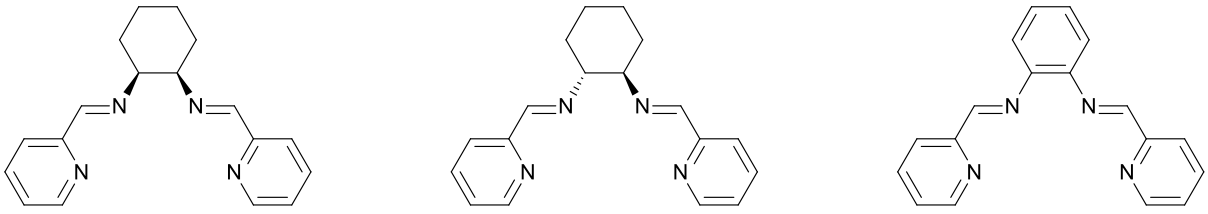

2.1 **2.2** **2.3**

Figure 2.1: Neutral bis-Schiff base ligands for the ion-pair extraction of divalent metal cations. (**a**) *cis*-BPIC; (**b**) *trans*-BPIC; (**c**) BPIB. [5]

Schiff bases have also proven to be highly efficient synthetic scaffolds in cyclometallation chemistry. Their design has allowed for regioselective synthesis of metallacycles forming either the *endo*- or *exo* product depending on the Schiff base and reaction conditions. Albert *et. al.*[6] reported cyclopalladation of Schiff-bases and showed that *exo*-palladacycles (**2.6** and **2.7**) can be obtained if the

ortho-positions of the benzal-ring are blocked by substituents such as halogen atoms (**Scheme 2.2**). However, when the ortho-substituents are replaced with hydrogen atoms, only *endo*-derivatives (**2.4** and **2.5**) were formed, which is consistent with reports of the strong tendency of Schiff bases to form *endo*-metallacycles. [7–9]

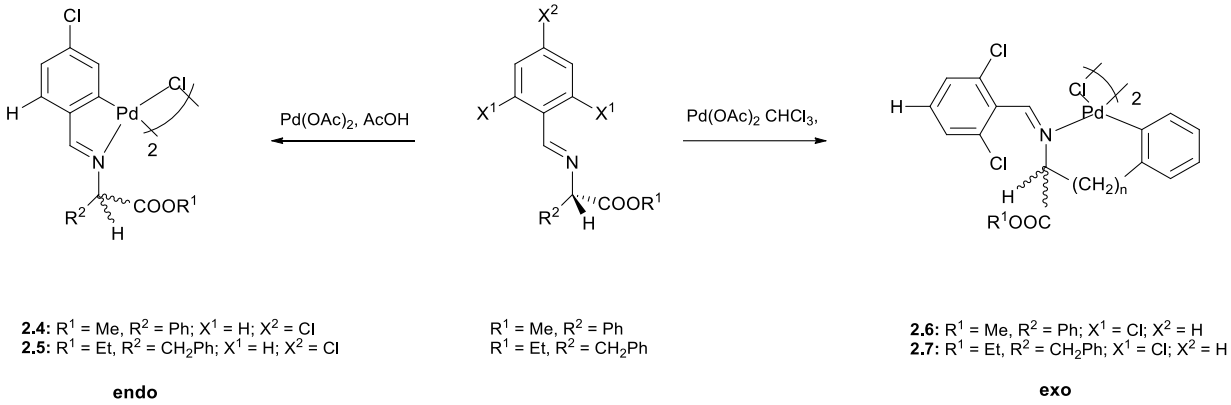

Scheme 2.2: Cyclopalladation of Schiff-base ligand via C-H bond activation forming *endo*- and *exo* palladacycles selectively. [6–9]

In this current study we report on the synthesis and characterization for a range of cyclopalladated complexes bearing different ortho-substituents on the cyclometallated ring derived from monofunctional Schiff-base ligands and subsequently the cleavage of these complexes with tertiary phosphines which differ in both steric and electronic effects.

2.2 Results and Discussion

2.2.1 Synthesis and characterization of monofunctional Schiff base imine ligands L1-L5.

A series of known monofunctional ligands were prepared by Schiff base condensation of 2,6-diisopropylaniline with various aromatic aldehydes bearing different ortho-substituents in a 1:1 ratio with the removal of water using anhydrous magnesium sulphate as shown in **Scheme 2.3.**

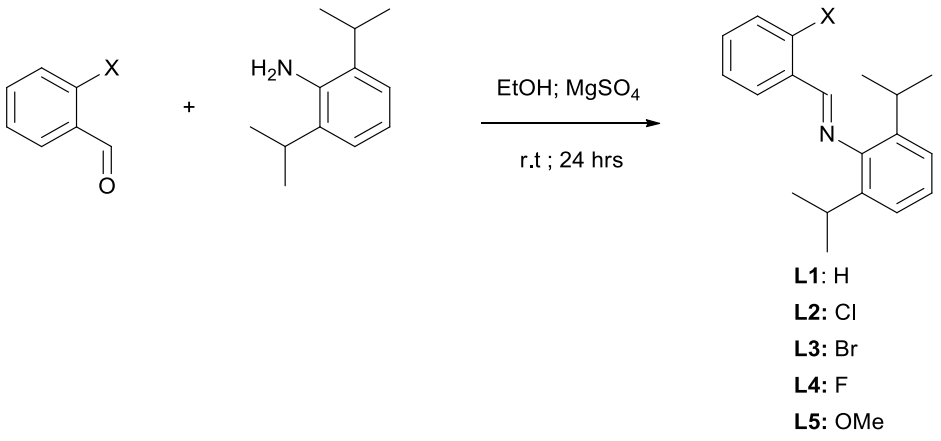

Scheme 2.3: Synthetic route to monofunctional Schiff base ligands, **L1-L5**.

All ligands were isolated in high yields (83 – 94%) as bright yellow crystals except for **L3** which was a pale yellow powder. All ligands were soluble in most polar organic solvents at room temperature. The ligands were also found to be relatively stable in both the solid state and in solution. Ligands **L1** [10,11], **L2-L3** [10,12], **L4** [13] and **L5** [14], were previously reported and fully characterized.

The choice of 2,6-diisopropylaniline in the architecture of the ligand is important since this moiety is sterically hindered due to the two isopropyl substituents (**Figure 2.2a**). The latter serves to incorporate steric bulkiness which could impact on the catalytic behaviour of complexes prepared from these ligand systems.[15,16] Additionally, bulky groups might decrease the rate of catalyst deactivation which could lead to higher catalytic activities.[17] A variety of aldehydes bearing different ortho-substituents ranging from electron withdrawing- to electron donating groups were also used to probe the effect of electronic properties for the ensuing cationic complexes as potentially active catalysts.

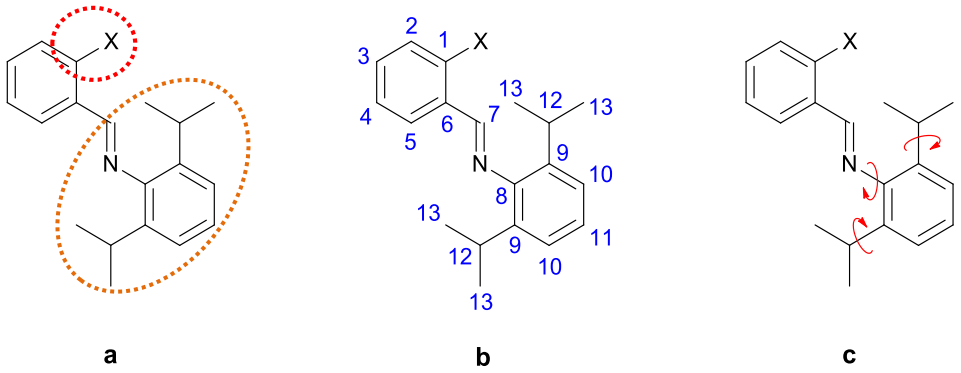

Figure 2.2: (a) Electronic- and steric group; **(b)** Labelled imine ligand with numbering for NMR spectra; **(c)** Free rotation of 2,6 diisopropylaniline moiety.

2.2.1.1 FT-IR- and ^{1}H NMR spectroscopy

The FT-IR spectra of all ligands showed a strong absorption in the range of 1636-1623 cm^{-1} unambiguously assignable to the $\nu_{C=N}$ absorption which clearly signifies that the condensation had occurred. The imine proton resonance (**H^{7}, Figure 2.2b**) in the ^{1}H NMR spectra of the ligands (**L1-L5**) was observed as a singlet in the downfield region of δ 8.66-8.20 ppm (**Table 2.1**). Furthermore, the equivalence of the methyl groups of the isopropyl moiety were observed as a doublet and is the most upfield signal integrating for a total of twelve protons. Hence, there exist free rotation along the N-C bond (**N-C^{8}**) and C-C bond (**C^{9}-C^{12}**) as shown in **Figure 2.2c**.

The nature of the imine proton resonance and the $\nu_{C=N}$ absorption are important since it reveals information regarding the arrangement of the coordination sphere around the metal centre for the impending palladium complexes that are generated from these ligands. Therefore, the relative position in wavenumber of the $\nu_{C=N}$ absorption and the splitting pattern, relative chemical shift and the broadness of the imine resonance are closely monitored throughout this project.

Table 2.1: ^{1}H NMR spectral data of monofunctional Schiff base ligands, **L1-L5.** [a]

Ligand	C=N***H***	Aromatic region	Aliphatic region		
			OC***H₃***	$(CH_3)_2C$***H***	$CH(C$***H₃***$)_2$
L1	δ 8.20 (s, 1H, H^7)	δ 7.96-7.88 (comp., 2H, $H^{1,5}$), δ 7.57-7.47 (comp, 3H, $H^{2,3,4}$), δ 7.20-7.07 (comp., 3H, $H^{10,11}$)		δ 2.98 (sept., $^3J_{H-H}$ = 6.9 Hz, 2H, H^{12})	δ 1.18 (d, $^3J_{H-H}$ = 6.9 Hz, 12H, H^{13})
L2	δ 8.66 (s, 1H, H^7)	δ 8.30-8.24 (m, 1H, H^2), δ 7.49-7.37 (comp, 3H, $H^{3,4,5}$), δ 7.21-7.06 (comp., 3H, $H^{10,11}$)		δ 2.97 (sept., $^3J_{H-H}$ = 7.1 Hz, 2H, H^{12})	δ 1.20 (d, $^3J_{H-H}$ = 6.9 Hz, 12H, H^{13})
L3	δ 8.58 (s, 1H, H^7)	δ 8.26 (dd, $^3J_{H-H}$ = 7.7 Hz, $^4J_{H-H}$ = 1.8 Hz, 1H, H^2), δ 7.65 (dd, $^3J_{H-H}$ = 7.9, $^4J_{H-H}$ = 1.3 Hz, 1H, H^5), δ 7.46 (t, $^3J_{H-H}$ = 7.3 Hz, 1H, H^3), δ 7.36 (td, $^3J_{H-H}$ = 7.9 Hz, $^4J_{H-H}$ = 1.8 Hz, 1H, H^4), δ 7.22-7.08 (comp., 3H, $H^{10,11}$)		δ 2.98 (sept., $^3J_{H-H}$ = 7.0 Hz, 2H, H^{12})	δ 1.20 (d, $^3J_{H-H}$ = 6.9 Hz, 12H, H^{13})
L4	δ 8.52 (s, 1H, H^7)	δ 8.23 (td, $^3J_{H-H}$ = 5.7 Hz, $^4J_{H-H}$ = 1.9 Hz, 1H, H^2), δ 7.54-7.45 (m, 1H, H^5), δ 7.29 (t, $^3J_{H-H}$ = 7.4 Hz, 1H, H^3), δ 7.20-7.07 (comp., 4H, $H^{4,10,11}$)		δ 2.96 (sept., $^3J_{H-H}$ = 6.9 Hz, 2H, H^{12})	δ 1.18 (d, $^3J_{H-H}$ = 7.0 Hz, 12H, H^{13})
L5	δ 8.64 (s, 1H, H^7)	δ 8.20 (dd, $^3J_{H-H}$ = 7.7 Hz, $^4J_{H-H}$ = 1.8 Hz, 1H, H^2), δ 7.48 (td, $^3J_{H-H}$ = 8.3 Hz, $^4J_{H-H}$ = 1.8 Hz, 1H, H^5), δ 7.19-7.05 (comp., 4H, $H^{3,10,11}$), δ 6.98 (d, $^3J_{H-H}$ = 8.5 Hz, 1H, H^4)	δ 3.87 (s, 3H, *o*-methoxy Me)	δ 3.00 (sept., $^3J_{H-H}$ = 7.0 Hz, 2H, H^{12})	δ 1.18 (d, $^3J_{H-H}$ = 6.9 Hz, 12H, H^{13})

[a] Spectra recorded in $CDCl_3$ at 298 K; chemical shifts reported as δ ppm values, referenced relative to the residual $CDCl_3$ resonance; superscripts denote protons as per numbering scheme **Figure 2.2b**; s = singlet, d = doublet, t = triplet, dd = doublet of doublets, td = triplet of doublets, sept. = septet, m = multiplet (denotes complex pattern for a single proton resonance), comp. = complex (denotes complex pattern of overlapping proton resonances)

2.2.2 Synthesis and characterization of μ-Cl binuclear palladacycles, C1-C5.

The syntheses of μ-Cl binuclear palladacycle complexes, **C1-C5**, were accomplished by the reaction of the palladium salt, bis(acetonitrile) palladium(II)chloride, in the presence of two equivalents sodium acetate using dichloromethane as solvent choice (**Scheme 2.4**). The cyclopalladation of the Schiff-base ligands proceeded *via* electrophilic C_{Ar}-H bond activation forming a five membered chelate ring. The presence of a base is important in facilitating palladacycle formation. The latter serves to remove the proton ortho to the imine functionality on the aryl ring of the Schiff-base ligand which promotes cyclopalladation.

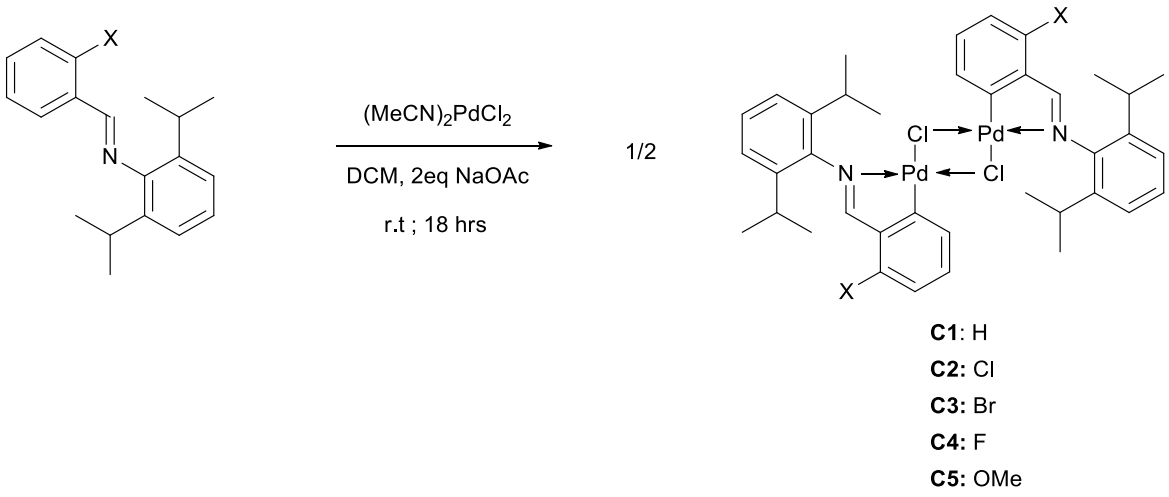

Scheme 2.4: Synthetic route to μ-Cl binuclear palladacycles, **C1-C5**.

The μ-Cl binuclear palladacycle complexes (**C1-C2, C4-C5**) were isolated in good yields (71 – 76%) as air-stable solids, however a yield of 59% was obtained for complex **C3**. All complexes displayed some degree of solubility in chlorinated organic solvents with only **C2** and in particular **C3** being sparingly soluble in these solvents. The solubility of these complexes were greatly influenced by the nature of the ortho-substituent on the cyclopalladated aromatic ring with the larger halide substituent decreasing the solubility of **C3**. The palladacycle complexes were also found to be relatively stable in solution since the formation of palladium black only formed gradually over time. Complexes **C1**[10], **C2**[12] and **C3**[10] were previously reported and fully characterized, whereas **C4** and **C5** were novel.

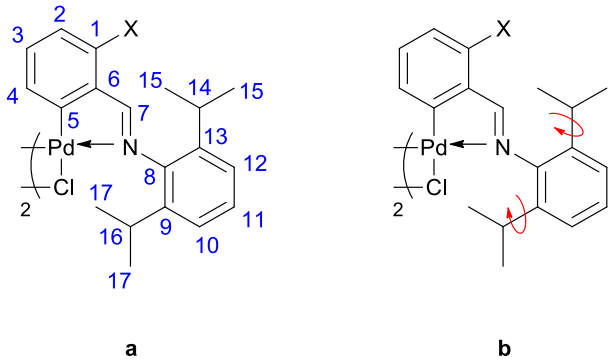

Figure 2.3: (**a**) μ-Cl Binuclear palladacycle with numbering for NMR data; (**b**) Free rotation about the C-C bond of the isopropyl moiety.

The complexes **C4** and **C5** were fully characterized using various analytical techniques. A summary of the general characterization data for complexes **C1-C5** is shown in **Table 2.2 - Table 2.4.**

2.2.2.1 FT-IR spectroscopy and thermal stability

The FT-IR spectra of μ-Cl binuclear palladacycles provided evidence of a successful reaction. The coordination of the imine nitrogen to the palladium metal centre was confirmed by a bathochromic (red) shift (37 cm^{-1} for **C1**, 44 cm^{-1} for **C2**, 39 cm^{-1} for **C3**, 26 cm^{-1} for **C4**, 44 cm^{-1} for **C5**) of the $\nu_{C=N}$ absorption which appear in the region 1605-1581 cm^{-1} in comparison to that of the free imine ligands, **L1-L5** (**Table 2.2**). This resulted in a decrease in the imine double-bond character of the imine functionality upon cyclopalladation.[18] It should be noted that coordination through the imine double-bond in a η^2 fashion would have resulted in a larger shift.[18,19]

Decomposition temperatures for **C1-C5** were significantly higher than the melting points determined for the corresponding ligands **L1-L5**, which shows the increased stability of the μ-Cl binuclear palladacycles.

Table 2.2: IR spectral data and decomposition temperatures for μ-Cl binuclear palladacycle complexes (**C1-C5**) and Schiff base ligands (**L1-L5**).

μ-Cl comp.	Decomposition temperature [a] (°C)	FT-IR [b] ($\nu_{C=N}$, cm^{-1})	Ligand	FT-IR [b] ($\nu_{C=N}$, cm^{-1})
C1	245-247	1599	**L1**	1636
C2	161-163	1585	**L2**	1629
C3	200-203	1584	**L3**	1623
C4	188-190	1605	**L4**	1631
C5	>250	1581	**L5**	1625

[a] Decomposition temperatures reported are uncorrected. No melting prior to decomposition was observed. [b] Recorded as neat spectra using a ZnSe ATR accessory.

2.2.2.2 ^{1}H- and ^{13}C NMR spectroscopy

The ^{1}H- and ^{13}C{^{1}H} NMR spectra of the μ-Cl binuclear palladacycles, **C1-C5**, confirmed the formation of a five-membered *endo*cyclic ring. The ^{1}H NMR spectra of **C1-C5** showed an upfield shift of the imine proton resonance (**H^{7}**, **Figure 2.3a**) in the range of δ 8.13-7.74 ppm (**Table 2.4**) relative to that of the imine proton resonance of the Schiff-base ligands. The observed upfield shift of δ 0.59-0.46 ppm with respect to the Schiff-base ligands is indicative of the imine moiety coordinating through the nitrogen lone pair to the palladium metal centre rather than through the π-electrons of the imine double-bond. In fact, if coordination occurred through the π-electrons of the imine double-bond, a larger chemical shift (2 ppm) would have been observed.[20] In the aromatic region, the disappearance of the *ortho*-proton resonance (**H^{5}**, **Figure 2.3a**) and the appearance of a series of aromatic resonances integrating for a total of fourteen protons (as in the case of **C1**) and twelve protons (as in the case of **C2-C5**) respectively were observed. This was attributed to the fact that cyclopalladation took place *via* electrophilic C-H bond activation of the aromatic ring [20] forming an *endo*-palladacycle and not *via* C-H bond activation of the isopropyl moieties which would have yielded *exo*-palladacycles (**Figure 2.4**).

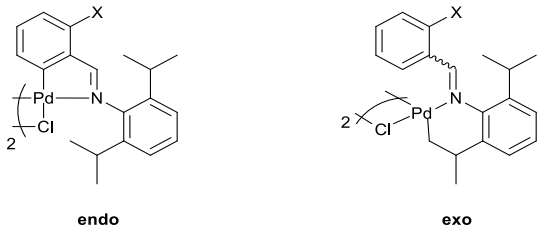

Figure 2.4: *Endo*- and *exo* μ-Cl binuclear palladacycles

Additionally, ^{1}H NMR spectral analysis also reveals crucial information regarding the rotation of the 2,6-diisopropylaniline moiety for the μ-Cl binuclear palladacycles. Upon cyclopalladation, the rotation along the N-C bond (**N-C^{8}**) was restricted (**Figure 2.3a**) and as a consequence, the symmetry of the 2,6 diisopropylaniline moiety that is present for the free ligands is absent for their respective complexes. The free rotation along the C-C bonds (**C^{13}-C^{14}**; **C^{9}-C^{16}**) still remained intact (**Figure 2.3b**). In the aliphatic region, the methine proton resonances (**H^{14,16}**) shifted downfield relative to resonances of the free imine ligands and appear in the region δ 3.60-3.39 ppm. Upon cyclopalladation, the signal no longer appears as a septet but rather as a multiplet (two overlapping septet resonances) revealing the chemically inequivalence of the methine protons. A significant change for the methyl resonances of the isopropyl moiety (**H^{15,17}**) was observed. The doublet, which integrates for twelve protons in the ligands, appeared as two distinct doublets integrating for twelve protons each for the μ-Cl binuclear palladacycles, revealing that **H^{15}** and **H^{17}** are chemically inequivalent (**Figure 2.5**). Hence, based on the observed spectra, rotation only occurred along the C-C bonds (**C^{13}-C^{14}**;**C^{9}-C^{16}**) in the 2,6 diisopropylaniline moiety.

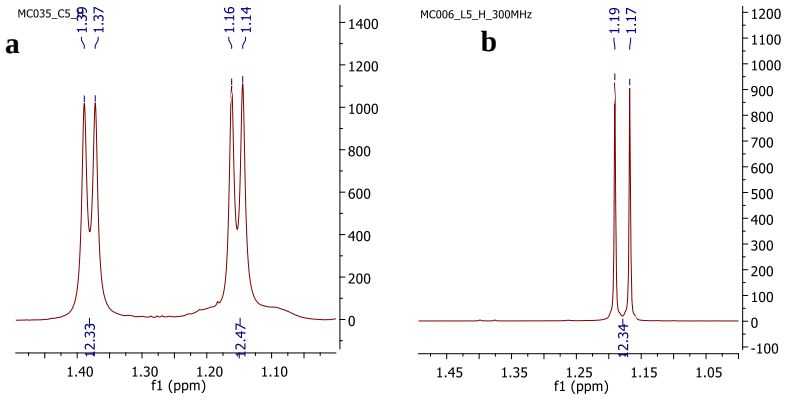

Figure 2.5: ^{1}H NMR spectrum showing the methyl resonances of the isopropyl moiety for (**a**) μ-Cl complex **C5**; (**b**) ligand **L5** in the region δ 1.50-1.00 ppm.

The $^{13}C\{^{1}H\}$ NMR spectra of previously reported μ-Cl binuclear palladacycles (**C1**, **C2** and **C3**) and novel μ-Cl binuclear palladacycles (**C4** and **C5**) showed the expected number of resonances. Coordination of the imine nitrogen to the palladium metal centre was confirmed by the downfield shifts of the imine carbon resonance (**C**[7]) in the region of δ 176.2-171.5 ppm in comparison to that of the imine carbon resonance of the Schiff-base ligands (**Table 2.3**).

Table 2.3: ^{13}C $\{^{1}H\}$ NMR spectral data for μ-Cl binuclear palladacycles (**C1-C5**) and Schiff-base ligands **(L1-L5**) showing the imine carbon resonance.

μ-Cl complex	**^{13}C $\{^{1}H\}$ NMR [a] ($\delta_{C=N}$, ppm)**	**Ligand**	**^{13}C $\{^{1}H\}$ NMR [a] ($\delta_{C=N}$, ppm)**
C1	176.2 [b]	**L1**	160.2 [b]
C2	174.8 [b]	**L2**	159.2 [b]
C3	174.2 [b]	**L3**	161.4 [b]
C4	171.5	**L4**	155.5 [c]
C5	173.2	**L5**	159.4 [d]

[a] Spectra recorded in $CDCl_3$ at 298 K; chemical shifts reported as δ ppm values, referenced relative to the residual $CDCl_3$ resonance. [b] Data obtained from reference. [12] [c] Data obtained from reference. [13] [d] Data obtained from reference. [14]

2.2.2.3 Mass spectrometry and elemental analysis

ESI-MS recorded in the positive ion mode, and elemental analysis were consistent with the proposed μ-Cl binuclear palladacycle structures. The isotopic pattern observed for the clusters was attributed to the presence of numerous palladium, nitrogen, chlorine and in the case of **C4**, fluorine isotopes.[21] The base peaks for complexes **C4** and **C5** at 429.1 *m/z* and 441.1 *m/z* respectively, correspond to the $[(m/2)\text{-Cl+MeCN}]^{2+}$ fragment ion. The exchange of ligands with molecules of solvent used in the analysis such as the observed chloride/acetonitrile exchange is common and is often observed in ESI-MS.[22] Furthermore, the fragments at 388.1 amu (**C4**) and 400.1 amu (**C5**) can be assigned to the $[(m/2)\text{-Cl}]^{2+}$ fragment, resulting from the loss of the acetonitrile ligand. Calculated isotopic clusters[23] for each assigned fragment coincide exactly with the experimentally observed isotopic fragments (**Figure 2.6**)

Further characterization of **C4** and **C5** by elemental analysis confirm product formation. The analytical found elemental analysis data corresponded well with the calculated values (see section 2.5), hence confirming a structure which consists of two palladium centres bridged by two chloride atoms (**Figure 2.7**).

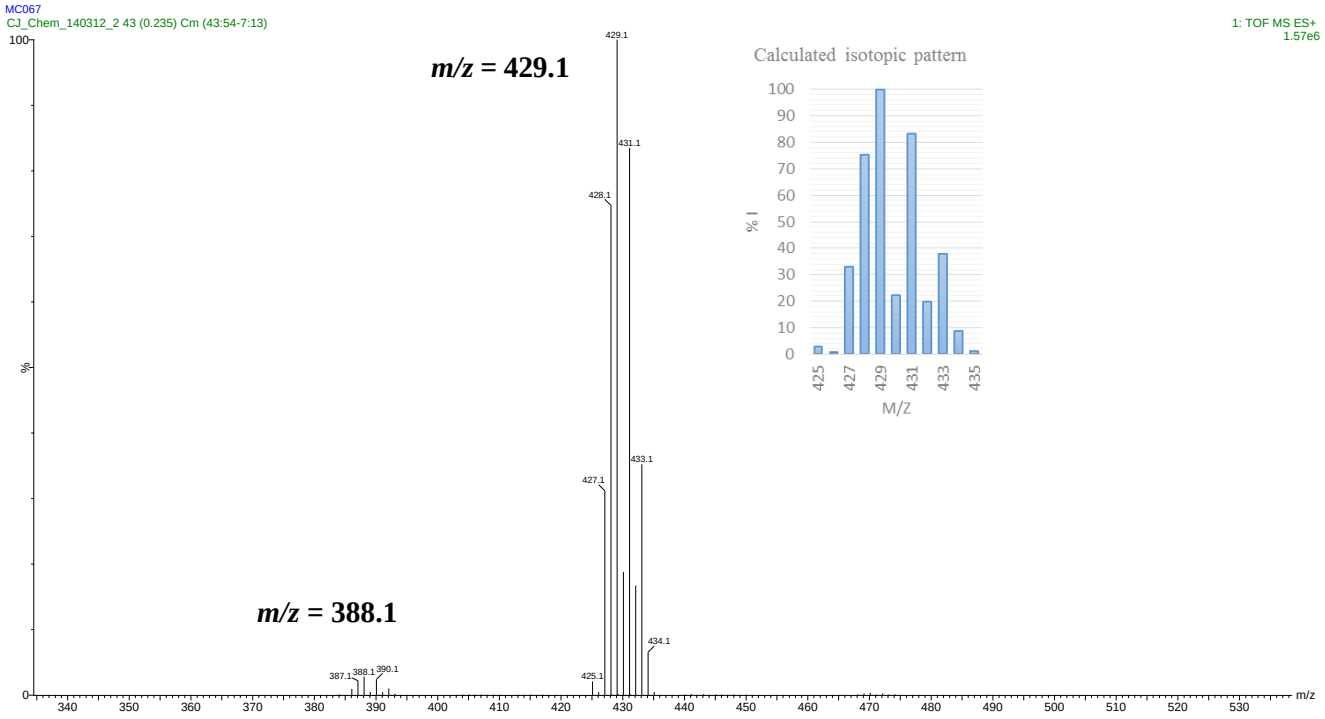

Figure 2.6: ESI-MS spectrum of μ-Cl binuclear palladacycle **C4** recorded in the positive mode. Clusters of peaks centred at 388.1 *m/z* and 429.1 *m/z* correspond to the $[(m/2)\text{-Cl}]^{2+}$ and $[(m/2)\text{-Cl+MeCN}]^{2+}$ fragments respectively. Inset shows calculated isotopic pattern for a specific fragmentation.

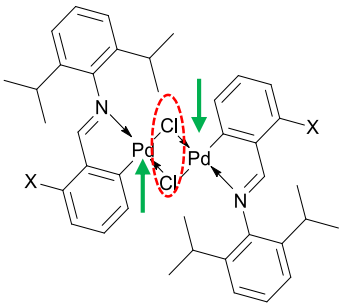

Figure 2.7: Typical μ-Cl palladacycles containing two palladium centres (green arrows) bridged by two chloride atoms (red circle).

Table 2.4: ^{1}H NMR spectral data of μ-Cl binuclear palladacycles, **C1-C5**. [a]

Complex	C=N***H***	Aromatic region	Aliphatic region		
			OC***H*$_3$**	$(CH_3)_2C$***H***	$CH(C$***H*$_3$**$)_2$
C1	δ 7.74 (s, 2H, H^{7})	δ 7.38-7.27 (comp., 4H, $H^{1,2}$), δ 7.24-7.14 (comp, 6H, $H^{10,11,12}$), δ 7.11-7.00 (comp., 4H, $H^{3,4}$)		δ 3.60-3.43 (m, 4H, $H^{14,16}$)	δ 1.39 (d, $^{3}J_{H\text{-}H}$ = 6.6 Hz, 12H, $H^{15,17}$), δ 1.15 (d, $^{3}J_{H\text{-}H}$ = 6.8 Hz, 12H, $H^{15,17}$).
C2	δ 8.13 (s, 2H, H^{7})	δ 7.38-7.27 (m, 2H, H^{2}), δ 7.24-7.15 (comp, 4H, Ar-H), δ 7.10-6.90 (comp., 6H, Ar-H)		δ 3.57-3.39 (m, 4H, $H^{14,16}$)	δ 1.39 (d, $^{3}J_{H\text{-}H}$ = 6.7 Hz, 12H, $H^{15,17}$), δ 1.18 (d, $^{3}J_{H\text{-}H}$ = 6.7 Hz, 12H, $H^{15,17}$)
C3	δ 8.12 (s, 2H, H^{7})	δ 7.33 (t, $^{3}J_{H\text{-}H}$ = 7.8 Hz, 2H, H^{2}), δ 7.23-7.15 (comp, 6H, $H^{10,11,12}$), δ 7.11 (d, $^{3}J_{H\text{-}H}$ = 8.0 Hz, 2H, H^{4}), δ 6.86 (t, $^{3}J_{H\text{-}H}$ = 8.0 Hz, 2H, H^{3})		δ 3.53-3.44 (m, 4H, $H^{14,16}$)	δ 1.39 (d, $^{3}J_{H\text{-}H}$ = 6.7 Hz, 12H, $H^{15,17}$), δ 1.18 (d, $^{3}J_{H\text{-}H}$ = 6.7 Hz, 12H, $H^{15,17}$)
C4	δ 8.02 (s, 2H, H^{7})	δ 7.37-7.28 (m, 2H, H^{2}), δ 7.24-7.15 (m, 4H, Ar-H), δ 7.11-7.00 (m, 2H, Ar-H), δ 6.99-6.91 (m, 2H, H^{4}), δ 6.73 (t, $^{3}J_{H\text{-}H}$ = 9.0 Hz, 2H, H^{3})		δ 3.56-3.40 (m, 4H, $H^{14,16}$)	δ 1.39 (d, $^{3}J_{H\text{-}H}$ = 6.7 Hz, 12H, $H^{15,17}$), δ 1.17 (d, $^{3}J_{H\text{-}H}$ = 6.7 Hz, 12H, $H^{15,17}$)
C5	δ 8.05 (s, 2H, H^{7})	δ 7.29 (t, $^{3}J_{H\text{-}H}$ = 7.7 Hz, 2H, H^{2}), δ 7.17 (d, $^{3}J_{H\text{-}H}$ = 7.5 Hz, 4H, $H^{10,12}$), δ 6.99 (t, $^{3}J_{H\text{-}H}$ = 8.1 Hz, 2H, H^{3}), δ 6.76 (d, $^{3}J_{H\text{-}H}$ = 8.1 Hz, 2H, H^{11}), δ 6.51 (d, $^{3}J_{H\text{-}H}$ = 8.6 Hz, 2H, H^{4})	δ 3.76 (s, 6H, *o*-methoxy Me)	δ 3.59-3.46 (m, 4H, $H^{14,16}$)	δ 1.38 (d, $^{3}J_{H\text{-}H}$ = 6.9 Hz, 12H, $H^{15,17}$), δ 1.15 (d, $^{3}J_{H\text{-}H}$ = 6.9 Hz, 12H, $H^{15,17}$)

[a] Spectra recorded in $CDCl_3$ at 298 K; chemical shifts reported as δ ppm values, referenced relative to the residual $CDCl_3$ resonance; superscripts denote protons as per numbering scheme **Figure 2.3a**; s = singlet, d = doublet, t = triplet, dd = doublet of doublets, td = triplet of doublets, sept. = septet, m = multiplet (denotes complex pattern for a single proton resonance), comp. = complex (denotes complex pattern of overlapping proton resonances)

2.2.3 Cleavage of μ-Cl binuclear palladacycles with various phosphine ligands with different steric and electronic properties.

The neutral mononuclear palladacycle complexes (**C6-C10**; **C16-C20; C26-C30**) were prepared by the reaction between the previously discussed μ-Cl binuclear palladacycles, **C1-C5**, and two molar equivalents of the phosphine ligand (**Scheme 2.5**). It is important to note that in some cases, addition of more than two equivalence could result in non-cyclopalladated complexes where the dissociation of the imine ligand from the palladium centre occurs with simultaneous coordination of two phosphine ligands.

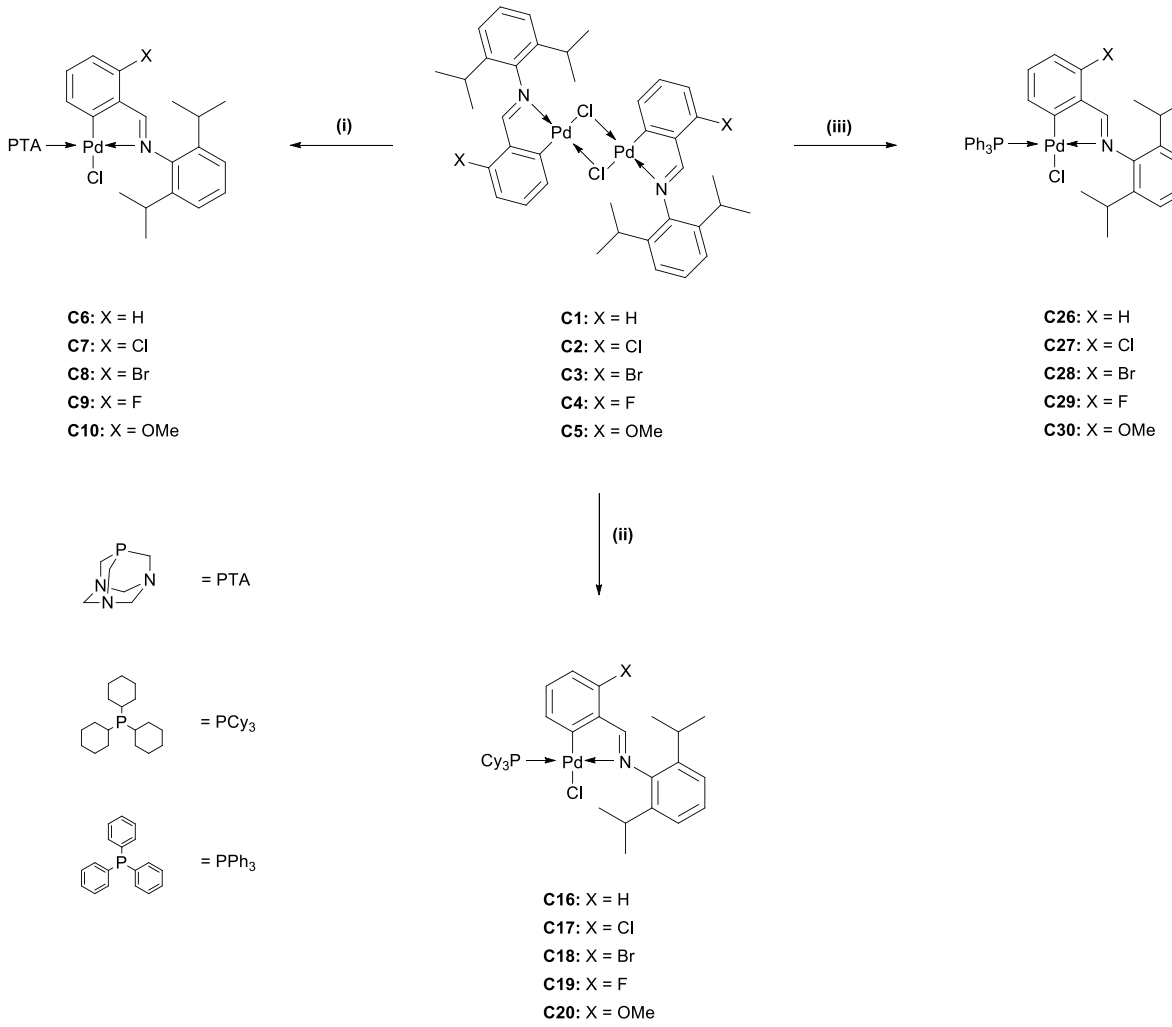

C6: X = H
C7: X = Cl
C8: X = Br
C9: X = F
C10: X = OMe

C1: X = H
C2: X = Cl
C3: X = Br
C4: X = F
C5: X = OMe

C26: X = H
C27: X = Cl
C28: X = Br
C29: X = F
C30: X = OMe

C16: X = H
C17: X = Cl
C18: X = Br
C19: X = F
C20: X = OMe

(**i**) 2eq PTA, DCM, 4h, rt.; (**ii**) 2eq PCy_3, DCM, 4h, rt.; (**iii**) 2eq PPh_3, DCM, 4h, rt.

Scheme 2.5: Cleavage of μ-Cl binuclear palladacycles using various phosphine ligands

All complexes were isolated in moderate to good yields (58 – 91 %) as yellow solids, however a yield of 58 % was obtained for complex **C8**. All analogues displays good solubility in chlorinated organic solvents but were found to be insoluble in alcohols, alkanes and ethers except for complexes **C16-C20,** which were partially soluble in diethyl ether. Although the free phosphine ligands oxidised when exposed to air, their complexes were found to be relatively stable in both solution and the solid state.

The choice to incorporate tertiary phosphine ligands into the architecture of the proposed palladacycle complexes is three-fold: (i) tertiary phosphines can stabilized an exceptionally wide variety of metal complexes,[24,25] (ii) tertiary phosphines impart desirable solubility properties to the resultant metal complexes, (iii) varying both the electronic and steric nature of the phosphine ligand in the complex can enhance activities and selectivities in homogeneous catalysis.[26,27] The selected phosphine ligands (**Figure 2.8, a-c**) exhibit a range of cone angles (Tolman steric parameter, θ_T) ranging between 103°-170° with different electronic properties (Tolman electronic parameter, υ). The cone angle indicates the approximate amount of space that the ligand occupies around the metal centre (**Figure 2.8**, **d**).

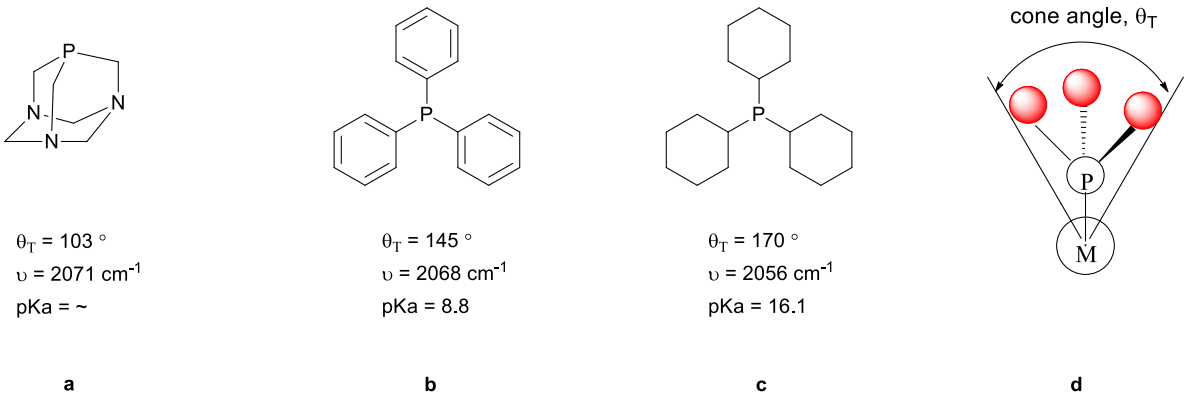

Figure 2.8: Tertiary phosphine ligands having different steric- and electronic properties. pKa measurements of phosphines in acetonitrile relative to pyridine. Tolman electronic parameter (υ) measured in dichloromethane (**a**) phosphatriazaadamantane with θ_T=103° [28–30], υ = 2071cm^{-1} [31]; (**b**) triphenylphosphine with θ_T=145° [32,33], υ = 2068cm^{-1} [33] and pKa=8.8 [34,35]; (**c**) tricyclohexylphosphine with θ_T=170° [32,33], υ = 2056cm^{-1} [33] and pKa=16.1 [35]; (**d**) cone angle representation about metal centre.[33]

Although there is no literature value for the pKa of phosphatriazaadamantane (PTA) in acetonitrile, Darensbourg *et al.* [31] reported a υ(CO) of 2071 cm^{-1} for $Ni(CO)_3PTA$ in dichloromethane which is slightly higher than the υ(CO) of triphenylphosphine (PPh_3). Based on this value, PTA can be assumed to be less donating (lower pKa) than PPh_3.

Neutral mononuclear palladacycle complexes **C6-C10, C16-C20** and **C29-C30** are all novel whereas complexes **C26-C28** were previously reported.[36] A variety of analytical techniques were employed for the characterization of these palladacycles. A summary of the general characterization data is shown in **Table 2.5 - Table 2.10**

2.2.3.1 FT-IR spectroscopy

The FT-IR spectra of the resulting products provided evidence for the formation of the desired neutral mononuclear palladacycles (**C6-C10; C16-C20; C29-C30**). The coordination of the phosphorous atom of the phosphine ligand to the palladium centre was confirmed by a slightly hypsochromic (blue) shift of the $\nu_{C=N}$ absorption bands of the neutral mononuclear palladacycles which appear in the region 1610-1597 cm^{-1} in comparison to their μ-Cl binuclear palladacycle counterparts, **C1-C5** (**Table 2.5**). The difference in the $\nu_{C=N}$ absorption between the neutral mononuclear palladacycles and μ-Cl binuclear palladacycles was attributed to an increase in the σ-donor ability of the 2-electron donor phosphine ligands compared to the previously coordinated chloride ligand which increases the electron density within the *endo*cycle ring leading to an enhancement of the metalloaromaticity of the metallacycle. This results in an increase in the imine double-bond character.[37]

Table 2.5: Spectral data for neutral mononuclear palladacycles and μ-Cl binuclear complexes showing the imine absorbance.

Neutral comp. (PTA)	FT-IR [a] ($\nu_{C=N}$, cm^{-1})	Neutral comp. (PCy_3)	FT-IR [a] ($\nu_{C=N}$, cm^{-1})	Neutral comp. (PPh_3)	FT-IR [a] ($\nu_{C=N}$, cm^{-1})	μ-Cl comp.	FT-IR [a] ($\nu_{C=N}$, cm^{-1})
C6	1606	**C16**	1610	**C26**	1605	**C1**	1599
C7	1600	**C17**	1606	**C27**	1607	**C2**	1585
C8	1597	**C18**	1604	**C28**	1603	**C3**	1584
C9	1606	**C19**	1610	**C29**	1608	**C4**	1605
C10	1597	**C20**	1609	**C30**	1597	**C5**	1581

[a] Recorded as neat spectra using a ZnSe ATR accessory.

2.2.3.2 ^{1}H NMR-, ^{13}C {^{1}H} NMR- and ^{31}P {^{1}H} NMR spectroscopy

^{1}H-, ^{13}C {^{1}H}- and ^{31}P {^{1}H} NMR spectra of the products confirm successful coordination of the phosphines (PTA, PCy_3, PPh_3) to the palladium centre. The ^{1}H NMR spectra of the neutral mononuclear palladacycles (**C6-C10; C16-C20; C26-C30**) showed a downfield shift of the imine proton resonance (**H^{7}**, **Figure 2.9a**) in the range δ 8.62-7.98 ppm (**Table 2.7 - Table 2.9**) in comparison to the μ-Cl binuclear palladacycles, **C1-C5**. This was attributed to an increase in the degree of electron delocalization within the *endo*cycle ring, hence deshielding the imine proton from the effect of the applied magnetic field. The imine proton resonance also appeared as a doublet integrating for one proton which was due to a heteronuclear $^{4}J_{H\text{-}P}$ coupling of the imine proton to the phosphorous atom of the phosphine ligand.[37] This splitting pattern confirms that the *endo*cycle ring is retained. [37–39] This also confirms that the coordination is *via* the phosphorous atom and not the nitrogen atoms in the case of the PTA-based palladacycles, **C6-C10**. The imine proton resonance of the neutral mononuclear palladacycles containing electron withdrawing groups in the same phosphine series appeared more downfield with respect to the imine proton resonance of the unsubstituted analogue.

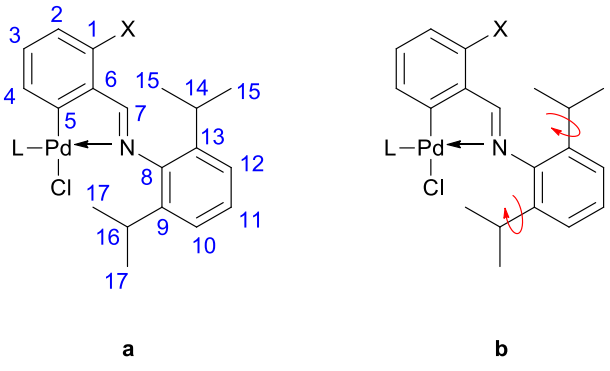

Figure 2.9: (a) Neutral mononuclear palladacycle with numbering for NMR data; (**b**) Free rotation about the C-C bond of the isopropyl moiety. L denotes the different phosphine ligands (L=PTA, PCy_3, PPh_3).

The cleavage of the μ-Cl binuclear palladacycles produced many multiplets with fine coupling-splittings for the PTA-based palladacycles in the aromatic region, particularly for **C6, C7** and **C9**. In addition, the ^{1}H NMR spectra shows a multiplet in the range δ 4.66-4.47 ppm which integrates for a total of twelve protons. This was assigned to the PTA ligand and the complexity of this multiplet is due to the overlapping of NC***H*$_2$**P (singlet) and NC***H*$_2$**N (AB quartet) methylene resonances. The proton atom (**H^4**) situated *ortho* to the metallated carbon atom was found to be the most shielded for the PPh_3-based palladacycles, **C26-C30**. This was attributed to the presence of the phenyl rings of the phosphine ligand coordinating in a *cis* fashion relative to the metallated carbon causing an anisotropic shielding.[37,40] In contrast, proton **H^4** shifted slightly downfield for the PCy_3-based palladacycles, **C16-C20** which are consistent with similar *N*-benzylideneamine complexes reported by Bedford *et al.*[41] Due to the different conformations (chair and boat) of the cyclohexyl rings of the PCy_3 ligand, many broad proton multiplets are observed in the aliphatic region of the ^{1}H NMR spectrum.

Similar to the μ-Cl binuclear palladacycles, the rotation along the N-C bond (**N-C^8**) remains restricted in solution for all neutral mononuclear palladacycles. The free rotation along the C-C bonds (**C^{13}-C^{14}**; **C^9-C^{16}**) remains intact (**Figure 2.9b**). In the aliphatic region, the methine multiplet (overlapping of two septet resonances) in the ^{1}H NMR spectra slightly shifted more upfield in the range δ 3.55-3.09 upon coordination of the phosphine to the palladium centre. The two distinct doublets integrating for a total of six protons respectively were observed for the methyl resonances of the isopropyl moiety (**H^{15}** and **H^{17}**) which resonate in the regions δ 1.39-1.31 ppm and δ 1.25-1.14 ppm compared to the μ-Cl binuclear palladacycles which resonate in the regions δ 1.39-1.38 ppm and 1.18-1.15 ppm. The smaller difference in the chemical shift between the two doublets for the neutral mononuclear palladacycles are due to these complexes being less chemical equivalent relative to their μ-Cl binuclear counterparts as shown in **Figure 2.10a** and **b**. In contrast, the methyl resonance of the isopropyl moiety for complex **C6** shows a very broad singlet instead of two distinct doublets (**Figure 2.10c**). This reveals that there is some degree of rotation which induces fast exchange of the two chemical environments for proton **H^{15}** and **H^{17}**.

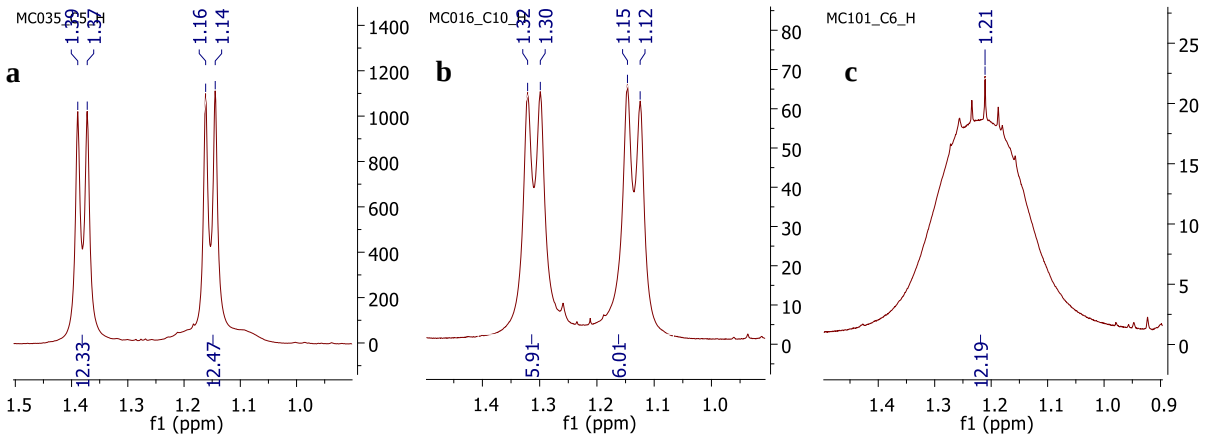

Figure 2.10: ^{1}H NMR spectrum showing the methyl resonances of the isopropyl moiety for (**a**) μ-Cl complex **C5**; (**b**) neutral complex **C10** and (**c**) neutral complex **C6** in the region δ 1.50-0.90 ppm.

The ^{13}C {^{1}H} NMR spectra for all neutral mononuclear palladacycles show the expected number of resonances. The imine carbon resonance (**C**^{7}) for all analogues appears in the downfield region of δ 177.8-170.7 ppm as a doublet due to a heteronuclear $^{3}J_{C\text{-}P}$ to the phosphorous atom of the phosphine ligand (**Table 2.6**). The latter provides further confirmation that the *endo*cycle is retained. Complexes **C6-C10** shows two distinct doublets resonating at δ 73.4 ppm and δ 52.6 ppm respectively. This was attributed to a heteronuclear $^{3}J_{C\text{-}P}$ and $^{1}J_{C\text{-}P}$ coupling of the N***C***H$_2$N and N***C***H$_2$P carbon atom to the phosphorous atom of the coordinating phosphine ligand respectively. Furthermore, three sets of doublets are observed in the aromatic region for complexes **C6-C10** and **C16-C20** due to heteronuclear coupling of the carbon atoms in the ligand backbone to the phosphorous atom of the phosphine ligand. More doublets are observed for complexes **C26-C30** which indicates that carbon atoms in both the ligand backbone and phenyl rings couples to the phosphorous atom.

Table 2.6: ^{13}C {^{1}H} NMR and ^{31}P {^{1}H} NMR spectral data for mononuclear complexes (**C6-C10; C16-C20; C26-C30**).

Neutral complex	^{13}C {^{1}H} NMR [a] ($\delta_{C=N}$, ppm)	^{31}P {^{1}H} NMR [b] (δ_{P}, ppm)
C6	177.1	-47.0
C7	175.7	-47.6
C8	177.7	-47.9
C9	171.6	-47.1
C10	173.7	-48.1
C16	176.2	43.2
C17	174.5	42.8
C18	176.8	42.6
C19	170.7	43.3
C20	172.9	42.2
C26	177.2	42.6
C27	175.6	42.2
C28	177.8	42.0
C29	171.8	42.2
C30	173.9	42.3

[a] Spectra recorded in $CDCl_3$ at 298 K; chemical shifts reported as δ ppm values, referenced relative to the residual $CDCl_3$ resonance. [b] Spectra recorded in $CDCl_3$ at 298 K; chemical shifts externally referenced relative to H_3PO_4.

The ^{31}P {^{1}H} NMR spectra exhibited a sharp singlet due to the phosphorous atom of the phosphine ligand in the region of δ -47-(-49) ppm, δ 42-44 ppm and δ 43-41 ppm for all neutral palladacycle analogues (**Table 2.6**), which is consistent with a *trans* arrangement of the phosphine relative to the imine moiety for PTA-,[38] PCy_3-[39] and PPh_3-based *N*-benzylideneamines palladium complexes[40] respectively. The presence of one phosphorous resonance implies that only one isomer was observed. Moreover, the phosphorous resonance for the complexes shifted downfield in comparison to the free phosphine ligand which provided further evidence of the phosphine ligand coordinating to the palladium centre.

Table 2.7: ^{1}H NMR spectral data of neutral mononuclear palladacycles, **C6-C10**. [a]

Complex	C=N***H***	Aromatic region	Phosphine	Aliphatic region		
				OC***H₃***	$(CH_3)_2C$***H***	$CH(C$***H₃***$)_2$
C6	δ 7.98 (d, $^4J_{H\text{-}P}$ = 7.7 Hz, 1H, H^7)	δ 7.46 (m, 1H, H^1), δ 7.35-7.14 (comp, 6H, Ar-H)	δ 4.66-4.50 (comp., 12H, PTA)		δ 3.29-3.13 (m, 2H, $H^{14,16}$)	δ 1.47-0.95 (comp., 12H, $H^{15,17}$)
C7	δ 8.47 (d, $^4J_{H\text{-}P}$ = 7.6 Hz, 1H, H^7)	δ 7.30-7.11 (comp, 6H, Ar-H)	δ 4.64-4.47 (comp., 12H, PTA)		δ 3.28-3.11 (m, 2H, $H^{14,16}$)	δ 1.32 (d, $^3J_{H\text{-}H}$ = 6.7 Hz, 6H, $H^{15,17}$), δ 1.15 (d, $^3J_{H\text{-}H}$ = 6.9 Hz, 6H, $H^{15,17}$)
C8	δ 8.47 (d, $^4J_{H\text{-}P}$ = 7.4 Hz, 1H, H^7)	δ 7.31 (d, $^3J_{H\text{-}H}$ = 8.0 Hz, 1H, H^2), δ 7.26 (t, $^3J_{H\text{-}H}$ = 7.8 Hz, 1H, H^3), δ 7.20-7.17 (comp., 3H, $H^{10,11,12}$), δ 7.09 (m, 1H, H^4)	δ 4.62-4.51 (comp., 12H, PTA)		δ 3.24-3.15 (m, 2H, $H^{14,16}$)	δ 1.33 (d, $^3J_{H\text{-}H}$ = 6.7 Hz, 6H, $H^{15,17}$), δ 1.16 (d, $^3J_{H\text{-}H}$ = 6.8 Hz, 6H, $H^{15,17}$)
C9	δ 8.31 (d, $^4J_{H\text{-}P}$ = 7.6 Hz, 1H, H^7)	δ 7.35-7.20 (comp., 2H, $H^{3,11}$), δ 7.19-7.14 (comp., 2H, $H^{10,12}$), δ 7.05 (dd, $^3J_{H\text{-}H}$ = 7.4 Hz, $^4J_{H\text{-}H}$ = 5.1 Hz 1H, H^2), δ 6.85 (m, 1H, H^4)	δ 4.65-4.50 (comp., 12H, PTA)		δ 3.26-3.09 (m, 2H, $H^{14,16}$)	δ 1.32 (d, $^3J_{H\text{-}H}$ = 6.8 Hz, 6H, $H^{15,17}$), δ 1.14 (d, $^3J_{H\text{-}H}$ = 6.8 Hz, 6H, $H^{15,17}$)
C10	δ 8.40 (d, $^4J_{H\text{-}P}$ = 7.4 Hz, 1H, H^7)	δ 7.30-7.12 (comp., 4H, $H^{3,10,11,12}$), δ 6.89-6.82 (m, 1H, H^4), δ 6.68 (d, $^3J_{H\text{-}H}$ = 8.0, 1H, H^2)	δ 4.65-4.48 (comp., 12H, PTA)	δ 3.80 (s, 3H, *o*-methoxy Me)	δ 3.31-3.15 (m, 2H, $H^{14,16}$)	δ 1.31 (d, $^3J_{H\text{-}H}$ = 6.5 Hz, 6H, $H^{15,17}$), δ 1.14 (d, $^3J_{H\text{-}H}$ = 6.5 Hz, 6H, $H^{15,17}$)

[a] Spectra recorded in $CDCl_3$ at 298 K; chemical shifts reported as δ ppm values, referenced relative to the residual $CDCl_3$ resonance; superscripts denote protons as per numbering scheme **Figure 2.9a**; s = singlet, d = doublet, t = triplet, dd = doublet of doublets, td = triplet of doublets, sept. = septet, m = multiplet (denotes complex pattern for a single proton resonance), comp. = complex (denotes complex pattern of overlapping proton resonances)

Table 2.8: ^{1}H NMR spectral data of neutral mononuclear palladacycles, **C16-C20.** [a]

Complex	C=N***H***	Aromatic region	Aliphatic region		
			OC***H₃***	$(CH_3)_2C$***H***	Phosphine & CH(C***H₃***)$_2$
C16	δ 8.01 (d, $^4J_{H\text{-}P}$ = 7.0 Hz, 1H, H^7)	δ 7.45 (d, $^3J_{H\text{-}H}$ = 5.9 Hz, 1H, H^1), δ 7.40 (d, $^3J_{H\text{-}H}$ = 6.6 Hz, 1H, H^4), δ 7.24-7.10 (comp., 5H, $H^{2,3,10,11,12}$).		δ 3.42-3.31 (m, 2H, $H^{14,16}$)	δ 2.70-2.56 (comp., 3H, $P(Cy)_3$), δ 2.11-1.99 (comp., 5H, $P(Cy)_3$), δ 1.85-1.60 (comp., 16H, $P(Cy)_3$), δ 1.36-1.19 (comp., 15H, $H^{15,17}$ & $P(Cy)_3$), δ 1.15 (d, $^3J_{H\text{-}H}$ = 6.7 Hz, 6H, $H^{15,17}$).
C17	δ 8.54 (d, $^4J_{H\text{-}P}$ = 6.7 Hz, 1H, H^7)	δ 7.31 (dd, $^3J_{H\text{-}H}$ = 7.5, $^4J_{H\text{-}H}$ = 2.9 Hz, 1H, H^2), δ 7.23 (t, $^3J_{H\text{-}H}$ = 7.6 Hz, 1H, H^{11}), δ 7.17-7.15 (comp., 2H, $H^{10,12}$), δ 7.10 (t, $^3J_{H\text{-}H}$ = 7.8 Hz, 1H, H^3), δ 7.08-7.05 (m, 1H, H^4).		δ 3.39-3.30 (m, 2H, $H^{14,16}$)	δ 2.65-2.55 (comp., 3H, $P(Cy)_3$), δ 2.07-1.98 (comp., 7H, $P(Cy)_3$), δ 1.84-1.74 (comp., 7H, $P(Cy)_3$), δ 1.74-1.61 (comp., 9H, $P(Cy)_3$), δ 1.33 (d, $^3J_{H\text{-}H}$ = 7.0 Hz, 6H, $H^{15,17}$), δ 1.28-1.20 (comp., 9H, $P(Cy)_3$), δ 1.17 (d, $^3J_{H\text{-}H}$ = 7.0 Hz, 6H, $H^{15,17}$).
C18	δ 8.53 (d, $^4J_{H\text{-}P}$ = 6.7 Hz, 1H, H^7)	δ 7.35 (dd, $^3J_{H\text{-}H}$ = 7.6, $^4J_{H\text{-}H}$ = 2.9 Hz, 1H, H^2), δ 7.27-7.20 (comp., 2H, $H^{4,11}$), δ 7.17-7.14 (comp., 2H, $H^{10,12}$), δ 7.00 (t, $^3J_{H\text{-}H}$ = 7.8 Hz, 1H, H^3)		δ 3.38-3.29 (m, 2H, $H^{14,16}$)	δ 2.64-2.53 (comp., 3H, $P(Cy)_3$), δ 2.06-1.98 (comp., 6H, $P(Cy)_3$), δ 1.82-1.74 (comp., 6H, $P(Cy)_3$), δ 1.74-1.59 (comp., 9H, $P(Cy)_3$), δ 1.36-1.13 (comp., 20H, $H^{15,17}$& $P(Cy)_3$).
C19	δ 8.37 (d, $^4J_{H\text{-}P}$ = 6.7 Hz, 1H, H^7)	δ 7.24-7.17 (comp., 3H, Ar-H), δ 7.17-7.13 (comp., 2H, Ar-H), δ 6.80-6.75 (m, 1H, H^{11})		δ 3.36-3.28 (m, 2H, $H^{14,16}$)	δ 2.67-2.57 (comp., 3H, $P(Cy)_3$), δ 2.08-1.99 (comp., 5H, $P(Cy)_3$), δ 1.82-1.74 (comp., 6H, $P(Cy)_3$), δ 1.73-1.61 (comp., 10H, $P(Cy)_3$), δ 1.32 (d, $^3J_{H\text{-}H}$ = 6.8 Hz, 6H, $H^{15,17}$), δ 1.29-1.18 (comp., 10H, $P(Cy)_3$), δ 1.15 (d, $^3J_{H\text{-}H}$ = 6.9 Hz, 6H, $H^{15,17}$).
C20	δ 8.46 (d, $^4J_{H\text{-}P}$ = 7.4 Hz, 1H, H^7)	δ 7.24-7.09 (comp., 4H, $H^{3,10,11,12}$), δ 6.99 (dd, $^3J_{H\text{-}H}$ = 7.8, $^4J_{H\text{-}H}$ = 3.0 Hz, 1H, H^2), δ 6.61 (d, $^4J_{H\text{-}P}$ = 7.6 Hz, 1H, H^4)	δ 3.78 (s, 3H, *o*-methoxy Me)	δ 3.45-3.30 (m, 2H, $H^{14,16}$)	δ 2.70-2.52 (comp., 3H, $P(Cy)_3$), δ 2.12-1.95 (comp., 6H, $P(Cy)_3$), δ 1.87-1.52 (comp., 16H, $P(Cy)_3$), δ 1.38-1.09 (comp., 20H, $P(Cy)_3$ & $H^{15,17}$).

[a] Spectra recorded in $CDCl_3$ at 298 K; chemical shifts reported as δ ppm values, referenced relative to the residual $CDCl_3$ resonance; superscripts denote protons as per numbering scheme **Figure 2.9a**; s = singlet, d = doublet, t = triplet, dd = doublet of doublets, td = triplet of doublets, sept. = septet, m = multiplet (denotes complex pattern for a single proton resonance), comp. = complex (denotes complex pattern of overlapping proton resonances)

Table 2.9: ^{1}H NMR spectral data of neutral mononuclear palladacycles, **C26-C30.** [a]

Complex	C=N***H***	Aromatic region	Aliphatic region		
			OC***H*$_3$**	$(CH_3)_2C$***H***	$CH(C$***H*$_3)_2$**
C26	δ 8.12 (d, $^{4}J_{H\text{-}P}$ = 7.8 Hz, 1H, H^{7})	δ 7.78-7.71 (comp., 6H, PPh_3), δ 7.44-7.40 (comp., 4H, PPh_3), δ 7.38-7.33 (comp., 6H, PPh_3 & H^{1}), δ 7.23-7.13 (comp., 3H, $H^{10,11,12}$), δ 7.01 (t, $^{3}J_{H\text{-}H}$ = 7.5 Hz 1H, H^{2}), δ 6.69 (t, $^{3}J_{H\text{-}H}$ = 7.8 Hz, 1H, H^{3}), δ 6.52-6.48 (m, 1H, H^{4}).		δ 3.50-3.42 (m, 2H, $H^{14,16}$)	δ 1.38 (d, $^{3}J_{H\text{-}H}$ = 6.8 Hz, 6H, $H^{15,17}$), δ 1.22 (d, $^{3}J_{H\text{-}H}$ = 6.9 Hz, 6H, $H^{15,17}$)
C27	δ 8.62 (d, $^{4}J_{H\text{-}P}$ = 8.1 Hz, 1H, H^{7})	δ 7.77-7.69 (comp., 6H, PPh_3), δ 7.46-7.40 (comp., 3H, PPh_3), δ 7.40-7.33 (comp., 6H, PPh_3), δ 7.24-7.19 (m, 1H, H^{11}), δ 7.18-7.15 (comp., 2H, $H^{10,12}$), δ 6.93 (d, $^{3}J_{H\text{-}H}$ = 8.1 Hz, 1H, H^{2}), δ 6.60 (t, $^{3}J_{H\text{-}H}$ = 7.5 Hz, 1H, H^{3}), δ 6.40-6.35 (m, 1H, H^{4}).		δ 3.48-3.41 (m, 2H, $H^{14,16}$)	δ 1.39 (d, $^{3}J_{H\text{-}H}$ = 6.8 Hz, 6H, $H^{15,17}$), δ 1.25 (d, $^{3}J_{H\text{-}H}$ = 6.9 Hz, 6H, $H^{15,17}$)
C28	δ 8.62 (d, $^{4}J_{H\text{-}P}$ = 7.9 Hz, 1H, H^{7})	δ 7.76-7.69 (comp., 6H, PPh_3), δ 7.46-7.40 (comp., 3H, PPh_3), δ 7.39-7.33 (comp., 6H, PPh_3), δ 7.25-7.14 (comp., 3H, $H^{10,11,12}$), δ 7.10 (d, $^{3}J_{H\text{-}H}$ = 7.9 Hz, 1H, H^{2}), δ 6.50 (t, $^{3}J_{H\text{-}H}$ = 7.8 Hz, 1H, H^{3}), δ 6.45-6.38 (m, 1H, H^{4}).		δ 3.52-3.38 (m, 2H, $H^{14,16}$)	δ 1.38 (d, $^{3}J_{H\text{-}H}$ = 6.7 Hz, 6H, $H^{15,17}$), δ 1.24 (d, $^{3}J_{H\text{-}H}$ = 6.8 Hz, 6H, $H^{15,17}$)
C29	δ 8.47 (d, $^{4}J_{H\text{-}P}$ = 8.0 Hz, 1H, H^{7})	δ 7.76-7.71 (comp., 6H, PPh_3), δ 7.45-7.41 (comp., 3H, PPh_3), δ 7.39-7.34 (comp., 6H, PPh_3), δ 7.23-7.18 (m, 1H, H^{11}), δ 7.17-7.14 (comp., 2H, $H^{10,12}$), δ 6.73-6.69 (m, 1H, H^{2}), δ 6.67-6.62 (t, $^{3}J_{H\text{-}H}$ = 8.4 Hz, 1H, H^{3}), δ 6.26-6.22 (m, 1H, H^{4}).		δ 3.47-3.39 (m, 2H, $H^{14,16}$)	δ 1.38 (d, $^{3}J_{H\text{-}H}$ = 6.8 Hz, 6H, $H^{15,17}$), δ 1.24 (d, $^{3}J_{H\text{-}H}$ = 6.8 Hz, 6H, $H^{15,17}$)
C30	δ 8.55 (d, $^{4}J_{H\text{-}P}$ = 7.9 Hz, 1H, H^{7})	δ 7.80-7.67 (comp., 6H, PPh_3), δ 7.47-7.29 (comp., 9H, PPh_3), δ 7.23-7.09 (comp., 3H, $H^{10,11,12}$), δ 6.67 (t, $^{3}J_{H\text{-}H}$ = 8.2 Hz, 1H, H^{3}), δ 6.46 (d, $^{3}J_{H\text{-}H}$ = 8.2 Hz, 1H, H^{2}), δ 6.07 (dd, $^{3}J_{H\text{-}H}$ = 7.1 Hz, $^{4}J_{H\text{-}P}$ = 6.0 Hz, 1H, H^{4}).	δ 3.77 (s, 3H, *o*-methoxy Me)	δ 3.55-3.40 (m, 2H, $H^{14,16}$)	δ 1.37 (d, $^{3}J_{H\text{-}H}$ = 6.8 Hz, 6H, $H^{15,17}$), δ 1.22 (d, $^{3}J_{H\text{-}H}$ = 6.9 Hz, 6H, $H^{15,17}$)

[a] Spectra recorded in $CDCl_3$ at 298 K; chemical shifts reported as δ ppm values, referenced relative to the residual $CDCl_3$ resonance; superscripts denote protons as per numbering scheme **Figure 2.9a**; s = singlet, d = doublet, t = triplet, dd = doublet of doublets, td = triplet of doublets, sept. = septet, m = multiplet (denotes complex pattern for a single proton resonance), comp. = complex (denotes complex pattern of overlapping proton resonances)

2.2.3.3 Mass spectrometry, elemental analysis and thermal stability

ESI-MS recorded in the positive ion mode together with elemental analysis provided further evidence of product formation. The isotopic pattern for clusters observed covering about 10 *m/z* units in the mass spectra of the complexes was attributed to the presence of numerous palladium, nitrogen, chlorine and in the case of **C9**, **C19** and **C29** fluorine isotopes.[21,42] **Table 2.10** reports the base peak observed in the spectra of all complexes, which corresponds to the $[M\text{-}Cl]^+$ fragment ion, unless stated otherwise. The protonated molecular ion, $[M+H]^+$, was only observed for complexes **C6-C10** but these signals were of rather low abundance (~5%) as shown in **Figure 2.11a** (red arrow) for **C10**. Complexes **C6-C10** show an ion cluster which corresponds to the fragment assigned as the $[M\text{-}Cl\text{-}PTA+MeCN]^+$ ion. Moreover, this fragment ion was observed as the base peak for **C7** and **C10.** As mentioned before, the exchange of ligands with solvent molecules such as the observed chloride/acetonitrile exchange is a common phenomenon and is often observed in ESI-MS.[22] The $[M\text{-}Cl]^+$ fragment ion was also observed which correspond to the further loss of the acetonitrile ligand. There are also two minor peaks corresponding to the sequential loss of a PTA ligand from the fragment $[M\text{-}Cl+MeCN]^+$ and $[M\text{-}Cl]^+$ fragments, generating the fragment ions $[M\text{-}Cl\text{-}PTA+MeCN]^+$ and $[M\text{-}Cl\text{-}PTA]^+$ respectively for complexes **C7-C8** and **C10**. Dimerization of **C7** and **C8** shown in **Scheme 2.6** also occurs which shows a minor peak at higher *m/z* (**Figure 2.11b**). The formation of dimeric fragment ions in ESI-MS, specifically for palladium complexes, has been previously reported.[22,43]

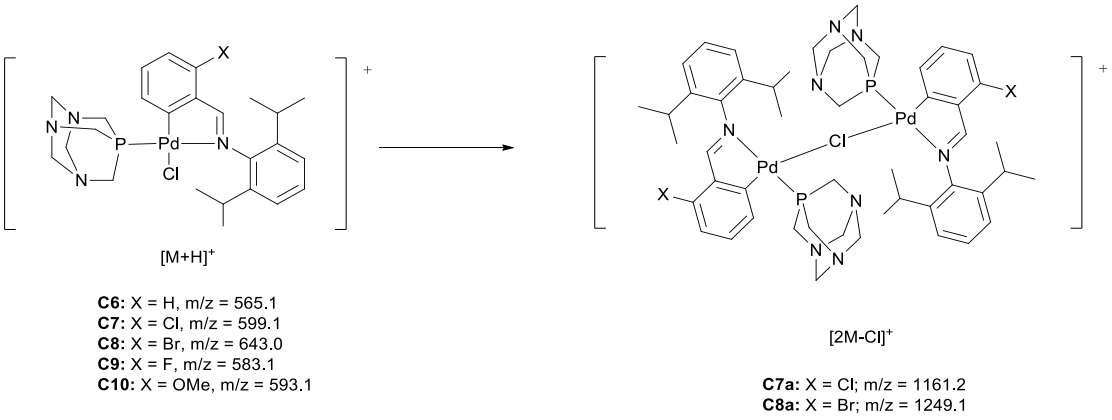

Scheme 2.6: Dimerization of neutral mononuclear palladacycle complexes.

Table 2.10: Mass spectral data and decomposition temperatures for neutral mononuclear palladacycle complexes (**C6-C10; C16-C20; C26-C30**).

Neutral complex	ESI-MS [a] (*m/z*)	Decomposition temperature [c] (°C)
C6	527	210-212
C7	447 [b]	209-211
C8	607	231-233
C9	545	194-197
C10	441 [b]	205-207
C16	650	221-223
C17	730	248-250
C18	730	>250 [d]
C19	668	227-230
C20	680	>250 [d]
C26	632	241-243
C27	668	247-249
C28	712	>250 [d]
C29	650	220-223
C30	662	246-248

ESI-MS recorded in the positive ion mode. [a] Reported ion corresponds to the $[M\text{-}Cl]^+$. [b] Reported ion corresponds to the $[M\text{-}Cl\text{-}PTA+MeCN]^+$. [c] Decomposition temperatures reported are uncorrected. No melting prior to decomposition was observed. [d] No decomposition was observed.

The only peak observed in the mass spectra of the tricyclohexylphosphine and triphenylphosphine analogues corresponded to the $[M\text{-}Cl]^+$ ion fragment with the exception for **C18** and **C20** which showed a minor cluster peak at 491.0 amu and 441.1 amu respectively, corresponding to the $[M\text{-}Cl\text{-}PCy_3+MeCN]^+$ fragment ion. Calculated isotopic clusters[23] for each assigned fragment were in good agreement with the experimentally observed isotopic fragments (**Figure 2.11**).

Further characterization of the neutral mononuclear complexes by elemental analysis were consistent with the calculated values, hence confirming the purity of these complexes. See methods and characterization **section 2.5** for further details. The complexes decomposed in the range of 194-249 °C which is similar to that of the μ-Cl binuclear palladacycles. No melting prior to the decomposition temperatures were observed. In general, the PTA-based palladacycles were thermally less stable than the tricyclohexylphosphine and triphenylphosphine analogues. Complexes which contained the bromo-substituent were thermally more stable in comparison to the other analogues. In the case of complexes **C18**, **C20** and **C28**, no decomposition was observed below 250 °C.

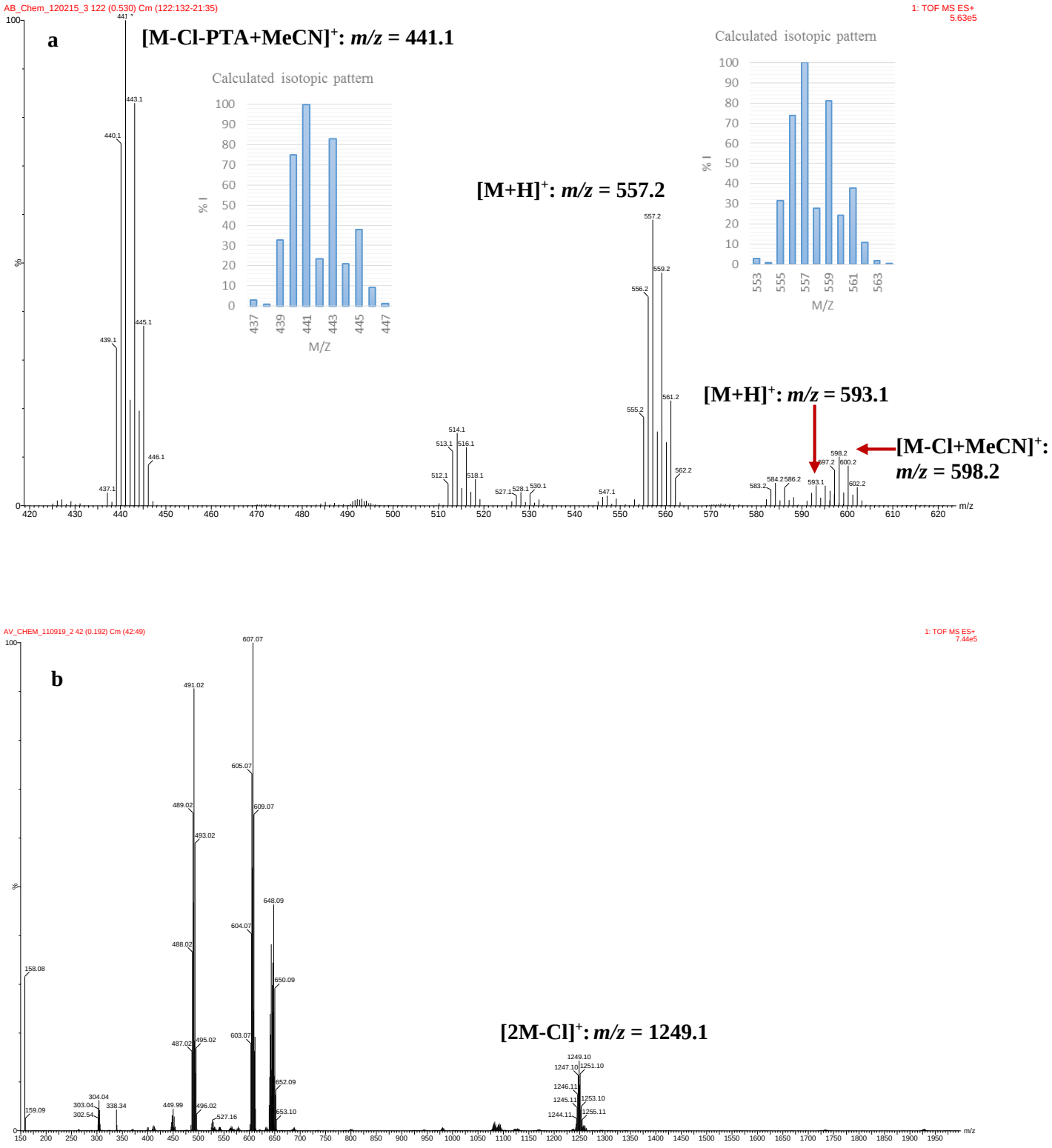

Figure 2.11: ESI-MS spectrum of neutral mononuclear palladacycle **C8** and **C10** recorded in the positive mode. (**a**) Clusters of peaks centred at 441.1 *m/z*, 557.2 *m/z*, 593.1 *m/z* and 598.2 *m/z* correspond to the $[M\text{-}Cl\text{-}PTA+MeCN]^+$, $[M\text{-}Cl]^+$, $[M+H]^+$ and $[M\text{-}Cl+MeCN]^+$ fragments respectively for **C10**. (**b**) Cluster of peaks centred at 1249.1 *m/z* correspond to the $[2M\text{-}Cl]^+$ dimerization fragment for **C8**. Inset shows calculated isotopic pattern for a specific fragmentation.

2.2.3.4 Single crystal diffraction

Suitable single crystals of complexes **C8, C9, C18** and **C30** were isolated from a 1:1 dichloromethane-diethyl ether solution by means of slow evaporation at room temperature which resulted in yellow needle-like crystals. The molecular structures were successfully determined by single crystal X-ray diffraction analyses. All atomic labels are given in the ORTEP pictures depicted in **Figure 2.12-Figure 2.14.** Crystallographic data as well as selected bond lengths, bond angles and torsion angle are shown in **Table 2.11** and **Table 2.12** respectively.

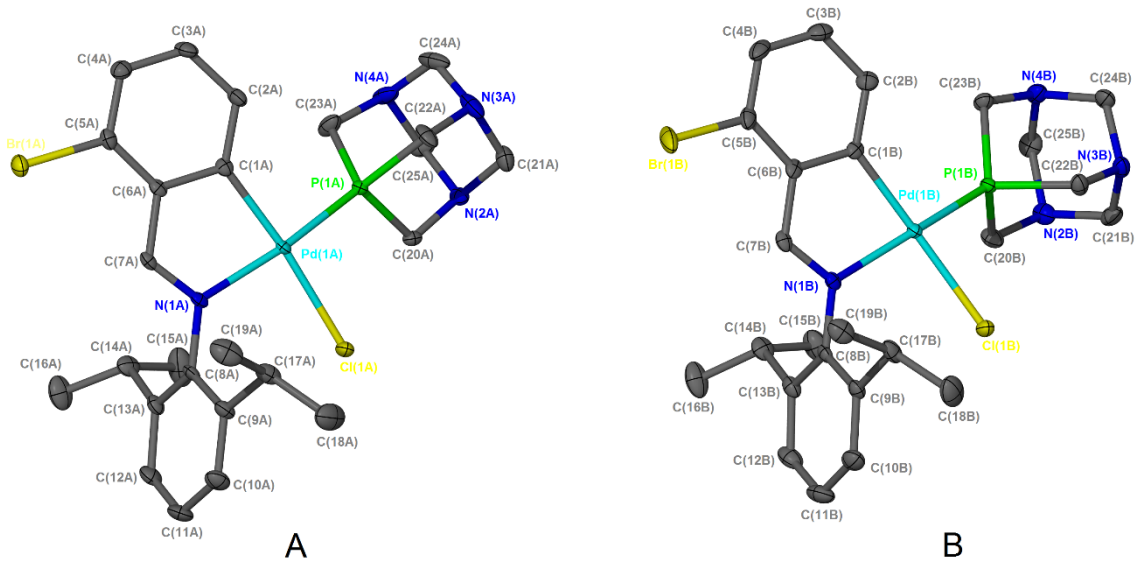

Figure 2.12: Molecular structures of complex **C8** with atomic numbering showing 50% probability ellipsoids. All hydrogen atoms are omitted for clarity. The two independent molecules in the asymmetric unit are labelled with suffix A and B.

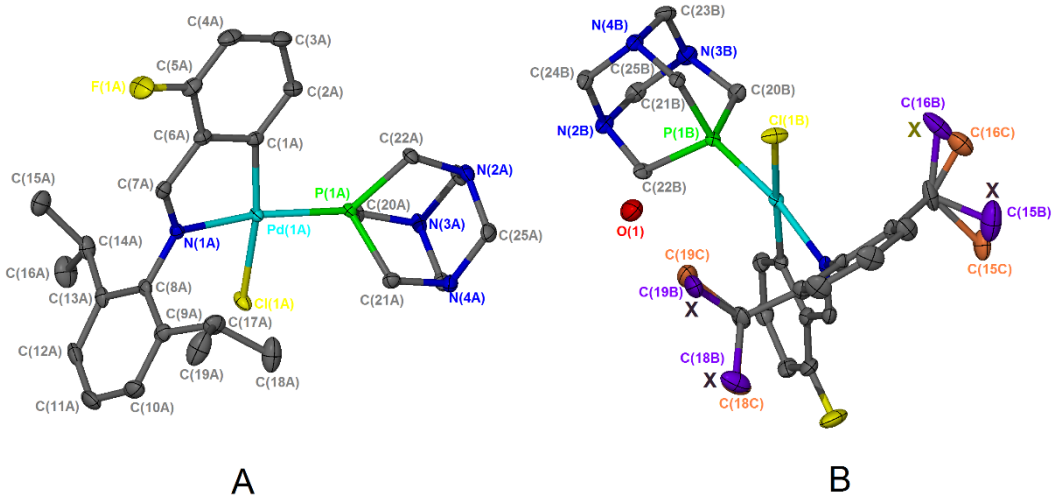

Figure 2.13: Molecular structures of complex **C9** with atomic numbering showing 50% probability ellipsoids. All hydrogen atoms are omitted for clarity. The two independent molecules in the asymmetric unit are labelled with suffix A and B.

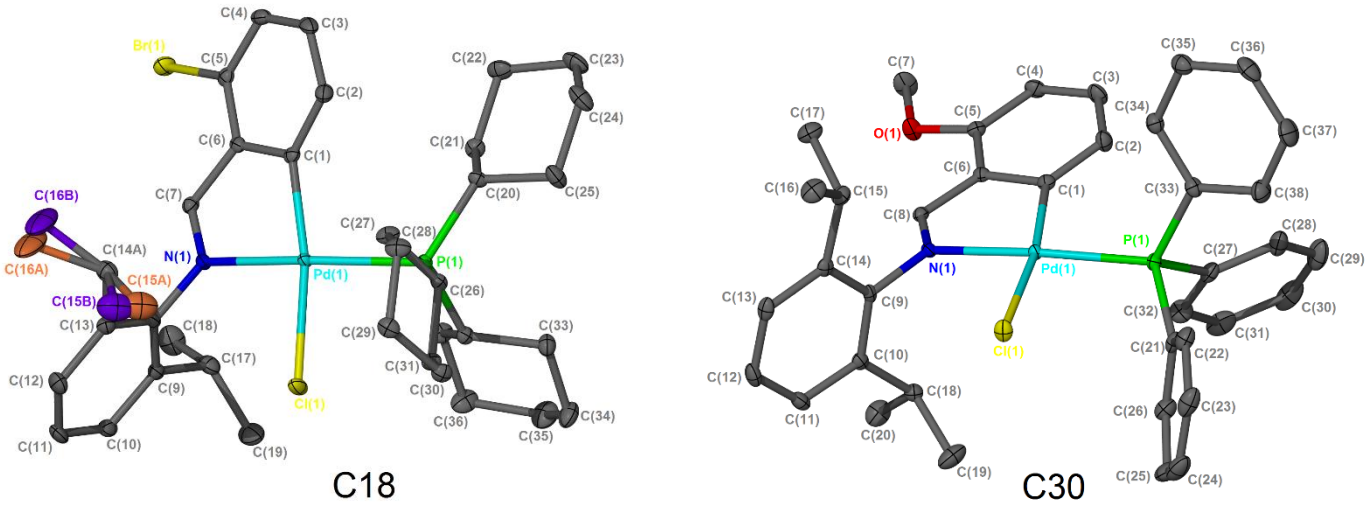

Figure 2.14: Molecular structures of complex **C18** and **C30** with atomic numbering showing 50% probability ellipsoids. All hydrogen atoms are omitted for clarity. For complex **C18**, disorder of the one isopropyl moiety is indicated in orange and purple.

In all complexes, the coordination sphere of palladium consists of a slightly distorted square-planar geometry with the *N*-benzylidene bound bidentate ligand (N^C) as well as the phosphine- and chloride ligand completing the coordination sphere of the palladium metal centre. The phosphine ligand (PTA, PCy_3, PPh_3) is situated *trans* relative to the imine moiety of which the imine nitrogen is included in the five-membered ring forming an *endo*cyclic palladacycle. The distortion of the square-planar geometry is discernibly demonstrated by the bond angles P(1)-Pd-C(1) and N(1)-Pd-C(1) for complexes **C8(B)**, **C9(A)**, **C18** and **C30** which occur in the range 101.20(1)° - 95.68(1)° and 81.55(1)°- 79.85(1)° respectively (**Table 2.12**) due to (C^N) chelation of the ligand to the palladium metal centre.[44] The sum of the angles around the palladium centre for all complexes are relative close to 360°**.**

The steric characteristics of phosphine ligands had a marked effect on the conformation of the five membered *endo*cycle ring of the palladacycle. The more sterically bulky phosphine ligand, tricyclohexylphosphine, in complex **C18** (**Figure 2.14**) appeared to increase the strain on the five-membered ring which resulted in the *endo*cycle being less planar in comparison to the complexes containing less bulkier phosphines, **C8**, **C9**, and **C30**.

The crystal structures of complexes **C8** and **C9** respectively contain two discrete molecules (labelled A and B) with different geometries within the asymmetric unit cell. The structural conformation of these complexes in terms of bond lengths and bond angles are slightly different and have been reported for related palladium complexes.[45] The structural difference for structures **C8(A)** and **C8(B)** is evident from the Cl(1)-Pd-P(1)-C(20) torsion angle (**Figure 2.12**). Structures **C8(A)** and **C8(B)** contain a torsion angles of -20.15(1)° and 60.59(1)° respectively as can be seen from the change in the position of the phosphine ligand relative to the metal centre. In the case of **C9(A)** and **C9(B)** in **Figure 2.13**, two different arrangements of the complex is observed. In addition, the isopropyl moieties of **C9(B)** are disordered due to fluxional motion of the methyl groups (purple and orange ellipsoid) of which carbon atoms C15/C16 and C18/C19 have site-occupancy factors of 0.61(3) and 0.39(4) respectively at position *X*. The disorder of the isopropyl moiety is also observed for complex **C18**.

Unsurprisingly, the cyclohexyl-rings of the phosphine ligand adopts the chair conformation which in fact is the more thermodynamically favoured conformation.

A number of weak non-covalent intermolecular interactions are present in the crystal lattice for complexes **C8**, **C9**, **C18** and **C30**. These include, C-H·····Cl; C-H·····N and C-H·····Br hydrogen bonding interactions with bond lengths and bond angles in the region of 2.8400(3) Å – 2.4400(3) Å and 178.0° - 137.0° respectively. The observed interactions increase the stability of these complexes. **Figure 2.15** shows the unit cell of complex **C9** with the entrapment of more than one water molecule. Only complex **C9(B)** participated in hydrogen bonding with the water molecule. The intermolecular distance of the oxygen atom of the water molecule and the hydrogen atom of the complex (C19B-H19B····O1) was measured to be 2.039 Å with an angle of 121.45°. No hydrogen bonding occurred through the hydrogen atoms of the water molecule.

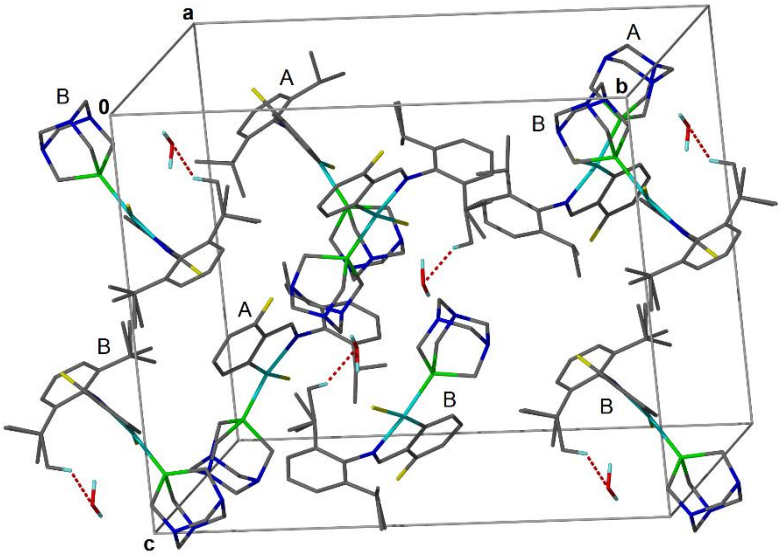

Figure 2.15: Hydrogen bonding indicated as a dashed red line between the water molecules and complex **C9.**

Table 2.11: Crystallographic data and structure refinement parameters for neutral mononuclear palladacycles **C8, C9, C18** and **C30.**

Parameter	Complex			
	C8	**C9**	**C18**	**C30**
Empirical formula	$C_{25}H_{33}BrClN_4PPd$	$C_{25}H_{33}FClN_4PPd.H_2O$	$C_{37}H_{54}BrClNPPd$	$C_{38}H_{39}ClNOPPd$
Mr (g/mol)	642.28	583.85	765.54	698.52
Crystal system	Monoclinic	Monoclinic	Monoclinic	Triclinic
Space group	P 21/c	P21/c	P21/n	P-1
***a* (Å)**	12.1346 (11)	12.2199 (12)	11.7324 (6)	8.845 (2)
***b* (Å)**	23.440 (2)	22.887 (2)	17.0465 (9)	9.157 (2)
***c* (Å)**	18.2523 (16)	18.1584 (17)	18.2408 (10)	21.178 (5)
***α* (deg)**	90	90	90	91.039 (3)
***β* (deg)**	93.544 (1)	95.258 (1)	105.564 (1)	95.483 (3)
***γ* (deg)**	90	90	90	106.516 (3)
Volume (Å^3)	5181.8 (8)	5057.2 (8)	3514.3 (3)	1635.1 (7)
Z	8	8	4	2
D_{calc} (g/cm^3)	1.647	1.534	1.447	1.419
F(000)	2592.0	2395.0	1584.0	720.0
λ (MoK$_a$) (Å)	0.71073	0.71073	0.71073	0.71073
Temperature (K)	100	100	173	100
2*θ* max (deg)	28.220	28.210	28.380	28.240
absorption corrections applied (mm^{-1})	2.445	0.932	1.813	0.729
Goodness-of-fit on F^2	1.023	1.050	1.033	1.036
Final R_1 indices [I>2σ(I)]	0.0241	0.0253	0.0209	0.0236
***wR*$_2$ (all reflections)**	0.0592	0.0624	0.0464	0.0511

Table 2.12: Selected bond lengths (Å), bond angles (°) and torsion angle (°) as determined for neutral mononuclear palladacycles **C8, C9, C18** and **C30.** [a]

	Complex					
	C8 (A)	**C8 (B)**	**C9(A)**	**C9(B)**	**C18**	**C30**
			Bond lengths			
Pd-C1	2.0061(2)	2.0049(2)	2.0069(2)	2.0069(2)	2.0101(1)	2.0167(5)
Pd-N1	2.0934(2)	2.0953(2)	2.0845(2)	2.0971(2)	2.0943(1)	2.0915(5)
Pd-Cl1	2.3700(2)	2.3720(2)	2.3696(2)	2.3567(2)	2.3792(1)	2.3631(6)
Pd-P1	2.2318(2)	2.2409(2)	2.2397(2)	2.2293(2)	2.3002(1)	2.2659(5)
N1-C9	-	-	-	-	-	1.4394(3)
N1-C8	1.4421(1)	1.4399(1)	1.4384(1)	1.4385(1)	1.4334(1)	1.2919(3)
N1-C7	1.2811(1)	1.2845(1)	1.2826(1)	1.2879(1)	1.2815(1)	-
C6-C7	1.4520(1)	1.4558(1)	1.4460(1)	1.4465(1)	1.4451(1)	-
C6-C8	-	-	-	-	-	1.4368(3)
Br1-C5	1.9068(2)	1.9010(2)	-	-	1.9035(1)	-
F1-C5	-	-	1.3622(1)	1.3608(1)	-	-
O1-C5	-	-	-	-	-	1.3633(3)
			Bond angles			
Cl1-Pd-N1	92.46(1)	94.08(1)	92.27(1)	91.18(1)	89.53(1)	90.72(1)
Cl1-Pd-P1	91.01(1)	86.43(1)	86.01(1)	91.42(1)	90.39(1)	92.87(1)
P1-Pd-C1	95.45(1)	100.14(1)	101.20(1)	95.21(1)	100.27(1)	95.68(1)
N1-Pd-C1	81.28(1)	81.36(1)	81.55(1)	81.84(1)	79.85(1)	80.97(1)
			Torsion angles			
Cl(1)-Pd-P(1)-C(20)	-20.16(1)	60.59(1)	51.48(1)	-109.85(1)	-	-

[a] Atoms are labelled as per numbering given in **Figure 2.12 - Figure 2.14.**

2.3 Conclusion

In this chapter, a series of neutral mononuclear palladacycle complexes bearing phosphine ligands with different electronic and steric properties were prepared and fully characterized by a range of analytical techniques. It is evident from the spectroscopy data that the *endocycle* remained intact upon coordination of the phosphine ligand to the metal which coincide with the crystal structures obtained. The incorporation of the bulky 2,6-diisopropylaniline moiety into the architecture of the ligand is responsible for the selective formation of five membered *endo*cycle complexes. Single crystal X-ray diffraction analysis reveals that the geometry around the metal centre is distorted square planar.

2.4 Experimental section

2.4.1 General remarks

All transformations were carried out under an inert atmosphere of dry nitrogen using a dual vacuum/nitrogen line and standard Schlenk techniques, unless specified otherwise. All reagents were acquired from Sigma-Aldrich, Merck and Alfa Aesar and used without further purification. Solvents were obtained from Merck and Kimix and purified by a Pure Solv^{TM} micro solvent purifier fitted with activated alumina columns. In the case of methanol and ethanol, the solvents were dried by distillation over a mixture of magnesium fillings and iodine. Acetonitrile was dried by distillation over phosphorous pentoxide. Reaction progress and product mixtures were monitored by thin-layer chromatography using precoated silica-gel F254. Selected complexes were purified by flash chromatography using an advanced automated Isolera One Biotage flash chromatography unit, equipped with a 200-450 nm variable UV detector. The palladium precursor, bis(acetonitrile) palladium(II)chloride, was prepared by the reaction of palladium(II)chloride with excess acetonitrile under reflux for 3 hours.[46]

2.4.2 Instruments

Melting points determinations were recorded on a Stuart Scientific SMP3 apparatus and are reported as uncorrected. FT-IR analyses were performed on a Thermo Nicolet AVATAR 330 instrument with a smart ATR performer and recorded as neat samples. ^{1}H, ^{13}C and ^{31}P NMR spectra were recorded on Varian VNMRS 300 MHz and Varian Unity Inova 400 MHz spectrometers. The chemical shifts for proton and carbon spectra are internally referenced to the residual deuterated solvents and externally referenced to tetramethyl silane (TMS). Chemical shifts for phosphorous spectra are externally referenced relative to 85% phosphoric acid (H_3PO_4). Elemental analyses were performed on a Thermo Elemental Analyser CHNS-O instrument at the University of Cape Town. ESI-MS analyses, recorded in the positive mode, were recorded on a Waters API Quattro Micro and Water API Q-TOF Ultima instruments by direct injections. Single X-ray diffraction intensity data were collected on a Bruker SMART Apex 2 diffractometer with a CCD area detector[47] using graphite monochromated Mo-Kα radiation (λ = 0.71073 Å). Data collection, reduction and refinement were performed using SMART and SAINT software.[48] Absorption corrections[49] and other systematic errors were accounted for using SADABS.[50] All structures were solved by Direct Methods using SHELXS-97 and refined using SHELXL-97.[51] The program X-Seed [52] was used as a graphical interface for the SHELX program. All non-hydrogen atoms were refined anisotropically. High resolution molecular diagrams were produced using the program POV-Ray.[53]

2.5 Methods and characterization

2.5.1 Synthesis of *μ*-Cl bridge palladacycles

2.5.1.1 $[PdCl(2\text{-}F\text{-}C_6H_3)CH{=}N\{2,6\text{-}^{i}Pr_2\text{-}C_6H_3\}]_2$ (C4)

Ligand **L4** (0.11 g, 0.386 mmol) was added to a stirring solution of $(MeCN)_2PdCl_2$ (0.1 g, 0.386 mmol) and sodium acetate (0.06 g, 0.771 mmol) dissolved in dichloromethane (10 mL) and the resulting reaction mixture was stirred for 24 hours at room temperature. After the allotted time, the solvent was

removed *in vacuo* and the yellow-orange solid residue was redissolved in dichloromethane (20 mL) and filtered through celite. The solvent was removed *in vacuo* from the yellow-orange filtrate and the light orange product (0.12 g, 73 %) was isolated by means of recrystallization from dichloromethane/hexane at room temperature. Melting point: 188-190 °C (decomposes without melting). ^{13}C {^{1}H} NMR (75 MHz, $CDCl_3$, numbering as per **Figure 2.3b**): δ 171.5 (C^{7}), δ 161.5 (Ar-C), δ 158.0 (Ar-C), δ 156.4 (Ar-C), δ 144.4 (Ar-C), δ 141.6 (Ar-C), δ 133.2 (Ar-C), δ 129.7 (Ar-C), δ 128.2 (Ar-C), δ 123.5 (Ar-C), δ 111.5 (d, $J_{C\text{-}F}$ = 18.9 Hz, C^{1}), δ 28.4 ($C^{14,16}$), δ 24.6 ($C^{15,17}$), δ 23.1 ($C^{15,17}$). ESI-MS (+.ve, m/z): 854.1 $[M\text{-}Cl+MeCN]^+$; 813.1 $[M\text{-}Cl]^+$; 429.1 $[(M/2)\text{-}Cl+MeCN]^{2+}$. *Anal. Calc.* for $C_{38}H_{42}Cl_2F_2N_2Pd_2$: C, 53.79; H, 4.99; N, 3.30. *Found:* C, 53.71; H, 5.41; N, 3.07.

2.5.1.2 [PdCl(2-OMe-C_6H_3)CH=N{2,6-$^{i}Pr_2$-C_6H_3}]$_2$ (C5)

μ-Cl Palladacycle **C5** was isolated as a yellow powder (0.13 g, 75 %) using the same synthetic procedure as outlined above for **C4**. Schiff base ligand **L5** was used as the appropriate reactant. Melting point: >250 °C. ^{13}C {^{1}H} NMR (151 MHz, $CDCl_3$, numbering as per **Figure 2.3b**): δ 173.2 (C^{7}), δ 158.5 (Ar-C), δ 157.5 (Ar-C), δ 145.0 (Ar-C), δ 141.9 (Ar-C), δ 134.0 (Ar-C), δ 132.9 (Ar-C), δ 127.7 (Ar-C), δ 126.5 (Ar-C), δ 123.3 (Ar-C), δ 106.9 (Ar-C), δ 55.5 (*o*-methoxy Me), δ 28.3 ($C^{14,16}$), δ 24.7 ($C^{15,17}$), δ 23.2 ($C^{15,17}$). ESI-MS (+.ve, m/z): 836.1 $[M\text{-}Cl]^+$; 441.1 $[(M/2)\text{-}Cl+MeCN]^{2+}$; 400.1 $[(M/2)\text{-}Cl]^{2+}$. *Anal. Calc.* for $C_{40}H_{48}Cl_2N_2O_2Pd_2$: C, 55.06; H, 5.54; N, 3.21. *Found:* C, 54.80; H, 5.96; N, 2.93.

2.5.2 Synthesis of neutral palladacycles with the monodentate phosphine, PTA

2.5.2.1 [Pd(PTA)(C_6H_4)CH=N{2,6-$^{i}Pr_2$-C_6H_3}Cl] (C6)

To a stirring solution of *μ*-Cl binuclear palladacycle complex (**C1**, 0.1 g, 0.123 mmol) in dichloromethane (10 mL) was added phosphatriazaadamantane (0.04 g, 0.246 mmol). The resulting light yellow solution was stirred under an inert atmosphere for 4 hours at room temperature. The solvent was removed *in vacuo* and the yellow residue was then recrystallized from dichloromethane/diethyl ether at room temperature which afforded the product **C6** as a yellow powder (0.13 g, 90 %). Melting point: 210-212 °C (decomposes without melting). ^{13}C {^{1}H} NMR (75 MHz, $CDCl_3$, numbering as per

Figure 2.9b): δ 177.1 (d, $^{3}J_{C\text{-}P}$ = 4.1 Hz, C^{7}), δ 158.2 (d, $^{3}J_{C\text{-}P}$ = 4.3 Hz, Ar-C), δ 148.0 (Ar-C), δ 144.4 (Ar-C), δ 141.0 (Ar-C), δ 136.4 (d, $J_{C\text{-}P}$ = 9.4 Hz, Ar-C), δ 132.1 (d, $J_{C\text{-}P}$ = 4.6 Hz, Ar-C), δ 130.2 (Ar-C), δ 127.4 (Ar-C), δ 125.1 (Ar-C), δ 123.0 (Ar-C), δ 73.4 (d, $^{3}J_{C\text{-}P}$ = 7.1 Hz, N-CH_2-N), δ 52.6 (d, $^{1}J_{C\text{-}P}$ = 16.2 Hz, N-CH_2-P), δ 28.5 ($C^{14,16}$), δ 24.5 ($C^{15,17}$), δ 23.7 ($C^{15,17}$). ^{31}P {^{1}H} NMR (121 MHz, $CDCl_3$): δ -47.0 (s). ESI-MS (+.ve, m/z): 568.2 $[M\text{-}Cl+MeCN]^+$; 565.1 $[M+H]^+$; 527.2 $[M\text{-}Cl]^+$. *Anal. Calc.* for $C_{25}H_{34}ClN_4PPd$: C, 53.29; H, 6.08; N, 9.94. *Found:* C, 53.40; H, 6.08; N, 9.29.

2.5.2.2 [Pd(PTA)(2-Cl-C_6H_3)CH=N{2,6-$^{i}Pr_2$-C_6H_3}Cl] (C7)

Neutral complex **C7** was isolated as yellow crystals (0.12 g, 79 %) using the same synthetic procedure as outlined above for **C6**. μ-Cl binuclear palladacycle complex **C2** and phosphatriazaadamantane were used as the appropriate reactants. Melting point: 209-211 °C (decomposes without melting). ^{13}C {^{1}H} NMR (75 MHz, $CDCl_3$, numbering as per **Figure 2.9b**): δ 175.7 (d, $^{3}J_{C\text{-}P}$ = 4.1 Hz, C^{7}), δ 160.4 (d, $^{3}J_{C\text{-}P}$ = 4.0 Hz, Ar-C), δ 144.6 (Ar-C), δ 144.5 (Ar-C), δ 140.9 (Ar-C), δ 135.0 (d, $J_{C\text{-}P}$ = 9.6 Hz, Ar-C), δ 134.6 (Ar-C), δ 133.4 (d, $J_{C\text{-}P}$ = 4.8 Hz, Ar-C), δ 127.6 (Ar-C), δ 126.0 (Ar-C), δ 123.1 (Ar-C), δ 73.4 (d, $^{3}J_{C\text{-}P}$ = 7.0 Hz, N-CH_2-N), δ 52.5 (d, $^{1}J_{C\text{-}P}$ = 15.9 Hz, N-CH_2-P), δ 28.6 ($C^{14,16}$), δ 24.7 ($C^{15,17}$), δ 23.0 ($C^{15,17}$). ^{31}P {^{1}H} NMR (121 MHz, $CDCl_3$): δ -47.6 (s). ESI-MS (+.ve, m/z): 1161.2 $[2M\text{-}Cl]^+$; 604.1 $[M\text{-}Cl+MeCN]^+$; 599.1 $[M+H]^+$; 563.1 $[M\text{-}Cl]^+$; 447.1 $[M\text{-}Cl\text{-}PTA+MeCN]^+$; 406.0 $[M\text{-}Cl+PTA]^+$. *Anal. Calc.* for $C_{25}H_{33}Cl_2N_4PPd$: C, 50.22; H, 5.56; N, 9.37. *Found:* C, 50.00; H, 5.54; N, 9.49.

2.5.2.3 [Pd(PTA)(2-Br-C_6H_3)CH=N{2,6-$^{i}Pr_2$-C_6H_3}Cl] (C8)

Neutral complex **C8** was isolated a yellow powder (0.09 g, 58 %) using the same synthetic procedure as outlined above for **C6**. μ-Cl binuclear palladacycle complex **C3** and phosphatriazaadamantane were used as the appropriate reactants. Melting point: 231-233 °C (decomposes without melting). ^{13}C {^{1}H} NMR (75 MHz, $CDCl_3$, numbering as per **Figure 2.9b**): δ 177.7 (d, $^{3}J_{C\text{-}P}$ = 4.2 Hz, C^{7}), δ 160.5 (d, $^{3}J_{C\text{-}P}$ = 4.0 Hz, Ar-C), δ 146.0 (Ar-C), δ 144.5 (Ar-C), δ 140.9 (Ar-C), δ 135.6 (d, $J_{C\text{-}P}$ = 9.3 Hz, Ar-C), δ 133.5 (d, $J_{C\text{-}P}$ = 4.9 Hz, Ar-C), δ 129.3 (Ar-C), δ 127.6 (Ar-C), δ 123.6 (Ar-C), δ 123.1 (Ar-C),

δ 73.4 (d, $^{3}J_{C\text{-}P}$ = 7.1 Hz, N-CH_2-N), δ 52.6 (d, $^{1}J_{C\text{-}P}$ = 16.1 Hz, N-CH_2-P), δ 28.6 ($C^{14,16}$), δ 24.7 ($C^{15,17}$), δ 23.0 ($C^{15,17}$). ^{31}P {^{1}H} NMR (162 MHz, $CDCl_3$): δ -47.9 (s). ESI-MS (+.ve, m/z): 1249.1 $[2M\text{-}Cl]^+$; 648.09 $[M\text{-}Cl+MeCN]^+$; 643.0 $[M+H]^+$; 607.07 $[M\text{-}Cl]^+$; 491.02 $[M\text{-}Cl\text{-}PTA+MeCN]^+$; 449.9 $[M\text{-}Cl\text{-}PTA]^+$. *Anal. Calc.* for $C_{25}H_{33}BrClN_4PPd$: C, 46.75; H, 5.18; N, 8.72. *Found:* C, 46.50; H, 6.38; N, 9.14.

2.5.2.4 [Pd(PTA)(2-F-C_6H_3)CH=N{2,6-$^{i}Pr_2$-C_6H_3}Cl] (C9)

Neutral complex **C9** was isolated as yellow crystals (0.13 g, 89 %) using the same synthetic procedure as outlined above for **C6**. *μ*-Cl binuclear palladacycle complex **C4** and phosphatriazaadamantane were used as the appropriate reactants. Melting point: 194-197 °C (decomposes without melting). ^{13}C {^{1}H} NMR (75 MHz, $CDCl_3$, numbering as per **Figure 2.9b**): δ 171.6 (d, $^{3}J_{C\text{-}P}$ = 3.8 Hz, C^7), δ 163.3 (Ar-C), δ 160.4 (Ar-C), δ 159.8 (Ar-C), δ 144.5 (Ar-C), δ 141.0 (Ar-C), δ 134.4 (dd, $J_{C\text{-}P}$ = 7.7, 4.9 Hz, Ar-C), δ 132.1 (dd, $J_{C\text{-}P}$ = 9.2, 3.2 Hz, Ar-C), δ 127.5 (Ar-C), δ 123.1 (Ar-C) δ 112.1 (d, $J_{C\text{-}P}$ = 19.7 Hz, Ar-C), δ 73.4 (d, $^{3}J_{C\text{-}P}$ = 7.0 Hz, N-CH_2-N), δ 52.7 (d, $^{1}J_{C\text{-}P}$ = 16.3 Hz, N-CH_2-P), δ 28.6 ($C^{14,16}$), δ 24.6 ($C^{15,17}$), δ 23.1 ($C^{15,17}$). ^{31}P {^{1}H} NMR (121 MHz, $CDCl_3$): δ -47.1 (s). ESI-MS (+.ve, m/z): 586.2 $[M\text{-}Cl+MeCN]^+$; 583.1 $[M+H]^+$; 545.1 $[M\text{-}Cl]^+$. *Anal. Calc.* for $C_{25}H_{33}ClFN_4PPd$: C, 51.65; H, 5.72; N, 9.64. *Found:* C, 51.60; H, 5.52; N, 9.65.

2.5.2.5 [Pd(PTA)(2-OMe-C_6H_3)CH=N{2,6-$^{i}Pr_2$-C_6H_3}Cl] (C10)

Neutral complex **C10** was isolated as yellow crystals (0.13 g, 87 %) using the same synthetic procedure as outlined above for **C6**. *μ*-Cl binuclear palladacycle complex **C5** and phosphatriazaadamantane were used as the appropriate reactants. Melting point: 205-207 °C (decomposes without melting). ^{13}C {^{1}H} NMR (75 MHz, $CDCl_3$, numbering as per **Figure 2.9b**): δ 173.7 (C^7), δ 160.3 (Ar-C), δ 159.9 (Ar-C), δ 145.0 (Ar-C), δ 141.2 (Ar-C), δ 135.6 (Ar-C), δ 134.1 (Ar-C), δ 128.8 (d, $J_{C\text{-}P}$ = 9.4 Hz, Ar-C), δ 127.1 (Ar-C), δ 122.9 (Ar-C) δ 107.7 (Ar-C), δ 73.4 (d, $^{3}J_{C\text{-}P}$ = 6.8 Hz, N-CH_2-N), δ 55.7 (*o*-methoxy Me), δ 52.6 (d, $^{1}J_{C\text{-}P}$ = 16.0 Hz, N-CH_2-P), δ 28.4 ($C^{14,16}$), δ 24.7 ($C^{15,17}$), δ 23.1 ($C^{15,17}$). ^{31}P {^{1}H} NMR (121 MHz, $CDCl_3$): δ -48.1 (s). ESI-MS (+.ve, m/z): 598.2 $[M\text{-}Cl+MeCN]^+$; 593.1 $[M+H]^+$; 557.2

$[M\text{-}Cl]^+$; 441.1 $[M\text{-}Cl\text{-}PTA+MeCN]^+$; 400.1 $[M\text{-}Cl\text{-}PTA]^+$. *Anal. Calc.* for $C_{26}H_{36}ClN_4OPPd$: C, 52.62; H, 6.11; N, 9.44. *Found:* C, 52.5; H, 6.09; N, 9.46.

2.5.3 Synthesis of neutral palladacycles with the monodentate phosphine, $P(Cy)_3$

2.5.3.1 $[Pd(P(Cy)_3)(C_6H_4)CH{=}N\{2,6\text{-}^iPr_2\text{-}C_6H_3\}Cl]$ (C16)

To a stirring solution of μ-Cl binuclear palladacycle complex (**C1**, 0.1 g, 0.123 mmol) in dichloromethane (10 mL) was added tricyclohexylphosphine (0.07 g, 0.246 mmol). The resulting light yellow solution was stirred under an inert atmosphere for 4 hours at room temperature, after which the solvent was removed *in vacuo*. The yellow solid residue obtained was redissolved in minimal amount of dichloromethane and purified by means of flash chromatography (95:5 hexane: ethyl acetate). The solvent was removed *in vacuo* which afforded the product **C16** as a pale yellow powder (0.11 g, 62 %). Melting point: 221-223 °C (decomposes without melting). $^{13}C\ \{^1H\}$ NMR (75 MHz, $CDCl_3$, numbering as per **Figure 2.9b**): δ 176.2 (d, $^3J_{C\text{-}P}$ = 3.8 Hz, C^7), δ 159.1 (d, $^3J_{C\text{-}P}$ = 2.5 Hz, Ar-C), δ 148.3 (Ar-C), δ 145.7 (Ar-C), δ 141.1 (Ar-C), δ 137.5 (d, $J_{C\text{-}P}$ = 5.1 Hz, Ar-C), δ 130.8 (d, $J_{C\text{-}P}$ = 3.5 Hz, Ar-C), δ 129.2 (Ar-C), δ 126.8 (Ar-C), δ 124.3 (Ar-C), δ 122.8 (Ar-C), δ 34.3 (d, $^1J_{C\text{-}P}$ = 21.7 Hz, $P(Cy)_3$), δ 30.5 ($P(Cy)_3$), δ 28.6 ($P(Cy)_3$), δ 27.8 (d, $^2J_{C\text{-}P}$ = 11.1 Hz, $P(Cy)_3$), δ 26.6 ($C^{14,16}$), δ 24.8 ($C^{15,17}$), δ 23.1 ($C^{15,17}$). $^{31}P\ \{^1H\}$ NMR (120 MHz, $CDCl_3$): δ 43.2 (s). ESI-MS (+.ve, m/z): 650.3 $[M\text{-}Cl]^+$. *Anal. Calc.* for $C_{37}H_{55}ClNPPd$: C, 64.72; H, 8.07; N, 2.04. *Found:* C, 64.38; H, 8.31; N, 1.60.

2.5.3.2 $[Pd(P(Cy)_3)(2\text{-}Cl\text{-}C_6H_3)CH{=}N\{2,6\text{-}^iPr_2\text{-}C_6H_3\}Cl]$ (C17)

Neutral complex **C17** was isolated as yellow crystals (0.13 g, 75 %) using the same synthetic procedure as outlined above for **C6**. μ-Cl binuclear palladacycle complex **C2** and tricyclohexylphosphine were used as the appropriate reactants. Melting point: 248-250 °C (decomposes without melting). $^{13}C\ \{^1H\}$ NMR (75 MHz, $CDCl_3$, numbering as per **Figure 2.9b**): δ 174.5 (d, $^3J_{C\text{-}P}$ = 4.0 Hz, C^7), δ 161.6 (d, $^3J_{C\text{-}P}$ = 2.2 Hz, Ar-C), δ 145.9 (Ar-C), δ 144.8 (Ar-C), δ 141.1 (Ar-C), δ 136.0 (d, $J_{C\text{-}P}$ = 5.3 Hz, Ar-C), δ 133.5 (Ar-C), δ 132.0 (Ar-C), δ 127.0 (Ar-C), δ 125.2 (Ar-C), δ 122.8 (Ar-C), δ 34.3 (d, $^1J_{C\text{-}P}$ = 21.7 Hz, $P(Cy)_3$), δ 30.6 ($P(Cy)_3$), δ 28.7 ($P(Cy)_3$), δ 27.9 (d, $^2J_{C\text{-}P}$ = 10.9 Hz, $P(Cy)_3$), δ 26.5

($C^{14,16}$), δ 24.9 ($C^{15,17}$), δ 23.0 ($C^{15,17}$). ^{31}P {^{1}H} NMR (120 MHz, $CDCl_3$): δ 42.8 (s). ESI-MS (+.ve, m/z): 730.2 $[M\text{-}Cl]^+$. *Anal. Calc.* for $C_{37}H_{54}Cl_2NPPd \bullet 1CH_2Cl_2$: C, 56.62; H, 7.00; N, 1.74. *Found:* C, 56.82; H, 6.63; N, 1.15.

2.5.3.3 [Pd(P(Cy)$_3$)(2-Br-C$_6$H$_3$)CH=N{2,6-^{i}Pr$_2$-C$_6$H$_3$}Cl] (C18)

Neutral complex **C18** was isolated as yellow crystals (0.15 g, 81 %) using the same synthetic procedure as outlined above for **C6**. μ-Cl binuclear palladacycle complex **C3** and tricyclohexylphosphine were used as the appropriate reactants. Melting point: >250 °C. ^{13}C {^{1}H} NMR (75 MHz, $CDCl_3$, numbering as per **Figure 2.9b**): δ 176.8 (d, $^{3}J_{C\text{-}P}$ = 3.9 Hz, C^7), δ 161.8 (d, $^{3}J_{C\text{-}P}$ = 2.0 Hz, Ar-C), δ 146.0 (Ar-C), δ 145.8 (Ar-C), δ 141.1 (Ar-C), δ 136.7 (d, $J_{C\text{-}P}$ = 5.0 Hz, Ar-C), δ 132.2 (d, $J_{C\text{-}P}$ = 3.4 Hz, Ar-C), δ 128.5 (Ar-C), δ 127.0 (Ar-C), δ 122.9 (Ar-C), δ 122.6 (Ar-C), δ 34.3 (d, $^{1}J_{C\text{-}P}$ = 23.5 Hz, P(Cy)$_3$), δ 30.5 (P(Cy)$_3$), δ 28.7 (P(Cy)$_3$), δ 27.8 (d, $^{2}J_{C\text{-}P}$ = 11.4 Hz, P(Cy)$_3$), δ 26.5 ($C^{14,16}$), δ 24.9 ($C^{15,17}$), δ 23.0 ($C^{15,17}$). ^{31}P {^{1}H} NMR (120 MHz, $CDCl_3$): δ 42.6 (s). ESI-MS (+.ve, m/z): 730.2 $[M\text{-}Cl]^+$; 491.0 $[M\text{-}Cl\text{-}PCy_3\text{+}MeCN]^+$. *Anal. Calc.* for $C_{37}H_{54}BrClNPPd$: C, 58.05; H, 7.11; N, 1.83. *Found:* C, 57.60; H, 6.54; N, 2.04.

2.5.3.4 [Pd(P(Cy)$_3$)(2-F-C$_6$H$_3$)CH=N{2,6-^{i}Pr$_2$-C$_6$H$_3$}Cl] (C19)

Neutral complex **C19** was isolated as yellow crystals (0.13 g, 74 %) using the same synthetic procedure as outlined above for **C6**. μ-Cl binuclear palladacycle complex **C4** and tricyclohexylphosphine were used as the appropriate reactants. Melting point: 227-230 °C (decomposes without melting). ^{13}C {^{1}H} NMR (75 MHz, $CDCl_3$, numbering as per **Figure 2.9b**): δ 170.7 (d, $^{3}J_{C\text{-}P}$ = 3.7 Hz, C^7), δ 162.8 (Ar-C), δ 161.6 (Ar-C), δ 159.3 (Ar-C), δ 145.8 (Ar-C), δ 141.1 (Ar-C), δ 135.3 (d, $J_{C\text{-}P}$ = 3.6 Hz, Ar-C), δ 133.1 (dq, $J_{C\text{-}P}$ = 18.3 Hz, $J_{C\text{-}P}$ = 3.6 Hz, Ar-C), δ 126.9 (Ar-C), δ 122.8 (Ar-C), δ 111.0 (Ar-C), δ 34.4 (d, $^{1}J_{C\text{-}P}$ = 21.1 Hz, P(Cy)$_3$), δ 30.5 (P(Cy)$_3$), δ 28.6 (P(Cy)$_3$), δ 27.8 (d, $^{2}J_{C\text{-}P}$ = 11.4 Hz, P(Cy)$_3$), δ 26.5 ($C^{14,16}$), δ 24.8 ($C^{15,17}$), δ 23.0 ($C^{15,17}$). ^{31}P {^{1}H} NMR (120 MHz, $CDCl_3$): δ 43.3 (s). ESI-MS (+.ve, m/z): 680.30 $[M\text{-}Cl]^+$. *Anal. Calc.* for $C_{37}H_{54}ClFNPPd \bullet 1CH_2Cl_2$: C, 57.80; H, 7.15; N, 1.77. *Found:* C, 58.18; H, 7.81; N, 1.33.

2.5.3.5 [Pd(P(Cy)$_3$)(2-OMe-C$_6$H$_3$)CH=N{2,6-^{i}Pr$_2$-C$_6$H$_3$}Cl] (C20)

Neutral complex **C20** was isolated as yellow crystals (0.13 g, 73 %) using the same synthetic procedure as outlined above for **C6**. μ-Cl binuclear palladacycle complex **C5** and tricyclohexylphosphine were used as the appropriate reactants. Melting point: >250 °C. ^{13}C {^{1}H} NMR (75 MHz, $CDCl_3$, numbering as per **Figure 2.9b**): δ 172.9 (d, $^3J_{C\text{-}P}$ = 4.2 Hz, C^7), δ 161.6 (Ar-C), δ 159.2 (Ar-C), δ 146.4 (Ar-C), δ 141.4 (Ar-C), δ 136.1 (Ar-C), δ 132.6 (Ar-C), δ 130.0 (d, $J_{C\text{-}P}$ = 4.8 Hz, Ar-C), δ 126.6 (Ar-C), δ 122.7 (Ar-C), δ 106.7 (Ar-C), δ 55.5 (*o*-methoxy Me), δ 34.3 (d, $^1J_{C\text{-}P}$ = 21.7 Hz, P(Cy)$_3$), δ 30.6 (P(Cy)$_3$), δ 28.5 (P(Cy)$_3$), δ 27.9 (d, $^2J_{C\text{-}P}$ = 10.9 Hz, P(Cy)$_3$), δ 26.6 ($C^{14,16}$), δ 24.9 ($C^{15,17}$), δ 23.1 ($C^{15,17}$). ^{31}P {^{1}H} NMR (120 MHz, $CDCl_3$): δ 42.2 (s). ESI-MS (+.ve, m/z): 680.3 $[M\text{-}Cl]^+$; 491.0 $[M\text{-}Cl\text{-}PCy_3\text{+}MeCN]^+$. *Anal. Calc.* for $C_{38}H_{57}ClNOPPd\bullet0.25CH_2Cl_2$: C, 62.26; H, 7.85; N, 1.90. *Found:* C, 62.13; H, 7.35; N, 2.22.

2.5.4 Synthesis of neutral palladacycles with the monodentate phosphine, PPh$_3$

2.5.4.1 [Pd(PPh$_3$)(C$_6$H$_4$)CH=N{2,6-^{i}Pr$_2$-C$_6$H$_3$}Cl] (C26)

Neutral complex **C26** was isolated as yellow crystals (0.13 g, 81 %) using the same synthetic procedure as outlined above for **C6**. μ-Cl binuclear palladacycle complex **C1** and triphenylphosphine were used as the appropriate reactants. Melting point: 241-243 °C (decomposes without melting). ^{13}C {^{1}H} NMR (151 MHz, $CDCl_3$, numbering as per **Figure 2.9b**): δ 177.2 (d, $^3J_{C\text{-}P}$ = 4.8 Hz, C^7), δ 160.0 (Ar-C), δ 145.3 (Ar-C), δ 141.5 (Ar-C), δ 141.0 (Ar-C), δ 138.2 (d, $J_{C\text{-}P}$ = 9.7 Hz, Ar-C), δ 135.5 (d, $J_{C\text{-}P}$ = 11.9 Hz, Ar-C), δ 131.5 (Ar-C), δ 131.1 (Ar-C), δ 130.9 (d, $J_{C\text{-}P}$ = 5.2 Hz, Ar-C), δ 130.7 (d, $J_{C\text{-}P}$ = 2.6 Hz, Ar-C), δ 129.0 (Ar-C), δ 128.2 (d, $J_{C\text{-}P}$ = 11.0 Hz, Ar-C), δ 127.0 (Ar-C), δ 124.1 (Ar-C), δ 124.3 (Ar-C), δ 122.9 (Ar-C), δ 28.7 ($C^{14,16}$), δ 24.7 ($C^{15,17}$), δ 23.2 ($C^{15,17}$). ^{31}P {^{1}H} NMR (121 MHz, $CDCl_3$): δ 42.6 (s). ESI-MS (+.ve, m/z): 632.17 $[M\text{-}Cl]^+$. *Anal. Calc.* for $C_{37}H_{37}ClNPPd$: C, 66.47; H, 5.58; N, 2.10. *Found:* C, 66.42; H, 5.54; N, 2.04.

2.5.4.2 [Pd(PPh$_3$)(2-Cl-C$_6$H$_3$)CH=N{2,6-^{i}Pr$_2$-C$_6$H$_3$}Cl] (C27)

Neutral complex **C27** was isolated as a yellow powder (0.14 g, 81 %) using the same synthetic procedure as outlined above for **C6**. μ-Cl binuclear palladacycle complex **C2** and triphenylphosphine were used as the appropriate reactants. Melting point: 247-249 °C (decomposes without melting). ^{13}C {^{1}H} NMR (151 MHz, $CDCl_3$, numbering as per **Figure 2.9b**): δ 175.6 (d, $^3J_{C\text{-}P}$ = 4.5 Hz, C^7), δ 162.1 (Ar-C), δ 145.5 (Ar-C), δ 144.8 (Ar-C), δ 140.9 (Ar-C), δ 136.7 (d, $J_{C\text{-}P}$ = 9.8 Hz, Ar-C), δ 135.4 (d, $J_{C\text{-}P}$ = 11.7 Hz, Ar-C), δ 133.3 (Ar-C), δ 132.3 (d, $J_{C\text{-}P}$ = 5.7 Hz, Ar-C), δ 131.2 (Ar-C), δ 130.9 (d, $J_{C\text{-}P}$ = 3.4 Hz, Ar-C), δ 128.3 (d, $J_{C\text{-}P}$ = 11.9 Hz, Ar-C), δ 127.3 (Ar-C), δ 125.1 (Ar-C), δ 123.0 (Ar-C), δ 28.8 ($C^{14,16}$), δ 24.7 ($C^{15,17}$), δ 23.1 ($C^{15,17}$). ^{31}P {^{1}H} NMR (121 MHz, $CDCl_3$): δ 42.2 (s). ESI-MS (+.ve, m/z): 668.13 $[M\text{-}Cl]^+$. *Anal. Calc.* for $C_{37}H_{36}Cl_2NPPd$: C, 63.22; H, 5.16; N, 1.99. *Found:* C, 63.18; H, 5.11; N, 1.92.

2.5.4.3 [Pd(PPh$_3$)(2-Br-C$_6$H$_3$)CH=N{2,6-^{i}Pr$_2$-C$_6$H$_3$}Cl] (C28)

Neutral complex **C28** was isolated as yellow crystals (0.15 g, 84 %) using the same synthetic procedure as outlined above for **C6**. μ-Cl binuclear palladacycle complex **C3** and triphenylphosphine were used as the appropriate reactants. Melting point: >250 °C. ^{13}C {^{1}H} NMR (151 MHz, $CDCl_3$, numbering as per **Figure 2.9b**): δ 177.8 (d, $^3J_{C\text{-}P}$ = 4.8 Hz, C^7), δ 162.2 (Ar-C), δ 145.4 (Ar-C), δ 141.2 (Ar-C), δ 140.9 (Ar-C), δ 137.3 (d, $J_{C\text{-}P}$ = 10.0 Hz, Ar-C), δ 135.4 (d, $J_{C\text{-}P}$ = 11.8 Hz, Ar-C), δ 132.5 (d, $^3J_{C\text{-}P}$ = 5.3 Hz, Ar-C), δ 131.1 (Ar-C), δ 130.9 (Ar-C), δ 130.8 (Ar-C), δ 128.5 (Ar-C), δ 128.3 (d, $J_{C\text{-}P}$ = 11.2 Hz, Ar-C), δ 127.3 (Ar-C), δ 123.0 (Ar-C), δ 122.3 (Ar-C), δ 28.8 ($C^{14,16}$), δ 24.7 ($C^{15,17}$), δ 23.1 ($C^{15,17}$). ^{31}P {^{1}H} NMR (121 MHz, $CDCl_3$): δ 42.0 (s). ESI-MS (+.ve, m/z): 712.08 $[M\text{-}Cl]^+$. *Anal. Calc.* for $C_{37}H_{36}BrClNPPd$: C, 59.46; H, 4.85; N, 1.87. *Found:* C, 58.85; H, 4.71; N, 1.41.

2.5.4.4 [Pd(PPh$_3$)(2-F-C$_6$H$_3$)CH=N{2,6-^{i}Pr$_2$-C$_6$H$_3$}Cl] (C29)

Neutral complex **C29** was isolated as a yellow powder (0.14 g, 85 %) using the same synthetic procedure as outlined above for **C6**. μ-Cl binuclear palladacycle complex **C4** and triphenylphosphine were used as the appropriate reactants. Melting point: 220-223 °C (decomposes without melting). ^{13}C

{^{1}H} NMR (151 MHz, $CDCl_3$, numbering as per **Figure 2.9b**): δ 171.8 (d, $^{3}J_{C\text{-}P}$ = 4.4 Hz, C^{7}), δ 162.1 (d, $J_{C\text{-}P}$ = 3.7 Hz, Ar-C), δ 161.7 (Ar-C), δ 160.0 (Ar-C), δ 145.4 (Ar-C), δ 140.9 (Ar-C), δ 135.4 (d, $J_{C\text{-}P}$ = 11.8 Hz, Ar-C), δ 133.8 (dd, $J_{C\text{-}P}$ = 10.0 Hz, $J_{C\text{-}P}$ = 3.1 Hz, Ar-C), δ 133.2 (dd, $J_{C\text{-}P}$ = 7.0 Hz, $J_{C\text{-}P}$ = 5.5 Hz, Ar-C), δ 131.3 (Ar-C), δ 130.9 (d, $J_{C\text{-}P}$ = 2.6 Hz, Ar-C), δ 128.2 (d, $J_{C\text{-}P}$ = 11.0 Hz, Ar-C), δ 127.2 (Ar-C), δ 123.0 (Ar-C), δ 111.0 (d, $J_{C\text{-}P}$ = 19.3 Hz, Ar-C), δ 28.8 ($C^{14,16}$), δ 24.7 ($C^{15,17}$), δ 23.2 ($C^{15,17}$). ^{31}P {^{1}H} NMR (121 MHz, $CDCl_3$): δ 42.2 (s). ESI-MS (+.ve, m/z): 650.16 $[M\text{-}Cl]^{+}$. *Anal. Calc.* for $C_{37}H_{36}ClFNPPd$: C, 64.73; H, 5.29; N, 2.04. *Found:* C, 64.29; H, 5.49; N, 1.57.

2.5.4.5 [Pd(PPh$_3$)(2-OMe-C$_6$H$_3$)CH=N{2,6-^{i}Pr$_2$-C$_6$H$_3$}Cl] (C30)

Neutral complex **C30** was isolated as yellow crystals (0.15 g, 89 %) using the same synthetic procedure as outlined above for **C6**. μ-Cl binuclear palladacycle complex **C5** and triphenylphosphine were used as the appropriate reactants. Melting point: 246-248 °C (decomposes without melting). ^{13}C {^{1}H} NMR (101 MHz, $CDCl_3$, numbering as per **Figure 2.9b**): δ 173.9 (d, $^{3}J_{C\text{-}P}$ = 4.8 Hz, C^{7}), δ 162.3 (Ar-C), δ 159.0 (Ar-C), δ 145.9 (Ar-C), δ 141.2 (Ar-C), δ 135.9 (Ar-C), δ 135.5 (d, $J_{C\text{-}P}$ = 12.1 Hz, Ar-C), δ 132.9 (d, $J_{C\text{-}P}$ = 6.2 Hz, Ar-C), δ 131.7 (Ar-C), δ 131.2 (Ar-C), δ 130.6 (Ar-C), δ 128.2 (d, $J_{C\text{-}P}$ = 10.8 Hz, Ar-C), δ 126.8 (Ar-C), δ 122.8 (Ar-C), δ 106.6 (Ar-C), δ 55.5 (*o*-methoxy Me), δ 28.7 ($C^{14,16}$), δ 24.7 ($C^{15,17}$), δ 23.2 ($C^{15,17}$). ^{31}P {^{1}H} NMR (162 MHz, $CDCl_3$): δ 42.3 (s). ESI-MS (+.ve, m/z): 662.18 $[M\text{-}Cl]^{+}$. *Anal. Calc.* for $C_{38}H_{39}ClNOPPd$: C, 65.33; H, 5.63; N, 2.01. *Found:* C, 65.11; H, 5.70; N, 1.60.

2.6 References

1 H. Schiff, *Ann. Suppl.*, 1864, **3**, 343.

2 H. Schiff, *Justus Liebigs Ann. Chem*, 1864, **131**, 118.

3 K. Campbell, A. H. Sommers and B. Campbell, *J. Am. Chem. Soc.*, 1944, **66**, 82.

4 C. Brewster, *J. Am. Chem. Soc.*, 1964, **46**, 2463.

5 S. Oshima, N. Hirayama, K. Kubono, H. Kokusen and T. Honjo, *Talanta*, 2003, **59**, 867.

6 J. Albert, J. M. Cadena, A. González, J. Granell, X. Solans and M. Font-Bardia, *J. Organomet. Chem.*, 2002, **663**, 277.

7 M. Gómez, J. Granell and M. Martinez, *Dalton. Trans.*, 1998, 37.

8 C. Lopez, R. Bosque, X. Solans, M. Font-bardia, J. Silverc and G. Fernc, *Dalton. Trans.*, 1995, 4053.

9 J. Granell and M. Martinez, *Organometallics*, 1997, **16**, 2539.

10 C. L. Chen, Y. H. Liu, S. M. Peng and S. T. Liu, *J. Organomet. Chem.*, 2004, **689**, 1806.

11 B. E. Love, T. S. Boston, B. T. Nguyen and J. R. Rorer, *Org. Prep. Proced. Int.*, 1999, **31**, 399.

12 N. Mungwe, A. J. Swarts, S. F. Mapolie and G. Westman, *J. Organomet. Chem.*, 2011, **696**, 3527.

13 J. Long, H. Gao, K. Song, F. Liu, H. Hu, L. Zhang, F. Zhu and Q. Wu, *Eur. J. Inorg. Chem.*, 2008, 4296.

14 D. Srimani and A. Sarkar, *Tetrahedron Lett.*, 2008, **49**, 6304.

15 Z. Zhang, S. Chen, X. Zhang, H. Li, Y. Ke, Y. Lu and Y. Hu, *J. Mol. Catal. A Chem.*, 2005, **230**, 1.

16 G. Britovsek, S. Mastroianni, G. Solan, S. Baugh, C. Redshaw, V. Gibson, A. White, D. Williams and M. Elsegood, *Chem. Eur. J.*, 2000, **6**, 2221.

17 L. K. Johnson, C. M. Killian and M. Brookhart, *J. Am. Chem. Soc.*, 1995, **117**, 6414.

18 H. Onoue and I. Moritani, *J. Organomet. Chem.*, 1972, **43**, 431.

19 M. Orchin and P. Schmidt, *Coord. Chem. Rev.*, 1968, **3**, 345.

20 V. A. Chertkov, Y. Ustynyuk and I. Barinov, *J. Organomet. Chem.*, 1971, **29**, 53.

21 L. Tušek-Božić, M. Komac, M. Ćurić, A. Lyčka, M. D'Alpaos, V. Scarcia and A. Furlani, *Polyhedron*, 2000, **19**, 937.

22 F. Tjosaas and A. Fiksdahl, *J. Organomet. Chem.*, 2007, **692**, 5429.

23 F. Antolasic, *Mol. Weight Calc.*, 2005, www.wsearch.com.au.

24 L. H. Slaugh and R. D. Mullineaux, *J. Organomet. Chem.*, 1968, **13**, 469.

25 A. R. Naziruddin, A. Hepp, T. Pape and F. E. Hahn, *Organometallics*, 2011, 5859.

26 P. Espinet and K. Soulantica, *Coord. Chem. Rev.*, 1999, **193-195**, 499.

27 P. Barbaro, C. Bianchini, G. Giambastiani and S. L. Parisel, *Coord. Chem. Rev.*, 2004, **248**, 2131.

28 J. Bravo, S. Bolaño, L. Gonsalvi and M. Peruzzini, *Coord. Chem. Rev.*, 2010, **254**, 555.

29 B. J. Frost, S. B. Miller, K. O. Rove, D. M. Pearson, J. D. Korinek, J. L. Harkreader, C. A. Mebi and J. Shearer, *Inorg. Chim. Acta*, 2006, **359**, 283.

30 A. D. Phillips, L. Gonsalvi, A. Romerosa, F. Vizza and M. Peruzzini, *Coord. Chem. Rev.*, 2004, **248**, 955.

31 D. J. Darensbourg, J. B. Robertson, D. L. Larkins and J. H. Reibenspies, *Inorg. Chem.*, 1999, **38**, 2473.

32 A. Brink, A. Roodt, G. Steyl and H. G. Visser, *Dalton Trans.*, 2010, **39**, 5572.

33 C. A. Tolman, *Chem. Rev.*, 1977, **77**, 313.

34 K. Haav, J. Saame, A. Kütt and I. Leito, *European J. Org. Chem.*, 2012, 2167.

35 J. N. Li, Y. Fu, L. Liu and Q. X. Guo, *Tetrahedron*, 2006, **62**, 11801.

36 A. J. Swarts, Mononuclear and Multinuclear Palladacycles as Catalyst Precursors, *MSc. Thesis*, Stellenbosch University, 2011.

37 J. Albert, M. Gomez, J. Granell and J. Sales, *Organometallics*, 1990, **9**, 1405.

38 J. Ruiz, N. Cutillas, F. López, G. López and D. Bautista, *Organometallics*, 2006, **25**, 5768.

39 R. B. Bedford, C. S. J. Cazin, M. B. Hursthouse, M. E. Light and V. J. M. Scordia, *Dalton Trans.*, 2004, 3864.

40 W. R. Jackson, S. M. Available, J. Albert, R. M. Ceder, M. Gómez, J. Granell and J. Sales, *Organometallics*, 1992, **11**, 1536.

41 R. B. Bedford, C. S. J. Cazin, S. J. Coles, T. Gelbrich, P. N. Horton, M. B. Hursthouse and M. E. Light, *Organometallics*, 2003, **22**, 987.

42 L. Tušek-Božić, M. Ćurić and P. Traldi, *Inorg. Chim. Acta*, 1997, **254**, 49.

43 W. Zawartka, A. Gniewek, A. M. Trzeciak, J. J. Ziółkowski and J. Pernak, *J. Mol. Catal. A Chem.*, 2009, **304**, 8.

44 L. Adrio, J. M. Antelo, J. M. Ortigueira, J. J. Fernández, A. Fernández, M. Teresa Pereira and J. M. Vila, *J. Organomet. Chem.*, 2009, **694**, 1273.

45 Y. Murata, H. Ohgi, T. Fujihara, J. Terao and Y. Tsuji, *Inorg. Chim. Acta*, 2011, **368**, 237.

46 F. R. Hartley, S. G. Murray and C. A. Mcauliffe, *Inorg. Chem.*, 1979, **18**, 1394.

47 Apex2, *Data Collect. Software*, Bruker AXS, 2010.

48 SAINT, *Data Reduct. Software*, Bruker AXS, 2003.

49 R. H. Blessing, *Acta Crystallogr. A.*, 1995, **51 (Pt 1)**, 33.

50 SADABS, *Version 2.05*, Bruker AXS, 2002.

51 G. M. Sheldrick, *Acta Crystallogr. Sect. A Found. Crystallogr.*, 2007, **64**, 112.

52 L. J. Barbour, *J. Supramol. Chem.*, 2001, **1**, 189.

53 POV-Ray, *Version 3.6*, Williamstown, Australia, Persistence of vision ray.

Chapter 3

The Synthesis and Characterization of Cationic Palladacycles Derived from Neutral Mononuclear Palladacycles

3.1 Introduction

The last two decades have witnessed phenomenal growth in the development of late transition metal complexes bearing multidentate ligands as catalysts for different olefin transformations.[1,2] Of particular significance is the development of bidentate α-diimine cationic palladium and nickel complexes by Brookhart *et. al.* for the selective oligomerization, polymerization or copolymerization of olefins depending on the steric bulk of the ligand backbone in the catalyst design (**Figure 3.1**).[3–6] In general, only oligomers were produced when the steric bulk of the *ortho*-substituent on the aryl-substituted α-diimine palladium and nickel complexes was reduced. In contrast, high molecular weight polymers were produced when bulky substituents were incorporated in the *ortho*-substituent of the aryl-substituted α-diimine ligand.

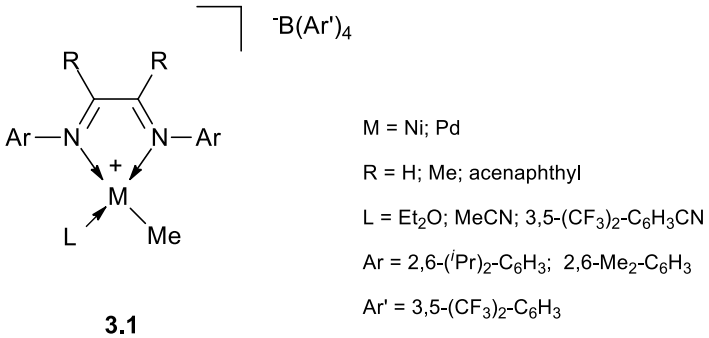

3.1

Figure 3.1: Cationic α-diimine Ni and Pd catalysts developed by Brookhart *et. al.* for different olefin transformations. [3–6]

Cationic complexes are often prepared by direct halide abstraction using silver, boron or alkali metal salts of a very weakly coordinating or non-coordinating anions to prevent unfavourable interaction with the metal centre.[2] Due to the low electrophilicity of the metal centre, late transition metal complexes are often less sensitive and unlikely to coordinate to the anion. Anions such as PF_6^-, BF_4^-, $B[Ar(CF_3)_2]_4^-$ and SbF_6^- are commonly used and regarded as weakly or non-coordinating.[7–9] The nature of the stabilizing ligand is crucial in the architecture of the cationic complexes. The latter serves to stabilize the catalyst's vacant site to such an extent that it will not compete with the incoming olefin yet would protect the vacant site in the absence of the olefin. **Scheme 3.1** represents a general route for the preparation of cationic complexes derived from their neutral counterparts.

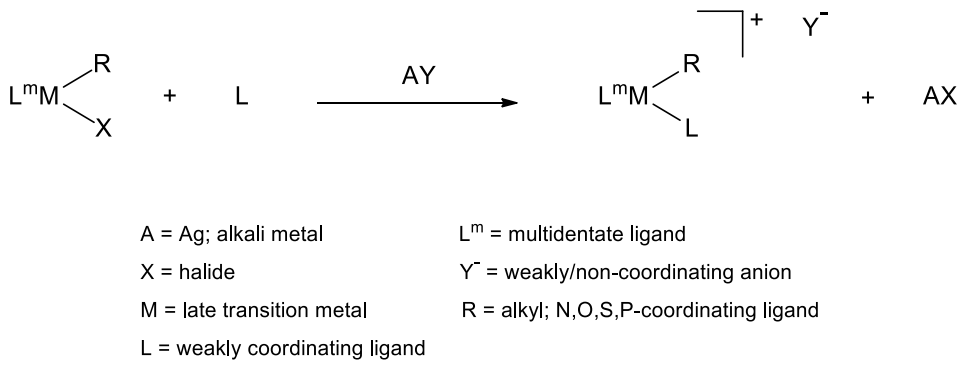

Scheme 3.1: General route for the preparation of multidentate cationic complexes.

It was envisaged that the interaction between the nitrogen atom of acetonitrile and the palladium centre would be strong enough to stabilize the complex's vacant site but weak enough to be displaced by the incoming olefin. Here, we report on the synthesis and characterization of series of cationic palladacycle complexes derived from their neutral counterparts as potential catalysts in the polymerization of phenylacetylene.

3.2 Results and Discussion

3.2.1 Synthesis and characterization of cationic palladacycle complexes with acetonitrile as coordinating solvent.

The cationic palladacycles complexes, **C11-C15**; **C21-C25** and **C31-35**, were prepared by the reaction of previous synthesized neutral complexes (**Chapter 2, section 2.2.3**) with $NaB(Ar)_4$ in the presence of acetonitrile (**Scheme 3.2**). The latter serves to firstly abstract the chloride ligand which creates a vacant site on the palladium centre which, in turn, is subsequently stabilized by weakly coordinating acetonitrile. Secondly, the non-coordinating $^{-}B(Ar)_4$ anion acts as the counterion to stabilize the positive charge on the palladium centre.

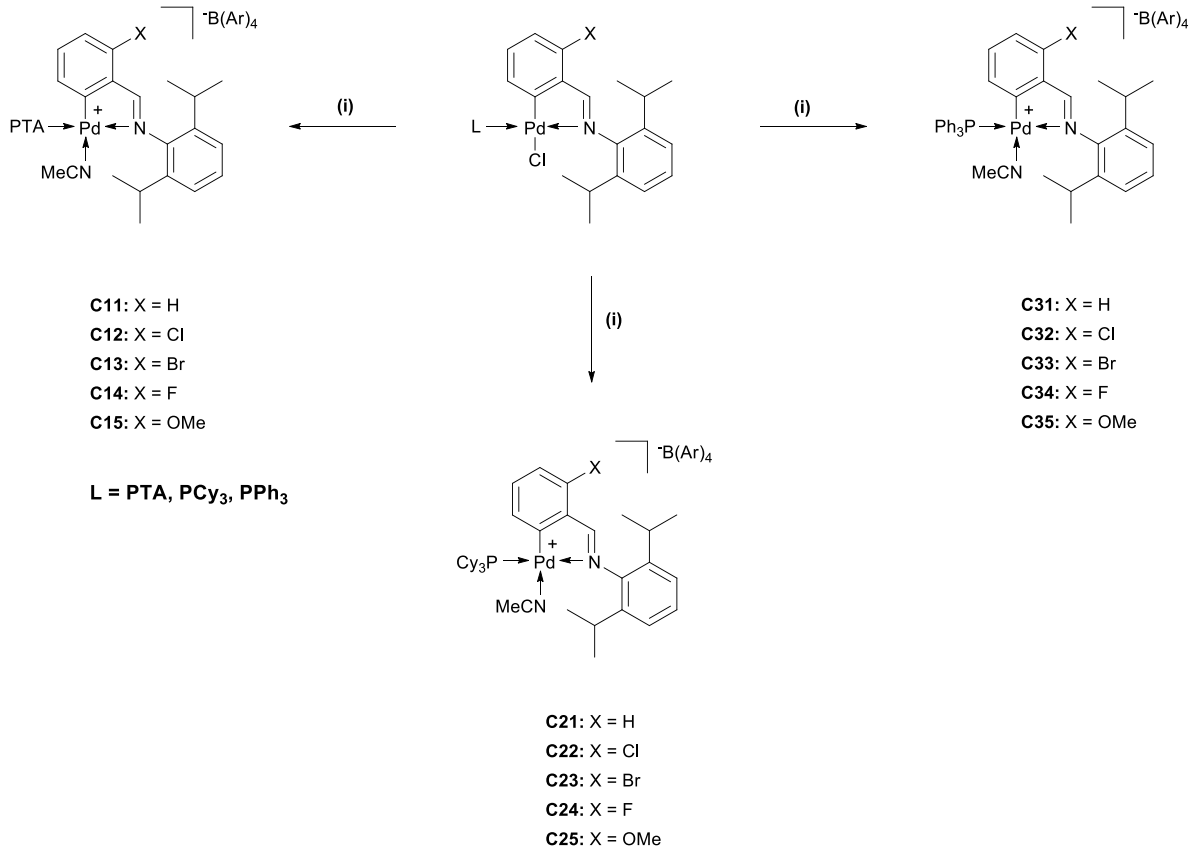

Scheme 3.2: Synthetic route to cationic palladacycles, **C11-C15, C21-C25** and **C31-C35**.

The cationic palladacycles were isolated after work-up and recrystallization from dichloromethane/*n*-hexane as off-white solids in high yields (80-91 %) and displayed solubility in chlorinated solvents, diethyl ether and alcohols, but were insoluble in alkanes. The complexes were stable in solution and in the solid state. The cationic palladacycle complexes containing the PTA and PCy_3 ligand are all novel, whereas the PPh_3 complexes **C31-C33** were previously reported.[10] A variety of analytical techniques were employed and a summary of the general characterization data for these palladacycles is shown in **Table 3.1-3.6.**

3.2.1.1 FT-IR spectroscopy

Characterization of the desired cationic palladacycles by FT-IR spectroscopy showed a hypsochromic shift of the $\nu_{C=N}$ absorption band which appears in the region 1620-1604 cm^{-1} (**Table 3.1**) in comparison to their neutral counterparts. In addition, strong ν_{C-F} absorption bands at ~ 1353, 1272 and 1112 cm^{-1} are observed for all analogues in the FT-IR spectra which are attributed to the various stretching vibration modes of the trifluoromethyl substituents in the $[B(Ar)_4]^-$ counterion.

Table 3.1: IR spectral data for cationic mononuclear palladacycles **C11-C15, C21-C25** and **C31-C35**.

Cationic comp. (PTA)	FT-IR [a] ($\nu_{C=N}$, cm^{-1})	Cationic comp. (PCy_3)	FT-IR [a] ($\nu_{C=N}$, cm^{-1})	Cationic comp. (PPh_3)	FT-IR [a] ($\nu_{C=N}$, cm^{-1})
C11	1620	**C21**	1615	**C31**	1613
C12	1611	**C22**	1616	**C32**	1611
C13	1612	**C23**	1613	**C33**	1616
C14	1611	**C24**	1611	**C34**	1612
C15	1605	**C25**	1604	**C35**	1604

[a] Recorded as neat spectra using a ZnSe ATR accessory.

3.2.1.2 ^{1}H-, $^{13}C\{^{1}H\}$- and $^{31}P\{^{1}H\}$ NMR spectroscopy

NMR spectroscopy of the desired cationic palladacycles confirmed successful coordination of the acetonitrile ligand to the palladium metal centre. The difference in the chemical shift of the imine proton resonance (**H^7, Figure 3.2a**) in the ^{1}H NMR spectra between the neutral palladacycles and their cationic

counterparts is discernible but not particularly significant. The *endo*cycle ring remains intact upon coordination of the acetonitrile ligand since the imine proton resonance still appeared as a doublet, demonstrating the existence of a heteronuclear $^{4}J_{H\text{-}P}$ coupling of the imine proton to the phosphorous atom of the phosphine ligand. In addition, two broad proton resonances assigned to the $[B(Ar)_4]^-$ counterion were observed downfield in the regions δ 7.76-7.63 ppm (**H^{21}**) and δ 7.57-7.46 ppm (**H^{23}**) which integrate for a total of eight- and four protons respectively for all cationic analogues. The complexity of the methylene resonances in the PTA ligand for cationic palladacycles **C11-C15** is reduced and showed two distinct resonances in the regions δ 4.58-4.42 ppm and δ 4.42-4.30 ppm for the NC***H*$_2$**N (AB quartet) and NC***H*$_2$**P (singlet) methylene resonances respectively (**Table 3.3**). This is in comparison to the observed multiplet for their neutral counterparts, **C6-C10**.

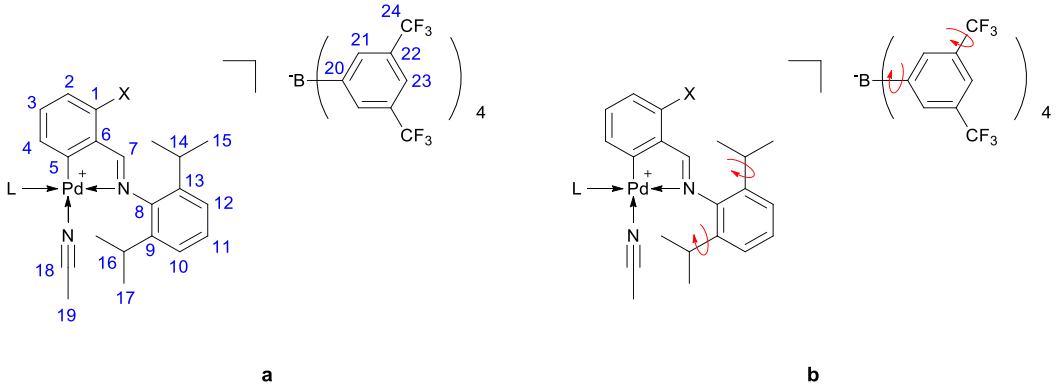

Figure 3.2: (a) Cationic palladacycle with numbering for NMR data; **(b)** Free rotation about the C-C bond of both the isopropyl and trifluoromethyl moiety and free rotation about the C-B bond in the counterion. L denotes the different phosphine ligands (L = PTA, PCy_3, PPh_3).

Similar to the *μ*-Cl binuclear- and neutral palladacycles, the ^{1}H NMR spectral data (**Table 3.3-Table 3.5**) of the cationic species revealed no rotation along the N-C bond (**N-C^{8}**) after coordination of the acetonitrile ligand, however free rotation along C-C bonds (**C^{13}-C^{14}; C^{9}-C^{16}**) remains intact (**Figure 3.2b**). In the aliphatic region, the methine resonance (**H^{14,16}**) shifted more upfield in the region δ 3.49-3.03 ppm relative to the methine resonance observed for the neutral analogues. The two doublets due to the **H^{15}** and **H^{17}** methyl protons of the isopropyl moiety overlap slightly, revealing

that their chemical inequivalence is somewhat reduced upon coordination of the acetonitrile ligand when compared to their neutral counterparts as shown in **Figure 3.3a** and **b**. In addition, a singlet was observed in the upfield region δ 1.44-1.38 ppm (for complexes **C11-C15** and **C21-C25**) and δ 1.05-1.04 ppm (for complexes **C31-C35**), integrating for a total of three protons which was assigned to the methyl protons (**H[19]**) of acetonitrile, hence confirming the successful coordination of the acetonitrile ligand to the palladium metal centre.

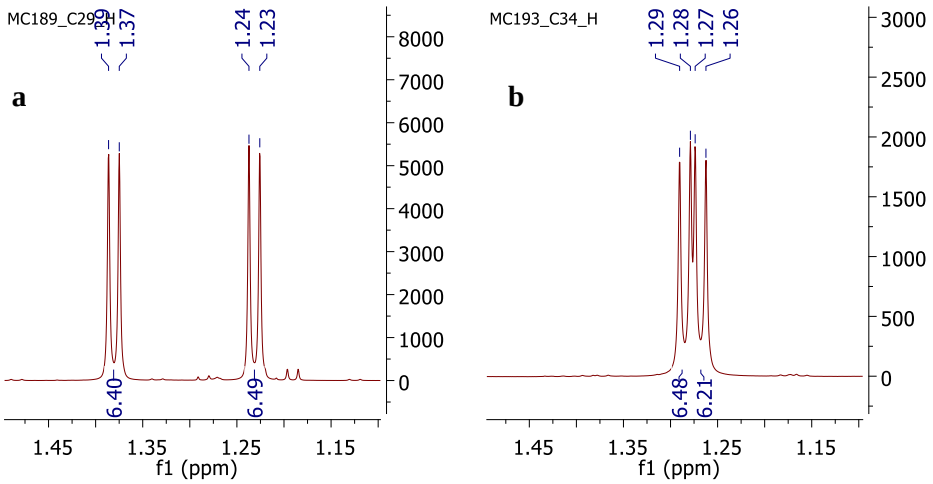

Figure 3.3: [1]H NMR spectrum showing the methyl resonances of the isopropyl moiety for (**a**) neutral palladacycle **C29**; (**b**) cationic palladacycle **C34** in the region δ 1.50-1.10 ppm.

Analogous resonances to the previously synthesized neutral palladacycles were observed in the ^{13}C {^{1}H} NMR spectra of all cationic palladacycle complexes. The imine carbon resonance (**C[7]**, **Figure 3.2a**) shifted slightly downfield in the region δ 179.1-172.5 ppm and appears as a doublet due to a heteronuclear $^{3}J_{C\text{-}P}$ coupling to the phosphorous atom of the phosphine ligand (**Table 3.2**). The latter also confirms that the *endo*cycle is retained. The $[B(Ar)_4]^-$ counterion consists of two NMR active nuclei atoms i.e. ^{11}B (with spin quantum number 3/2) and ^{19}F (with spin quantum number 1/2), therefore predictable splitting patterns are expected in the $^{13}C\{^{1}H\}$ NMR spectra. A quartet (1:1:1:1) which resonates in the downfield region of ~ δ 161.8 ppm was assigned to carbon **C[20]** due to heteronuclear $^{1}J_{C\text{-}B}$ coupling to the boron atom in the $[B(Ar)_4]^-$ counterion. Carbon **C[22]** appears as quartet

of quartets which resonates in the region ~ δ 129.0 ppm due to $^{2}J_{C\text{-}F}$ coupling to the fluorine atom and $^{3}J_{C\text{-}B}$ coupling to the boron atom. Furthermore carbon **C^{23}** resonates as a septet in the region ~ δ 117.6 ppm due to $^{3}J_{C\text{-}F}$ coupling to the fluorine atoms of both trifluoromethyl substituents. In addition, free rotation is possible along the C-B bond (**C^{20}-B**) and C-C bond (**C^{22}-C^{24}**) in the counterion as evident from the ^{13}C {^{1}H} NMR spectral data.

The ^{31}P {^{1}H} NMR spectra showed a well-defined singlet in the region δ 48.2-41.0 ppm for the PCy_3- and PPh_3 cationic analogues and in the region δ -46.3-(-48.1) ppm for the PTA cationic complexes (**Table 3.2**). The presence of only one phosphorous resonance implies that only one isomer was observed.

Table 3.2: ^{13}C {^{1}H} NMR and ^{31}P {^{1}H} NMR spectral data for cationic complexes (**C11-C15; C21-C25; C31-C35**).

Cationic complex	^{13}C {^{1}H} NMR [a] ($\delta_{C=N}$, ppm)	^{31}P {^{1}H} NMR [b] (δ_{P}, ppm)
C11	178.1	-46.9
C12	176.5	-46.9
C13	178.9	-47.8
C14	172.8	-46.3
C15	174.8	-48.1
C21	177.8	47.7
C22	176.2	47.5
C23	178.5	47.3
C24	172.5	48.2
C25	174.5	46.7
C31	178.5	41.6
C32	176.8	41.2
C33	179.1	41.0
C34	173.1	41.2
C35	175.1	41.1

[a] Spectra recorded in $CDCl_3$ at 298 K; chemical shifts reported as δ ppm values, referenced relative to the residual $CDCl_3$ resonance. [b] Spectra recorded in $CDCl_3$ at 298 K; chemical shifts externally referenced relative to H_3PO_4.

Table 3.3: ^{1}H NMR spectral data of neutral mononuclear palladacycles, **C11-C15**. [a]

Complex	C=N***H***	Aromatic region	Phosphine	Aliphatic region			
				OC***H*₃**	$(CH_3)_2C\boldsymbol{H}$	$CH(C\boldsymbol{H}_3)_2$	$C\boldsymbol{H}_3CN$
C11	δ 8.00 (d, $^{4}J_{H\text{-}P}$ = 7.2 Hz, 1H, H^{7})	δ 7.74-7.66 (comp., 8H, $B(Ar)_4$), δ 7.56-7.49 (comp., 4H, $B(Ar)_4$), δ 7.35 (t, $^{3}J_{H\text{-}H}$ = 7.6 Hz, 1H, H^{2}), δ 7.32-7.22 (comp., 5H, $H^{1,3,10,11,12}$), δ 7.14 (m, 1H, H^{4})	δ 4.58-4.48 (comp., 6H, PTA), δ 4.42-4.35 (comp., 6H, PTA)		δ 3.17-3.07 (m, 2H, $H^{14,16}$)	δ 1.24 (d, $^{3}J_{H\text{-}H}$ = 6.8 Hz, 6H, $H^{15,17}$), δ 1.16 (d, $^{3}J_{H\text{-}H}$ = 6.8 Hz, 6H, $H^{15,17}$)	δ 1.43 (s, 3H, H^{19})
C12	δ 8.46 (d, $^{4}J_{H\text{-}P}$ = 7.0 Hz, 1H, H^{7})	δ 7.73-7.65 (comp., 8H, $B(Ar)_4$), δ 7.56-7.50 (comp., 4H, $B(Ar)_4$), δ 7.37-7.20 (comp., 5H, $H^{2,3,10,11,12}$), δ 7.03-6.93 (m, 1H, H^{4})	δ 4.55-4.45 (comp., 6H, PTA), δ 4.40-4.30 (comp., 6H, PTA)		δ 3.20-3.02 (m, 2H, $H^{14,16}$)	δ 1.25 (d, $^{3}J_{H\text{-}H}$ = 6.8 Hz, 6H, $H^{15,17}$), δ 1.19 (d, $^{3}J_{H\text{-}H}$ = 6.8 Hz, 6H, $H^{15,17}$)	δ 1.40 (s, 3H, H^{19})
C13	δ 8.47 (d, $^{4}J_{H\text{-}P}$ = 7.3 Hz, 1H, H^{7})	δ 7.75-7.64 (comp., 8H, $B(Ar)_4$), δ 7.56-7.49 (comp., 4H, $B(Ar)_4$), δ 7.42 (d, $^{3}J_{H\text{-}H}$ = 7.6 Hz, 1H, H^{2}), δ 7.37-7.23 (comp., 3H, $H^{10,11,12}$), δ 7.17 (t, $^{3}J_{H\text{-}H}$ = 8.0 Hz, 1H, H^{3}), δ 7.06-6.98 (m, 1H, H^{4})	δ 4.58-4.42 (comp., 6H, PTA), δ 4.41-4.30 (comp., 6H, PTA)		δ 3.20-3.03 (m, 2H, $H^{14,16}$)	δ 1.25 (d, $^{3}J_{H\text{-}H}$ = 6.8 Hz, 6H, $H^{15,17}$), δ 1.19 (d, $^{3}J_{H\text{-}H}$ = 6.7 Hz, 6H, $H^{15,17}$)	δ 1.42 (s, 3H, H^{19})
C14	δ 8.32 (d, $^{4}J_{H\text{-}P}$ = 7.6 Hz, 1H, H^{7})	δ 7.76-7.65 (comp., 8H, $B(Ar)_4$), δ 7.56-7.49 (comp., 4H, $B(Ar)_4$), δ 7.43-7.21 (comp., 4H, $H^{3,10,11,12}$), δ 7.00-6.86 (comp., 2H, $H^{2,4}$)	δ 4.58-4.45 (comp., 6H, PTA), δ 4.43-4.32 (comp., 6H, PTA)		δ 3.17-3.03 (m, 2H, $H^{14,16}$)	δ 1.24 (d, $^{3}J_{H\text{-}H}$ = 7.0 Hz, 6H, $H^{15,17}$), δ 1.18 (d, $^{3}J_{H\text{-}H}$ = 7.0 Hz, 6H, $H^{15,17}$)	δ 1.44 (s, 3H, H^{19})
C15	δ 8.38 (d, $^{4}J_{H\text{-}P}$ = 7.7 Hz, 1H, H^{7})	δ 7.75-7.64 (comp., 8H, $B(Ar)_4$), δ 7.56-7.48 (comp., 4H, $B(Ar)_4$), δ 7.35-7.19 (comp., 4H, $H^{3,10,11,12}$), δ 6.75 (d, $^{3}J_{H\text{-}H}$ = 8.5 Hz, 1H, H^{2}), δ 6.68-6.63 (m, 1H, H^{4})	δ 4.57-4.47 (comp., 6H, PTA), δ 4.40-4.35 (comp., 6H, PTA)	δ 3.82 (s, 3H, *o*-methoxy Me),	δ 3.20-3.07 (m, 2H, $H^{14,16}$)	δ 1.24 (d, $^{3}J_{H\text{-}H}$ = 6.8 Hz, 6H, $H^{15,17}$), δ 1.17 (d, $^{3}J_{H\text{-}H}$ = 6.8 Hz, 6H, $H^{15,17}$)	δ 1.41 (s, 3H, H^{19})

[a] Spectra recorded in $CDCl_3$ at 298 K; chemical shifts reported as δ ppm values, referenced relative to the residual $CDCl_3$ resonance; superscripts denote protons as per numbering scheme **Figure 3.2a**; s = singlet, d = doublet, t = triplet, dd = doublet of doublets, td = triplet of doublets, sept. = septet, m = multiplet (denotes complex pattern for a single proton resonance), comp. = complex (denotes complex pattern of overlapping proton resonances)

Table 3.4: ^{1}H NMR spectral data of neutral mononuclear palladacycles, **C21-C25.** [a]

Complex	C=N***H***	Aromatic region	Aliphatic region			
			OC***H*₃**	$(CH_3)_2C$***H***	Phosphine & CH(C***H*₃**)$_2$	C***H*₃**CN
C21	δ 8.03 (d, $^{4}J_{H\text{-}P}$ = 6.6 Hz, 1H, H^{7})	δ 7.74-7.65 (comp., 8H, B(Ar)$_4$), δ 7.55-7.50 (comp., 4H, B(Ar)$_4$), δ 7.50-7.46 (m, 1H, H^{1}), δ 7.33-7.19 (comp., 6H, Ar-H)		δ 3.35-3.21 (m, 2H, $H^{14,16}$)	δ 2.25-2.09 (comp., 4H, P(Cy)$_3$), δ 2.02-1.90 (comp., 6H, P(Cy)$_3$), δ 1.89-1.79 (comp., 6H, P(Cy)$_3$), δ 1.78-1.68 (comp., 3H, P(Cy)$_3$), δ 1.67-1.52 (comp., 7H, P(Cy)$_3$), δ 1.31-1.08 (comp., 19H, P(Cy)$_3$ & $H^{15,17}$)	δ 1.39 (s, 3H, H^{19})
C22	δ 8.52 (d, $^{4}J_{H\text{-}P}$ = 6.6 Hz, 1H, H^{7})	δ 7.74-7.65 (comp., 8H, B(Ar)$_4$), δ 7.56-7.48 (comp., 4H, B(Ar)$_4$), δ 7.36-7.24 (comp., 3H, Ar-H), δ 7.22-7.05 (comp., 3H, Ar-H)		δ 3.36-3.17 (m, 2H, $H^{14,16}$)	δ 2.25-2.04 (comp., 5H, P(Cy)$_3$), δ 2.02-1.47 (comp., 21H, P(Cy)$_3$), δ 1.34-1.03 (comp., 19H, P(Cy)$_3$ & $H^{15,17}$).	δ 1.40 (s, 3H, H^{19})
C23	δ 8.53 (d, $^{4}J_{H\text{-}P}$ = 6.7 Hz, 1H, H^{7})	δ 7.76-7.63 (comp., 8H, B(Ar)$_4$), δ 7.57-7.48 (comp., 4H, B(Ar)$_4$), δ 7.42-7.22 (comp., 4H, Ar-H), δ 7.17-7.03 (comp., 2H, Ar-H)		δ 3.36-3.16 (m, 2H, $H^{14,16}$)	δ 2.23-1.46 (comp., 26H, P(Cy)$_3$), δ 1.35-1.03 (comp., 19H, P(Cy)$_3$ & $H^{15,17}$)	δ 1.39 (s, 3H, H^{19})
C24	δ 8.63 (d, $^{4}J_{H\text{-}P}$ = 6.7 Hz, 1H, H^{7})	δ 7.74-7.60 (comp., 8H, B(Ar)$_4$), δ 7.54-7.46 (comp., 4H, B(Ar)$_4$), δ 7.33-7.20 (comp., 4H, Ar-H), δ 6.99-6.93 (m, 1H, Ar-H), δ 6.92-6.86 (m, 1H, H^{11})		δ 3.29-3.17 (m, 2H, $H^{14,16}$)	δ 2.21-2.07 (comp., 4H, P(Cy)$_3$), δ 1.98-1.87 (comp., 6H, P(Cy)$_3$), δ 1.87-1.77 (comp., 6H, P(Cy)$_3$), δ 1.75-1.66 (comp., 3H, P(Cy)$_3$), δ 1.64-1.49 (comp., 6H, P(Cy)$_3$), δ 1.31-1.07 (comp., 20H, P(Cy)$_3$ & $H^{15,17}$)	δ 1.38 (s, 3H, H^{19})
C25	δ 8.44 (d, $^{4}J_{H\text{-}P}$ = 6.9 Hz, 1H, H^{7})	δ 7.74-7.65 (comp., 8H, B(Ar)$_4$), δ 7.55-7.48 (comp., 4H, B(Ar)$_4$), δ 7.33-7.17 (comp., 4H, Ar-H), δ 6.79-6.65 (comp., 2H, Ar-H)	δ 3.81 (s, 3H, *o*-methoxy Me),	δ 3.29-3.21 (m, 2H, $H^{14,16}$)	δ 2.25-2.05 (comp., 4H, P(Cy)$_3$), δ 2.02-1.46 (comp., 21H, P(Cy)$_3$), δ 1.34-1.05 (comp., 20H, P(Cy)$_3$ & $H^{15,17}$)	δ 1.39 (s, 3H, H^{19})

[a] Spectra recorded in $CDCl_3$ at 298 K; chemical shifts reported as δ ppm values, referenced relative to the residual $CDCl_3$ resonance; superscripts denote protons as per numbering scheme **Figure 3.2a**; s = singlet, d = doublet, t = triplet, dd = doublet of doublets, td = triplet of doublets, sept. = septet, m = multiplet (denotes complex pattern for a single proton resonance), comp. = complex (denotes complex pattern of overlapping proton resonances)

Table 3.5: ^{1}H NMR spectral data of neutral mononuclear palladacycles, **C31-C35.** [a]

Complex	C=N***H***	Aromatic region	Aliphatic region			
			OC***H*₃**	$(CH_3)_2C$***H***	$CH(C$***H*₃**$)_2$	C***H*₃**CN
C31	δ 8.11 (d, $^{4}J_{H\text{-}P}$ = 7.7 Hz, 1H, H^{7})	δ 7.74-7.61 (comp., 15H, PPh_3 & $B(Ar)_4$), δ 7.55-7.39 (comp., 13H, PPh_3 & $B(Ar)_4$ & H^{1}), δ 7.27-7.17 (comp., 3H, $H^{10,11,12}$), δ 7.12 (t, $^{3}J_{H\text{-}H}$ = 7.2 Hz, 1H, H^{2}), δ 6.77 (t, $^{3}J_{H\text{-}H}$ = 7.6 Hz, 1H, H^{3}), δ 6.50-6.44 (m, 1H, H^{4}).		δ 3.40-3.27 (m, 2H, $H^{14,16}$)	δ 1.28 (d, $^{3}J_{H\text{-}H}$ = 7.0 Hz, 6H, $H^{15,17}$), δ 1.25 (d, $^{3}J_{H\text{-}H}$ = 7.0 Hz, 6H, $H^{15,17}$)	δ 1.04 (s, 3H, H^{19})
C32	δ 8.59 (d, $^{4}J_{H\text{-}P}$ = 7.6 Hz, 1H, H^{7})	δ 7.72-7.68 (comp., 7H, $B(Ar)_4$), δ 7.67-7.62 (comp., 6H, PPh_3), δ 7.53-7.49 (comp., 5H, $B(Ar)_4$), δ 7.46-7.41 (comp., 6H, PPh_3), δ 7.29-7.19 (comp., 3H, $H^{10,11,12}$), δ 7.05 (d, $^{3}J_{H\text{-}H}$ = 7.5 Hz, 1H, H^{2}), δ 6.69 (t, $^{3}J_{H\text{-}H}$ = 7.7 Hz, 1H, H^{3}), δ 6.38-6.31 (m, 1H, H^{4}).		δ 3.37-3.29 (m, 2H, $H^{14,16}$)	δ 1.29 (d, $^{3}J_{H\text{-}H}$ = 7.0 Hz, 6H, $H^{15,17}$), δ 1.28 (d, $^{3}J_{H\text{-}H}$ = 7.0 Hz, 6H, $H^{15,17}$)	δ 1.05 (s, 3H, H^{19})
C33	δ 8.59 (d, $^{4}J_{H\text{-}P}$ = 7.5 Hz, 1H, H^{7})	δ 7.75-7.58 (comp., 15H, $B(Ar)_4$ & PPh_3), δ 7.55-7.48 (comp., 6H, $B(Ar)_4$), δ 7.47-7.39 (comp., 6H, PPh_3), δ 7.30-7.18 (comp., 4H, $H^{2,10,11,12}$), δ 6.58 (t, $^{3}J_{H\text{-}H}$ = 7.9 Hz, 1H, H^{3}), δ 6.43-6.35 (m, 1H, H^{4}).		δ 3.39-3.26 (m, 2H, $H^{14,16}$)	δ 1.29 (d, $^{3}J_{H\text{-}H}$ = 6.8 Hz, 6H, $H^{15,17}$), δ 1.28 (d, $^{3}J_{H\text{-}H}$ = 6.8 Hz, 6H, $H^{15,17}$)	δ 1.04 (s, 3H, H^{19})
C34	δ 8.44 (d, $^{4}J_{H\text{-}P}$ = 7.6 Hz, 1H, H^{7})	δ 7.72-7.68 (comp., 7H, $B(Ar)_4$), δ 7.67-7.62 (comp., 8H, PPh_3), δ 7.53-7.48 (comp., 5H, $B(Ar)_4$), δ 7.47-7.40 (comp., 7H, PPh_3), δ 7.28-7.19 (comp., 3H, $H^{10,11,12}$), δ 6.84-6.74 (comp., 2H, $H^{2,3}$), δ 6.25-6.20 (m, 1H, H^{4}).		δ 3.36-3.27 (m, 2H, $H^{14,16}$)	δ 1.29 (d, $^{3}J_{H\text{-}H}$ = 6.8 Hz, 6H, $H^{15,17}$), δ 1.27 (d, $^{3}J_{H\text{-}H}$ = 6.9 Hz, 6H, $H^{15,17}$)	δ 1.05 (s, 3H, H^{19})
C35	δ 8.52 (d, $^{4}J_{H\text{-}P}$ = 8.0 Hz, 1H, H^{7})	δ 7.74-7.60 (comp., 15H, $B(Ar)_4$ & PPh_3), δ 7.54-7.47 (comp., 6H, $B(Ar)_4$), δ 7.46-7.39 (comp., 6H, PPh_3), δ 7.25-7.16 (comp., 3H, $H^{10,11,12}$), δ 6.74 (t, $^{3}J_{H\text{-}H}$ = 8.2 Hz, 1H, H^{3}), δ 6.57 (d, $^{3}J_{H\text{-}H}$ = 8.5 Hz, 1H, H^{2}), δ 6.05-5.98 (m, 1H, H^{4}).	δ 3.79 (s, 3H, *o*-methoxy Me),	δ 3.49-3.30 (m, 2H, $H^{14,16}$)	δ 1.28 (d, $^{3}J_{H\text{-}H}$ = 6.7 Hz, 6H, $H^{15,17}$), δ 1.26 (d, $^{3}J_{H\text{-}H}$ = 6.6 Hz, 6H, $H^{15,17}$)	δ 1.04 (s, 3H, H^{19})

[a] Spectra recorded in $CDCl_3$ at 298 K; chemical shifts reported as δ ppm values, referenced relative to the residual $CDCl_3$ resonance; superscripts denote protons as per numbering scheme **Figure 3.2a**; s = singlet, d = doublet, t = triplet, dd = doublet of doublets, td = triplet of doublets, sept. = septet, m = multiplet (denotes complex pattern for a single proton resonance), comp. = complex (denotes complex pattern of overlapping proton resonances)

3.2.1.3 Mass spectrometry, elemental analysis and thermal stability

ESI-MS spectra recorded in both the positive and negative ion mode were consistent with the proposed structures for cationic palladacycle complexes **C11-C15**, **C21-C25** and **C31-C35**. The mass spectral data for complexes **C11-C15** showed a $[M\text{-}PTA]^+$ fragment ion as the base peak (**Figure 3.4a**) whereas the base peak for complexes **C21-C25** and **C31-C35** corresponds to the $[M\text{-}MeCN]^+$ fragment ion (**Table 3.6**). The molecular ion $[M]^+$ was only observed for complexes **C11-C15**. Complexes **C12-C15** also show peaks which correspond to the μ-Cl dimeric species $[2M\text{-}2MeCN+Cl]^+$ observed at higher *m/z*. It has been reported that the formation of dimeric ions in ESI-MS studies is common for palladium complexes.[11] The only fragment in the negative ion mode for all analogues corresponds to the mass of the $[B(Ar)_4]^-$ counterion (**Figure 3.4b**). Calculated isotopic clusters[12] for each assigned fragment coincide exactly with the experimentally observed isotopic fragments. Further characterization by elemental analysis corresponds well with the calculated values. The results indicate the entrapment of dichloromethane molecules which is supported by both ^1H NMR spectroscopy and X-ray diffraction analysis. Decomposition temperatures for the cationic palladacycle complexes were lower than those determined for their neutral counterparts.

Table 3.6: Mass spectral data and decomposition temperatures for cationic palladacycle complexes

Cationic complex	ESI-MS [a] (*m/z*)	Decomposition temperature [c] (°C)
C11	568 [b]	145-143
C12	604 [b]	147-145
C13	648 [b]	164-161
C14	586 [b]	143-141
C15	598 [b]	157-155
C21	650	169-168
C22	684	163-160
C23	730	170-168
C24	668	146-143
C25	680	150-147
C31	632	167-165
C32	666	162-160
C33	712	143-140
C34	650	137-134
C35	662	160-158

ESI-MS recorded in the positive ion mode. [a] Reported ion corresponds to the $[M\text{-}MeCN]^+$, unless otherwise stated. [b] Reported ion corresponds to the $[M]^+$. [c] Decomposition temperatures reported are uncorrected. No melting prior to decomposition.

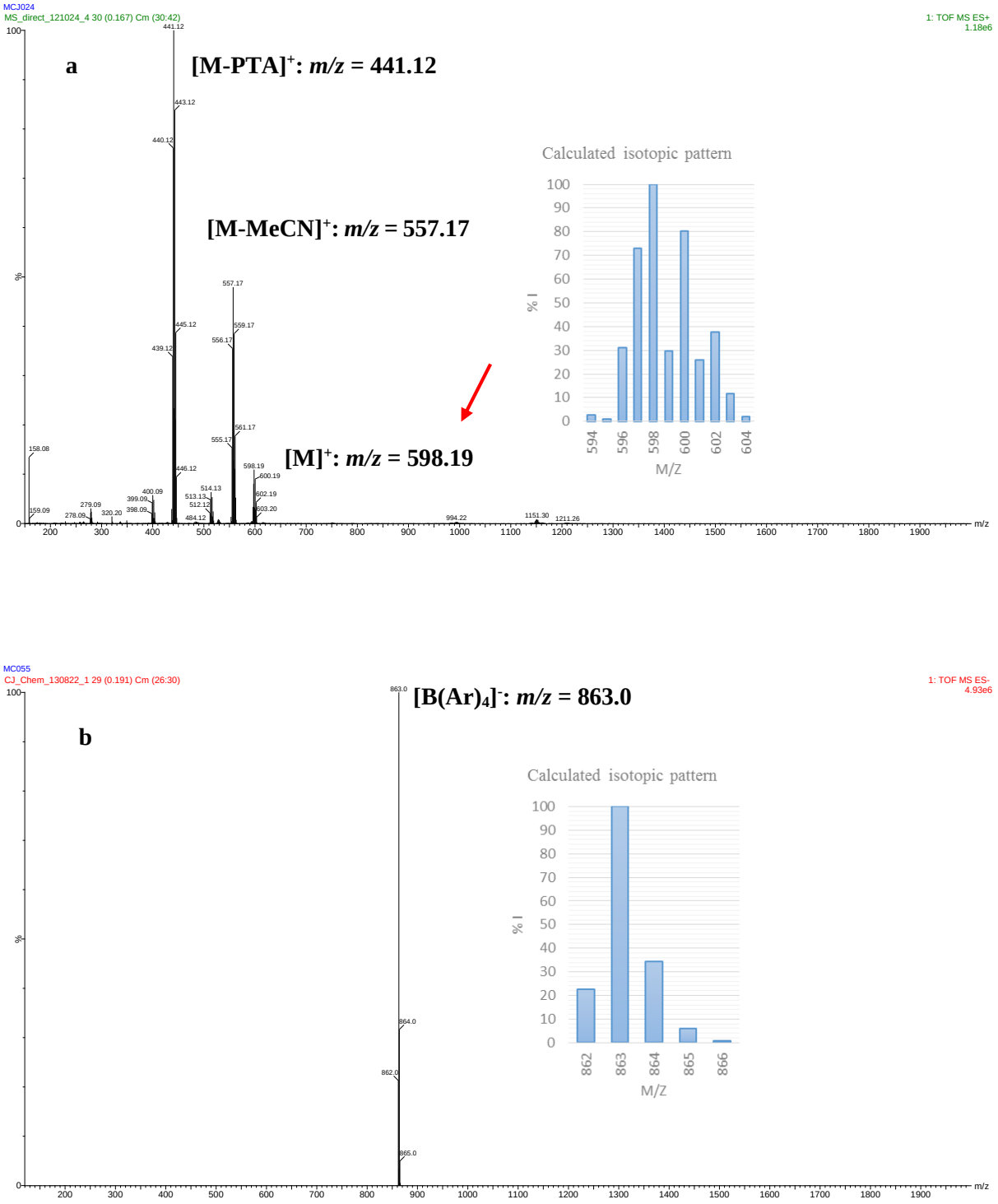

Figure 3.4: ESI-MS spectrum of cationic palladacycle **C15** and **C23** recorded in the positive and negative mode repectively. (**a**) Clusters of peaks centred at 441.1 *m/z*, 557.2 *m/z* and 598.2 *m/z* correspond to the $[M\text{-}PTA]^+$, $[M\text{-}MeCN]^+$ and $[M]^+$ fragments respectively. (**b**) Cluster of peaks centred at 863.0 *m/z* correspond to the $[B(Ar)_4]^-$ counterion fragment for **C23**. Inset shows calculated isotopic pattern for a specific fragmentation.

3.2.1.4 Single crystal x-ray diffraction

Single crystals suitable for X-ray diffraction analysis of complexes **C15** and **C25** were isolated by slow diffusion of hexane into a dichloromethane solution at room temperature which resulted in formation of colourless crystals. All atomic labels are given in the ORTEP pictures depicted in **Figure 3.5** and **Figure 3.6**. Crystallographic data for **C15** and **C25** are presented in **Table 3.7** while selected bond lengths, bond angles and torsion angle are presented in **Table 3.8**.

The molecular structures of the complexes exhibit a slightly distorted square-planar geometry around the palladium centre in which the coordination sphere of the metal is occupied by the *N*-benzylidene bound bidentate ligand (N^C) as well as the phosphine ligand. The vacant coordination site is occupied by the weakly coordinating acetonitrile molecule. The orientation of the phosphine ligands remain *trans* relative to the imine moiety upon coordination of the acetonitrile ligand. The distorted square planar geometry around the metal is discernibly demonstrated by the bond angles N(1)-Pd-C(1) and C(1)-Pd-P(1) which occur in the range 81.7°-80.7° and 98.6°-94.5° respectively (**Table 3.8**). Similar to the molecular structures of the neutral complexes (**Chapter 2)**, the more sterically bulky PCy_3 ligand in complex **C25** (**Figure 3.6**) seems to increase the strain on the five-membered ring which results in the *endo*cycle being less planar in comparison to complex **C15** containing the less bulkier PTA ligand (**Figure 3.5**). The torsion angle C(8)-N(1)-C(9)-C(10) for both complexes **C15** and **C25** is -88.55(1)° and 108.22(1)° respectively, which reveals that the plane of the 2,6-diisopropylaniline moiety is nearly perpendicular to the plane of the five-membered *endo*cycle ring. The Pd-N(1) bond length for complexes **C15** and **C25** are 2.0975(2) Å and 2.0995(2) Å respectively and are within the range observed for analogues *endo*cyclic complexes.[13]

The counterion consists of a boron atom of which the coordination sphere is occupied by four 3,5-*bis*-(trifluoromethyl)phenyl groups. Some of the trifluoromethyl substituents are disordered due to fluxional motion (purple and orange ellipsoid) of the fluoride atoms. A number of weak non-covalent intermolecular interactions are present in the crystal lattice for complex **C15** and **C25,** which include

C-H·····F and C-H·····N hydrogen bonding interactions with bond lengths and bond angles in the region of 2.5700(3) Å - 2.4600(3) Å and 175.0° – 120.0° respectively.

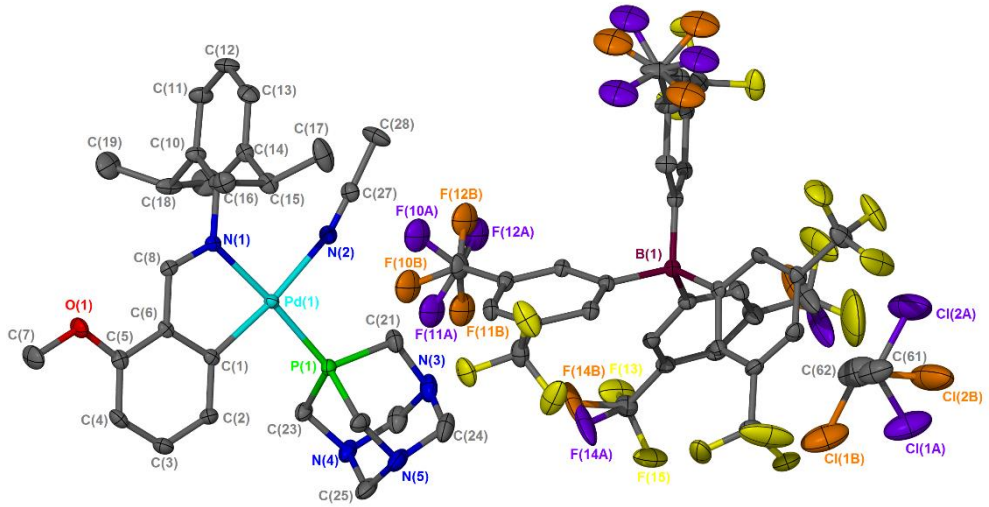

Figure 3.5: Molecular structure of solvated complex **C15** with atomic numbering, drawn at 50% probability ellipsoids. All hydrogen atoms are omitted for clarity. Disorder of the trifluoromethyl substituents of the counterion is indicated in orange and purple.

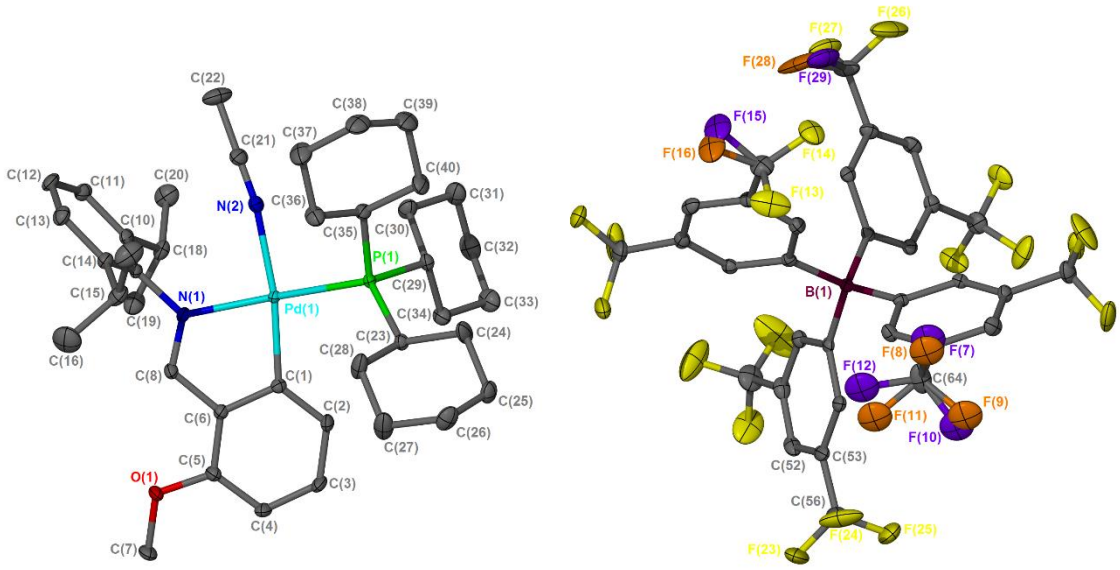

Figure 3.6: Molecular structure of complex **C25** with atomic numbering, drawn at 50% probability ellipsoids. All hydrogen atoms are omitted for clarity. Disorder of the trifluoromethyl substituents of the counterion is indicated in orange and purple.

Table 3.7: Crystallographic data and structure refinement parameters for cationic palladacycles **C15** and **C25**.

Parameter	Complex	
	C15	**C25**
Empirical formula	$C_{61}H_{53}BCl_2F_{24}N_5OPPd$	$C_{72}H_{72}BF_{24}N_2OPPd$
Mr (g/mol)	1547.16	1585.50
Crystal system	Orthorhombic	Triclinic
Space group	P2(1)2(1)2(1)	P-1
***a* (Å)**	13.9241(13)	10.0762(10)
***b* (Å)**	18.1629(17)	18.3919(19)
***c* (Å)**	25.815(2)	19.844(2)
***α* (deg)**	90	101.149(1)
***β* (deg)**	90	92.522(1)
***γ* (deg)**	90	92.592(1)
Crystal dimension (mm)	0.33 × 0.34 × 0.40	0.15 × 0.19 × 0.22
Volume (Å^3)	6528.7(10)	3599.1(6)
Z	4	2
D_{calc} (g/cm^3)	1.574	1.463
F(000)	3112.0	1616
λ (MoK_a) (Å)	0.71073	0.71073
Temperature (K)	100	100
2*θ* max (deg)	28.270	28.480
absorption corrections applied (mm^{-1})	0.504	0.387
Goodness-of-fit on F^2	1.018	1.039
Final R_1 indices [I>2σ(I)]	0.0444	0.0383
wR_2 (all reflections)	0.1084	0.0942

Table 3.8: Selected bond lengths (Å), bond angles (°) and torsion angle (°) as determined for cationic palladacycles **C15** and **C25.** [a]

	Complex	
	C15	**C25**
Bond lengths		
Pd-C1	2.0091(2)	2.0015(2)
Pd-N1	2.0975(2)	2.0995(2)
Pd-N2	2.0872(2)	2.1079(2)
Pd-P1	2.2415(2)	2.3086(2)
N1-C8	1.0757(1)	1.2835(1)
N1-C9	1.4435(1)	1.4369(1)
C6-C8	1.4340(1)	1.4403(1)
O1-C5	1.3579(1)	1.3580(1)
Bond angles		
N1-Pd-N2	90.24(1)	89.62(1)
N1-Pd-C1	81.61(1)	80.75(1)
C1-Pd-P1	94.62(1)	98.59(1)
P1-Pd-N2	93.62(1)	92.59(1)
Torsion angles		
C8-N1-C9-C10	-88.55(1)	108.22(1)

[a] Atoms are labelled as per numbering given in **Figure 3.5** and **Figure 3.6**

3.3 Conclusion

In this chapter, a series of cationic palladacycle complexes (**C11-C15; C21-C25; C31-C35**) containing acetonitrile as the coordinating ligand were prepared *via* a chloride abstraction reaction of the previously discussed neutral palladacycle complexes (**C6-C10; C16-C20; C26-C30**) with $NaB(Ar)_4$. Various analytical techniques were employed for the successful characterization of these complexes. Spectroscopy data revealed the successful coordination of acetonitrile to the metal centre which was confirmed by the crystal structures isolated. Complexes **C15** and **C25** have a distorted square planar geometry around the metal centre with the plane of the 2,6-diisopropylaniline moiety almost perpendicular to the plane of the *endo*cycle ring.

3.4 Experimental section

3.4.1 General remarks

All transformations were carried out under an inert atmosphere of dry nitrogen using a dual vacuum/nitrogen line and standard Schlenk techniques, unless specified otherwise. All reagents were acquired from Sigma-Aldrich, Merck or Alfa Aesar and used without further purification. Solvents were obtained from Merck and Kimix and purified by a Pure Solv^{TM} micro solvent purifier fitted with activated alumina columns. In the case of methanol and ethanol, the solvents were dried by distillation over a mixture of magnesium fillings and iodine. Acetonitrile was dried by distillation over phosphorous pentoxide. Reaction progress and product mixtures were monitored by thin-layer chromatography using precoated silica-gel F254. Selected complexes were purified by flash chromatography using an advanced automated Isolera One Biotage flash chromatography unit, equipped with a 200-450 nm variable UV detector. The palladium precursor, bis(acetonitrile) palladium(II)chloride, was prepared by the reaction of palladium(II)chloride with excess acetonitrile under reflux for 3 hours.[14]

3.4.2 Instruments

Melting points determinations were recorded on a Stuart Scientific SMP3 apparatus and are reported as uncorrected. FT-IR analyses were performed on a Thermo Nicolet AVATAR 330 instrument with a smart ATR performer and recorded as neat samples. ^{1}H, ^{13}C ^{19}F and ^{31}P NMR spectra were recorded on Varian VNMRS 300 MHz and Varian Unity Inova 400 and 600 MHz spectrometers. The chemical shifts for proton and carbon spectra are internally referenced to the residual deuterated solvents and externally referenced to tetramethyl silane (TMS). Chemical shifts for phosphorous spectra are externally referenced relative to 85% phosphoric acid (H_3PO_4). Elemental analyses were performed on a Thermo Elemental Analyser CHNS-O instrument at the University of Cape Town. ESI-MS analyses, recorded in the positive mode, were recorded on a Waters API Quattro Micro and Water API Q-TOF Ultima instruments by direct injections. Single X-ray diffraction intensity data were collected on a Bruker SMART Apex 2 diffractometer with a CCD area detector[15] using graphite monochromated Mo-Kα radiation (λ = 0.71073 Å). Data collection, reduction and refinement were performed using SMART and SAINT software.[16] Absorption corrections[17] and other systematic errors were accounted for using SADABS.[18] All structures were solved by Direct Methods using SHELXS-97 and refined using SHELXL-97.[19] The program X-Seed [20] was used as a graphical interface for the SHELX program. All non-hydrogen atoms were refined anisotropically. High resolution molecular diagrams were produced using the program POV-Ray.[21]

3.5 Methods and characterization

3.5.1 Synthesis of cationic palladacycles with monodentate phosphine, PTA

3.5.1.1 $[Pd(PTA)(MeCN)(C_6H_4)CH{=}N\{2,6\text{-}^{i}Pr_2\text{-}C_6H_3\}]^+ [B(Ar)_4]^-$ (C11)

To a stirring solution of the neutral mononuclear palladacycle complex (**C6**, 0.08 g, 0.142 mmol) in dichloromethane (7 mL) was added 1.2 equivalence $Na[B(Ar)_4]$ (0.15 g, 0.170 mmol) dissolved in acetonitrile (3 mL). The resulting off-white solution was stirred under an inert atmosphere for 2 hours at room temperature. The solvent was removed *in vacuo* leaving an off-white oily residue which was

redissolved in dichloromethane (10 mL). The sodium chloride precipitate which formed was filtered off after which the solvent was removed from the filtrate *in vacuo*. The product was isolated as an off-white powder (0.17 g, 83%) by triturating the oily residue with *n*-hexane. Recrystallization of palladacycle **C11** was achieved by means of slow evaporation of a dichloromethane/*n*-hexane solution of the compound at room temperature. Melting point: 143 – 145 °C (decomposes without melting). FT-IR *ν*(C=N) 1620 cm^{-1}; *ν*(C-F) 1352; 1274; 1117 cm^{-1}. ^{13}C {^{1}H} NMR (151 MHz, $CDCl_3$, numbering as per **Figure 3.2a**): δ 178.1 (d, $^{3}J_{C-P}$ = 4.0 Hz, C^{7}), δ 161.8 (q, $^{1}J_{C-B}$ = 48.2 Hz, C^{20}), δ 152.8 (d, J_{C-P} = 6.1, Ar-C), δ 147.5 (Ar-C), δ 143.0 (Ar-C), δ 140.8 (Ar-C), δ 136.2 (Ar-C), δ 136.1 (Ar-C), δ 134.9 (br, C^{21}), δ 133.7 (d, J_{C-P} = 6.1, Ar-C), δ 132.0 (Ar-C), δ 129.0 (qq, $^{2}J_{C-F}$ = 31.5, $^{3}J_{C-B}$ = 3.0 Hz, C^{22}), δ 128.7 (Ar-C), δ 127.4 (Ar-C), δ 127.3 (Ar-C), δ 125.6 (Ar-C), δ 124.1 (Ar-C), δ 123.8 (Ar-C), δ 122.0 (Ar-C), δ 121.7 (C^{18}), δ 117.6 (sept., $^{3}J_{C-F}$ = 3.8 Hz, C^{23}), δ 73.2 (d, $^{3}J_{C-P}$ = 7.4 Hz, N-***C***H_2-N), δ 52.1 (d, $^{3}J_{C-P}$ = 14.4 Hz, N-***C***H_2-P), δ 28.6 ($C^{14,16}$), δ 24.4 ($C^{15,17}$), δ 22.8 ($C^{15,17}$), δ 0.8 (C^{19}). ^{31}P {^{1}H} NMR (121 MHz, $CDCl_3$): δ -46.9 (s). ESI-MS (+.ve, m/z): 568.18 $[M]^+$; 527.16 $[M\text{-}MeCN]^+$; 411.11 $[M\text{-}PTA]^+$; 370.08 $[M\text{-}PTA\text{-}MeCN]^+$. *Anal. Calc.* for $C_{59}H_{49}BF_{24}N_5PPd$: C, 49.48; H, 3.45; N, 4.89. *Found:* C, 49.87; H, 3.24; N, 4.43.

3.5.1.2 [Pd(PTA)(MeCN)(2-Cl-C_6H_3)CH=N{2,6-$^{i}Pr_2$-C_6H_3}]$^+$ [B(Ar)$_4$]$^-$ (C12)

The cationic palladacycle **C12** was isolated as an off-white powder (0.16 g, 81 %) using the same synthetic procedure as outlined above for **C11**. The neutral palladacycle **C7** was used as the corresponding reactant. Melting point: 145 – 147 °C (decomposes without melting). FT-IR *ν*(C=N) 1611 cm^{-1}; *ν*(C-F) 1353; 1272; 1110 cm^{-1}. ^{13}C {^{1}H} NMR (75 MHz, $CDCl_3$, numbering as per **Figure 3.2a**): δ 176.5 (d, $^{3}J_{C-P}$ = 4.2 Hz, C^{7}), δ 161.8 (q, $^{1}J_{C-B}$ = 50.6 Hz, C^{20}), δ 150.7 (Ar-C), δ 144.6 (Ar-C), δ 143.2 (Ar-C), δ 140.8 (Ar-C), δ 136.2 (Ar-C), δ 134.9 (br, C^{21}), δ 134.5 (Ar-C), δ 131.2 (Ar-C), δ 130.1 (Ar-C), δ 129.2 (Ar-C), δ 129.0 (qq, $^{2}J_{C-F}$ = 29.9, $^{3}J_{C-B}$ = 2.7 Hz, C^{22}), δ 128.9 (Ar-C), δ 128.2 (Ar-C), δ 126.5 (Ar-C), δ 124.2 (Ar-C), δ 122.9 (Ar-C), δ 119.3 (C^{18}), δ 117.6 (sept., $^{3}J_{C-F}$ = 3.7 Hz, C^{23}), δ 73.1 (d, $^{3}J_{C-P}$ = 6.8 Hz, N-***C***H_2-N), δ 52.0 (d, $^{3}J_{C-P}$ = 14.1 Hz, N-***C***H_2-P), δ 28.6 ($C^{14,16}$), δ 24.5 ($C^{15,17}$), δ 22.7 ($C^{15,17}$), δ 0.8 (C^{19}). ^{31}P {^{1}H} NMR (121 MHz, $CDCl_3$): δ -46.9 (s). ESI-MS (+.ve, m/z):

1161.20 [2M-2MeCN+Cl]$^+$; 604.14 [M]$^+$; 563.12 [M-MeCN]$^+$; 447.07 [M-PTA]$^+$; 406.04 [M-PTA-MeCN]$^+$. *Anal. Calc.* for $C_{59}H_{48}BClF_{24}N_5PPd$: C, 48.32; H, 3.30; N, 4.78. *Found:* C, 48.66; H, 3.05; N, 4.22.

3.5.1.3 [Pd(PTA)(MeCN)(2-Br-C_6H_3)CH=N{2,6-^{i}Pr$_2$-C_6H_3}]$^+$ [B(Ar)$_4$]$^-$ (C13)

The cationic palladacycle **C13** was isolated as an off-white powder (0.15 g, 80 %) using the same synthetic procedure as outlined above for **C11**. The neutral palladacycle **C8** was used as the corresponding reactant. Melting point: 161 – 164 °C (decomposes without melting). FT-IR *ν*(C=N) 1612 cm^{-1}; *ν*(C-F) 1353; 1272; 1112 cm^{-1}. ^{13}C {^{1}H} NMR (151 MHz, $CDCl_3$, numbering as per **Figure 3.2a**): δ 178.9 (d, $^3J_{C\text{-}P}$ = 3.9 Hz, C^7), δ 161.9 (q, $^1J_{C\text{-}B}$ = 50.6 Hz, C^{20}), δ 154.2 (d, $J_{C\text{-}P}$ = 5.7, Ar-C), δ 145.9 (Ar-C), δ 143.2 (Ar-C), δ 140.8 (Ar-C), δ 135.2 (Ar-C), δ 135.1 (Ar-C), δ 134.9 (br, C^{21}), δ 131.5 (Ar-C), δ 129.0 (qq, $^2J_{C\text{-}F}$ = 31.2, $^3J_{C\text{-}B}$ = 2.7 Hz, C^{22}), δ 128.9 (Ar-C), δ 127.4 (Ar-C), δ 125.6 (Ar-C), δ 125.0 (Ar-C), δ 124.2 (Ar-C), δ 123.8 (Ar-C), δ 122.0 (Ar-C), δ 121.9 (C^{18}), δ 117.6 (sept., $^3J_{C\text{-}F}$ = 4.3 Hz, C^{23}), δ 73.2 (d, $^3J_{C\text{-}P}$ = 7.6 Hz, N-***C***H$_2$-N), δ 52.1 (d, $^3J_{C\text{-}P}$ = 14.5 Hz, N-***C***H$_2$-P), δ 28.7 (C^{14,16}), δ 24.5 (C^{15,17}), δ 22.8 (C^{15,17}), δ 0.8 (C^{19}). ^{31}P {^{1}H} NMR (121 MHz, $CDCl_3$): δ -47.8 (s). ESI-MS (+.ve, m/z): 1249.10 [2M-2MeCN+Cl]$^+$; 648.09 [M]$^+$; 607.07 [M-MeCN]$^+$; 491.02 [M-PTA]$^+$; 449.99 [M-PTA-MeCN]$^+$. ESI-MS (-.ve, m/z): 863.07 [B(Ar)$_4$]$^-$. *Anal. Calc.* for $C_{59}H_{48}BBrF_{24}N_5PPd{\bullet}1CH_2Cl_2$: C, 45.15; H, 3.16; N, 4.39. *Found:* C, 45.09; H, 2.88; N, 4.59.

3.5.1.4 [Pd(PTA)(MeCN)(2-F-C6H3)CH=N{2,6-iPr2-C6H3}]+ [B(Ar)4]- (C14)

The cationic palladacycle **C14** was isolated as an off-white powder (0.17 g, 86 %) using the same synthetic procedure as outlined above for **C11**. The neutral palladacycle **C9** was used as the corresponding reactant. Melting point: 141 – 143 °C (decomposes without melting). FT-IR *ν*(C=N) 1611 cm^{-1}; *ν*(C-F) 1353; 1272; 1111 cm^{-1}. ^{13}C {^{1}H} NMR (101 MHz, $CDCl_3$, numbering as per **Figure 3.2a**): δ 172.8 (d, $^3J_{C\text{-}P}$ = 4.0 Hz, C^7), δ 163.2 (Ar-C), δ 161.8 (q, $^1J_{C\text{-}B}$ = 51.1 Hz, C^{20}), δ 160.6 (Ar-C), δ 153.9 (d, $J_{C\text{-}P}$ = 6.3, Ar-C), δ 143.2 (Ar-C), δ 140.8 (Ar-C), δ 136.2 (dd, $J_{C\text{-}P}$ = 8.3, 5.7 Hz, Ar-C), δ 134.9 (br, C^{21}), δ 131.8 (dd, $J_{C\text{-}P}$ = 11.6, 3.3 Hz, Ar-C), δ 129.0 (qq, $^2J_{C\text{-}F}$ = 31.4, $^3J_{C\text{-}B}$ = 3.0 Hz, C^{22}),

δ 128.8 (Ar-C), δ 128.7 (Ar-C), δ 126.1 (Ar-C), δ 124.1 (Ar-C), δ 123.3 (Ar-C), δ 121.9 (Ar-C), δ 120.0 (C^{18}), δ 117.6 (sept., $^{3}J_{C\text{-}F}$ = 3.8 Hz, C^{23}), δ 172.8 (d, $J_{C\text{-}P}$ = 19.3 Hz, Ar-C), δ 73.1 (d, $^{3}J_{C\text{-}P}$ = 7.6 Hz, N-***C***H_2-N), δ 52.2 (d, $^{3}J_{C\text{-}P}$ = 14.5 Hz, N-***C***H_2-P), δ 28.6 ($C^{14,16}$), δ 24.4 ($C^{15,17}$), δ 22.8 ($C^{15,17}$), δ 0.8 (C^{19}). ^{31}P {^{1}H} NMR (162 MHz, $CDCl_3$): δ -46.3 (s). ESI-MS (+.ve, m/z): 1127.25 $[2M\text{-}2MeCN+Cl]^+$; 586.17 $[M]^+$; 545.15 $[M\text{-}MeCN]^+$; 429.10 $[M\text{-}PTA]^+$; 388.07 $[M\text{-}PTA\text{-}MeCN]^+$. *Anal. Calc.* for $C_{59}H_{48}BF_{25}N_5PPd$: C, 48.86; H, 3.34; N, 4.83. *Found:* C, 49.25; H, 3.18; N, 4.34.

3.5.1.5 [Pd(PTA)(MeCN)(2-F-C_6H_3)CH=N{2,6-^{i}Pr$_2$-C_6H_3}]$^+$ [B(Ar)$_4$]$^-$ (C15)

The cationic palladacycle **C15** was isolated as an off-white powder (0.17 g, 85 %) using the same synthetic procedure as outlined above for **C11**. The neutral palladacycle **C10** was used as the corresponding reactant. Melting point: 155 – 157 °C (decomposes without melting). FT-IR *ν*(C=N) 1605 cm^{-1}; *ν*(C-F) 1352; 1273; 1112 cm^{-1}. ^{13}C {^{1}H} NMR (75 MHz, $CDCl_3$, numbering as per **Figure 3.2a**): δ 174.8 (d, $^{3}J_{C\text{-}P}$ = 4.0 Hz, C^7), δ 161.8 (q, $^{1}J_{C\text{-}B}$ = 50.0 Hz, C^{20}), δ 160.9 (Ar-C), δ 154.7 (Ar-C), δ 143.7 (Ar-C), δ 141.2 (Ar-C), δ 135.9 (Ar-C), δ 135.1 (Ar-C), δ 134.9 (br, C^{21}), δ 130.1 (Ar-C), δ 129.0 (qq, $^{2}J_{C\text{-}F}$ = 31.6, $^{3}J_{C\text{-}B}$ = 2.9 Hz, C^{22}), δ 128.4 (Ar-C), δ 128.2 (Ar-C), δ 126.5 (Ar-C), δ 123.9 (Ar-C), δ 122.9 (Ar-C), δ 121.6 (Ar-C), δ 119.3 (C^{18}), δ 117.6 (sept., $^{3}J_{C\text{-}F}$ = 4.1 Hz, C^{23}), δ 109.9 (Ar-C), δ 73.2 (d, $^{3}J_{C\text{-}P}$ = 7.7 Hz, N-***C***H_2-N), δ 56.0 (*o*-methoxy Me), δ 52.1 (d, $^{3}J_{C\text{-}P}$ = 14.4 Hz, N-***C***H_2-P), δ 28.5 ($C^{14,16}$), δ 24.5 ($C^{15,17}$), δ 22.8 ($C^{15,17}$), δ 0.8 (C^{19}). ^{31}P {^{1}H} NMR (121 MHz, $CDCl_3$): δ -48.1 (s). ^{19}F {^{1}H} NMR (282 MHz, $CDCl_3$): δ -62.6 (s). ESI-MS (+.ve, m/z): 1151.30 $[2M\text{-}2MeCN+Cl]^+$; 598.19 $[M]^+$; 557.17 $[M\text{-}MeCN]^+$; 441.12 $[M\text{-}PTA]^+$; 400.09 $[M\text{-}PTA\text{-}MeCN]^+$. *Anal. Calc.* for $C_{60}H_{51}BF_{24}N_5OPPd\bullet 1CH_2Cl_2$: C, 47.35; H, 3.45; N, 4.53. *Found:* C, 47.62; H, 3.27; N, 4.59.

3.5.2 Synthesis of cationic palladacycles with monodentate phosphine, PCy_3

3.5.2.1 [Pd(PCy_3)(MeCN)(C_6H_4)CH=N{2,6-^{i}Pr$_2$-C_6H_3}]$^+$ [B(Ar)$_4$]$^-$ (C21)

The cationic palladacycle **C21** was isolated as an off-white powder (0.15 g, 85 %) using the same synthetic procedure as outlined above for **C11**. The neutral palladacycle **C16** was used as the corresponding reactant. Melting point: 168 – 169 °C (decomposes without melting). FT-IR *ν*(C=N)

1615 cm^{-1}; *v*(C-F) 1354; 1271; 1113 cm^{-1}. ^{13}C {^{1}H} NMR (101 MHz, $CDCl_3$, numbering as per **Figure 3.2a**): δ 177.8 (d, $^{3}J_{C-P}$ = 4.0 Hz, C^{7}), δ 161.8 (q, $^{1}J_{C-B}$ = 50.6 Hz, C^{20}), δ 153.0 (Ar-C), δ 147.9 (Ar-C), δ 143.9 (Ar-C), δ 141.1 (Ar-C), δ 137.5 (d, J_{C-P} = 5.7 Hz, Ar-C), δ 134.9 (br, C^{21}), δ 132.5 (d, J_{C-P} = 3.8 Hz, Ar-C), δ 129.0 (qq, $^{2}J_{C-F}$ = 31.3, $^{3}J_{C-B}$ = 2.9 Hz, C^{22}), δ 128.8 (Ar-C), δ 128.5 (Ar-C), δ 126.6 (Ar-C), δ 126.1 (Ar-C), δ 124.2 (Ar-C), δ 123.3 (Ar-C), δ 120.6 (C^{18}), δ 117.6 (sept., $^{3}J_{C-F}$ = 3.9 Hz, C^{23}), δ 34.8 (d, $^{1}J_{C-P}$ = 21.2 Hz, PCy_3), δ 30.4 (PCy_3), δ 28.7 (PCy_3), δ 27.8 (d, $^{2}J_{C-P}$ = 10.4 Hz, PCy_3), δ 26.0 ($C^{14,16}$), δ 24.4 ($C^{15,17}$), δ 22.7 ($C^{15,17}$), δ 0.9 (C^{19}). ^{31}P {^{1}H} NMR (121 MHz, $CDCl_3$): δ 47.7 (s). ESI-MS (+.ve, m/z): 650.3 $[M\text{-}MeCN]^+$; 411.1 $[M\text{-}P(Cy)_3]^+$. ESI-MS (-.ve, m/z): 863.07 $[B(Ar)_4]^-$. *Anal. Calc.* for $C_{71}H_{70}BF_{24}N_2PPd \bullet 0.5CH_2Cl_2$: C, 53.74; H, 4.48; N, 1.75. *Found:* C, 53.61; H, 4.82; N, 1.30.

3.5.2.2 $[Pd(PCy_3)(MeCN)(2\text{-}Cl\text{-}C_6H_3)CH{=}N\{2,6\text{-}^{i}Pr_2\text{-}C_6H_3\}]^+ [B(Ar)_4]^-$ (C22)

The cationic palladacycle **C22** was isolated as an off-white powder (0.15 g, 85 %) using the same synthetic procedure as outlined above for **C11**. The neutral palladacycle **C17** was used as the corresponding reactant. Melting point: 160 – 163 °C (decomposes without melting). FT-IR *v*(C=N) 1616 cm^{-1}; *v*(C-F) 1354; 1276; 1116 cm^{-1}. ^{13}C {^{1}H} NMR (75 MHz, $CDCl_3$, numbering as per **Figure 3.2a**): δ 176.2 (d, $^{3}J_{C-P}$ = 3.9 Hz, C^{7}), δ 161.8 (q, $^{1}J_{C-B}$ = 50.4 Hz, C^{20}), δ 154.6 (Ar-C), δ 144.7 (Ar-C), δ 144.1 (Ar-C), δ 141.0 (Ar-C), δ 136.0 (d, J_{C-P} = 5.2 Hz, Ar-C), δ 135.3 (Ar-C), δ 134.9 (br, C^{21}), δ 133.6 (d, J_{C-P} = 4.0 Hz, Ar-C), δ 130.1 (Ar-C), δ 129.0 (qq, $^{2}J_{C-F}$ = 31.5, $^{3}J_{C-B}$ = 3.3 Hz, C^{22}), δ 128.7 (Ar-C), δ 127.6 (Ar-C), δ 126.5 (Ar-C), δ 124.3 (Ar-C), δ 122.9 (Ar-C), δ 119.3 (C^{18}), δ 117.6 (sept., $^{3}J_{C-F}$ = 3.7 Hz, C^{23}), δ 34.8 (d, $^{1}J_{C-P}$ = 21.2 Hz, PCy_3), δ 30.4 (PCy_3), δ 28.8 (PCy_3), δ 27.7 (d, $^{2}J_{C-P}$ = 11.2 Hz, PCy_3), δ 26.0 ($C^{14,16}$), δ 24.5 ($C^{15,17}$), δ 22.7 ($C^{15,17}$), δ 0.9 (C^{19}). ^{31}P {^{1}H} NMR (121 MHz, $CDCl_3$): δ 47.5 (s). ESI-MS (+.ve, m/z): 684.27 $[M\text{-}MeCN]^+$. *Anal. Calc.* for $C_{71}H_{69}BClF_{24}N_2PPd \bullet 1CH_2Cl_2$: C, 51.63; H, 4.27; N, 1.67. *Found:* C, 51.29; H, 4.26; N, 1.01.

3.5.2.3 [Pd(PCy$_3$)(MeCN)(2-Br-C$_6$H$_3$)CH=N{2,6-^{i}Pr$_2$-C$_6$H$_3$}]$^+$ [B(Ar)$_4$]$^-$ (C23)

The cationic palladacycle **C23** was isolated as an off-white powder (0.14 g, 83 %) using the same synthetic procedure as outlined above for **C11**. The neutral palladacycle **C18** was used as the corresponding reactant. Melting point: 168 – 170 °C (decomposes without melting). FT-IR *ν*(C=N) 1613 cm^{-1}; *ν*(C-F) 1353; 1275; 1115 cm^{-1}. ^{13}C {^{1}H} NMR (75 MHz, $CDCl_3$, numbering as per **Figure 3.2a**): δ 178.5 (d, $^3J_{C\text{-}P}$ = 3.6 Hz, C^7), δ 161.8 (q, $^1J_{C\text{-}B}$ = 52.0 Hz, C^{20}), δ 154.8 (Ar-C), δ 146.0 (Ar-C), δ 144.1 (Ar-C), δ 141.0 (Ar-C), δ 136.7 (d, $J_{C\text{-}P}$ = 5.4 Hz, Ar-C), δ 134.9 (br, C^{21}), δ 133.7 (d, $J_{C\text{-}P}$ = 4.0 Hz, Ar-C), δ 130.9 (Ar-C), δ 130.1 (Ar-C), δ 129.0 (qq, $^2J_{C\text{-}F}$ = 32.0, $^3J_{C\text{-}B}$ = 2.5 Hz, C^{22}), δ 128.8 (Ar-C), δ 126.5 (Ar-C), δ 124.3 (Ar-C), δ 124.2 (Ar-C), δ 122.9 (Ar-C), δ 119.3 (C^{18}), δ 117.6 (sept., $^3J_{C\text{-}F}$ = 3.8 Hz, C^{23}), δ 34.8 (d, $^1J_{C\text{-}P}$ = 22.1 Hz, PCy$_3$), δ 30.4 (PCy$_3$), δ 28.8 (PCy$_3$), δ 27.7 (d, $^2J_{C\text{-}P}$ = 11.3 Hz, PCy$_3$), δ 26.0 (C^{14,16}), δ 24.5 (C^{15,17}), δ 22.7 (C^{15,17}), δ 0.9 (C^{19}). ^{31}P {^{1}H} NMR (121 MHz, $CDCl_3$): δ 47.3 (s). ESI-MS (+.ve, m/z): 730.2 [M-MeCN]$^+$; 491.0 [M-P(Cy)$_3$]$^+$. ESI-MS (-.ve, m/z): 863.0 [B(Ar)$_4$]$^-$. *Anal. Calc.* for $C_{71}H_{69}BBrF_{24}N_2PPd{\bullet}2CH_2Cl_2$: C, 48.60; H, 4.08; N, 1.55. *Found:* C, 48.31; H, 4.40; N, 1.35.

3.5.2.4 [Pd(PCy$_3$)(MeCN)(2-F-C$_6$H$_3$)CH=N{2,6-^{i}Pr$_2$-C$_6$H$_3$}]$^+$ [B(Ar)$_4$]$^-$ (C24)

The cationic palladacycle **C24** was isolated as an off-white powder (0.15 g, 86 %) using the same synthetic procedure as outlined above for **C11**. The neutral palladacycle **C19** was used as the corresponding reactant. Melting point: 143 – 146 °C (decomposes without melting). FT-IR *ν*(C=N) 1611 cm^{-1}; *ν*(C-F) 1353; 1276; 1119 cm^{-1}. ^{13}C {^{1}H} NMR (75 MHz, $CDCl_3$, numbering as per **Figure 3.2a**): δ 172.5 (d, $^3J_{C\text{-}P}$ = 4.1 Hz, C^7), δ 163.3 (Ar-C), δ 161.8 (q, $^3J_{C\text{-}B}$ = 50.4 Hz, C^{20}), δ 159.8 (Ar-C), δ 154.2 (Ar-C), δ 144.1 (Ar-C), δ 141.1 (Ar-C), δ 134.9 (br, C^{21}), δ 133.2 (Ar-C), δ 130.1 (Ar-C), δ 129.0 (qq, $^2J_{C\text{-}F}$ = 31.6, $^3J_{C\text{-}B}$ =2.9 Hz, C^{22}), δ 128.7 (Ar-C), δ 126.5 (Ar-C), δ 124.2 (Ar-C), δ 122.9 (Ar-C), δ 119.3 (C^{18}), δ 117.6 (sept., $^3J_{C\text{-}F}$ = 4.0 Hz, C^{23}), δ 113.8 (Ar-C), δ 113.6 (Ar-C), δ 34.9 (d, $^1J_{C\text{-}P}$ = 22.1 Hz, PCy$_3$), δ 30.4 (PCy$_3$), δ 28.7 (PCy$_3$), δ 27.7 (d, $^2J_{C\text{-}P}$ = 11.4 Hz, PCy$_3$), δ 26.0 (C^{14,16}), δ 24.4 (C^{15,17}), δ 22.7 (C^{15,17}), δ 0.9 (C^{19}). ^{31}P {^{1}H} NMR (121 MHz, $CDCl_3$): δ 48.2 (s). ESI-MS

(+.ve, m/z): 668.30 $[M\text{-}MeCN]^+$. *Anal. Calc.* for $C_{71}H_{69}BF_{25}N_2PPd \bullet 0.5CH_2Cl_2$: C, 53.14; H, 4.37; N, 1.73. *Found:* C, 52.83; H, 4.00; N, 1.95.

3.5.2.5 $[Pd(PCy_3)(MeCN)(2\text{-}OMe\text{-}C_6H_3)CH{=}N\{2,6\text{-}^iPr_2\text{-}C_6H_3\}]^+ [B(Ar)_4]^-$ (C25)

The cationic palladacycle **C25** was isolated as an off-white powder (0.15 g, 82 %) using the same synthetic procedure as outlined above for **C11**. The neutral palladacycle **C20** was used as the corresponding reactant. Melting point: 147 – 150 °C (decomposes without melting). FT-IR *ν*(C=N) 1604 cm^{-1}; *ν*(C-F) 1352; 1273; 1120 cm^{-1}. ^{13}C $\{^1H\}$ NMR (75 MHz, $CDCl_3$, numbering as per **Figure 3.2a**): δ 174.5 (d, $^3J_{C\text{-}P}$ = 3.7 Hz, C^7), δ 161.8 (q, $^3J_{C\text{-}B}$ = 50.6 Hz, C^{20}), δ 160.4 (Ar-C), δ 155.2 (Ar-C), δ 144.6 (Ar-C), δ 141.4 (Ar-C), δ 135.5 (Ar-C), δ 134.9 (br, C^{21}), δ 134.5 (d, $J_{C\text{-}P}$ = 4.2 Hz, Ar-C), δ 130.1 (Ar-C), δ 129.0 (qq, $^2J_{C\text{-}F}$ = 30.9, $^3J_{C\text{-}B}$ =2.4 Hz, C^{22}), δ 128.2 (Ar-C), δ 126.5 (Ar-C), δ 124.1 (Ar-C), δ 122.9 (Ar-C), δ 117.6 (sept., $^3J_{C\text{-}F}$ = 4.0 Hz, C^{23}), δ 109.1 (C^{18}), δ 55.9 (methoxy C), δ 34.8 (d, $^1J_{C\text{-}P}$ = 21.3 Hz, PCy_3), δ 30.4 (PCy_3), δ 28.6 (PCy_3), δ 27.7 (d, $^2J_{C\text{-}P}$ = 10.6 Hz, PCy_3), δ 26.0 ($C^{14,16}$), δ 24.5 ($C^{15,17}$), δ 22.7 ($C^{15,17}$), δ 0.9 (C^{19}). ^{31}P $\{^1H\}$ NMR (121 MHz, $CDCl_3$): δ 46.7 (s). ESI-MS (+.ve, m/z): 680.3 $[M\text{-}MeCN]^+$; 441.1 $[M\text{-}P(Cy)_3]^+$. ESI-MS (-.ve, m/z): 863.0 $[B(Ar)_4]^-$. *Anal. Calc.* for $C_{72}H_{72}BF_{24}N_2OPPd \bullet 0.5CH_2Cl_2$: C, 53.49; H, 4.52; N, 1.72. *Found:* C, 53.14; H, 4.71; N, 1.29.

3.5.3 Synthesis of cationic palladacycles with monodentate phosphine, PPh_3

3.5.3.1 $[Pd(PPh_3)(MeCN)(C_6H_4)CH{=}N\{2,6\text{-}^iPr_2\text{-}C_6H_3\}]^+ [B(Ar)_4]^-$ (C31)

The cationic palladacycle **C31** was isolated as an off-white powder (0.16 g, 85 %) using the same synthetic procedure as outlined above for **C11**. The neutral palladacycle **C26** was used as the corresponding reactant. Melting point: 165 - 167°C (decomposes without melting). FT-IR *ν*(C=N) 1613 cm^{-1}; *ν*(C-F) 1353; 1273; 1117 cm^{-1}. ^{13}C $\{^1H\}$ NMR (151 MHz, $CDCl_3$, numbering as per **Figure 3.2a**): δ 178.4 (d, $^3J_{C\text{-}P}$ = 4.9 Hz, C^7), δ 161.8 (q, $^1J_{C\text{-}B}$ = 48.9 Hz, C^{20}), δ 154.1 (Ar-C), δ 147.8 (Ar-C), δ 144.0 (Ar-C), δ 140.6 (Ar-C), δ 139.1 (Ar-C), δ 139.0 (Ar-C), δ 134.9 (br, C^{21}), δ 134.8 (Ar-C), δ 134.7 (Ar-C), δ 132.7 (d, $J_{C\text{-}P}$ = 6.6, Ar-C), δ 132.4 (Ar-C), δ 130.9 (Ar-C), δ 129.3 (Ar-C), δ 129.2 (Ar-C), δ 128.9 (qq, $^2J_{C\text{-}F}$ = 33.5, $^3J_{C\text{-}B}$ = 3.5 Hz, C^{22}), δ 128.5 (Ar-C), δ 128.4 (Ar-C), δ 127.4 (Ar-C), δ 126.6

(Ar-C), δ 125.6 (Ar-C), δ 123.8 (Ar-C), δ 123.7 (Ar-C), δ 122.0 (Ar-C), δ 119.4 (C^{18}), δ 117.6 (sept., $^{3}J_{C\text{-}F}$ = 3.6 Hz, C^{23}), δ 28.8 ($C^{14,16}$), δ 24.3 ($C^{15,17}$), δ 22.8 ($C^{15,17}$), δ 0.3 (C^{19}). ^{31}P {^{1}H} NMR (121 MHz, $CDCl_3$): δ 41.6 (s). ESI-MS (+.ve, m/z): 632.1711 $[M\text{-}MeCN]^+$. *Anal. Calc.* for $C_{71}H_{52}BF_{24}N_2PPd$: C, 55.47; H, 3.41; N, 1.82. *Found:* C, 55.01; H, 3.14; N, 1.43.

3.5.3.2 [Pd(PPh$_3$)(MeCN)(2-Cl-C$_6$H$_3$)CH=N{2,6-^{i}Pr$_2$-C$_6$H$_3$}]$^+$ [B(Ar)$_4$]$^-$ (C32)

The cationic palladacycle **C32** was isolated as an off-white powder (0.16 g, 88 %) using the same synthetic procedure as outlined above for **C11**. The neutral palladacycle **C27** was used as the corresponding reactant. Melting point: 160 - 162°C (decomposes without melting). FT-IR *ν*(C=N) 1611 cm^{-1}; *ν*(C-F) 1353; 1275; 1111 cm^{-1}. ^{13}C {^{1}H} NMR (151 MHz, $CDCl_3$, numbering as per **Figure 3.2a**): δ 176.8 (d, $^{3}J_{C\text{-}P}$ = 4.4 Hz, C^7), δ 161.9 (q, $^{1}J_{C\text{-}B}$ = 49.9 Hz, C^{20}), δ 155.4 (Ar-C), δ 144.9 (Ar-C), δ 142.2 (Ar-C), δ 140.5 (Ar-C), δ 137.5 (Ar-C), δ 137.4 (Ar-C), δ 134.9 (br, C^{21}), δ 134.8 (Ar-C), δ 134.7 (Ar-C), δ 133.9 (d, $J_{C\text{-}P}$ = 6.5, Ar-C), δ 132.6 (Ar-C), δ 129.4 (Ar-C), δ 129.3 (Ar-C), δ 129.0 (qq, $^{2}J_{C\text{-}F}$ = 31.2, $^{3}J_{C\text{-}B}$ = 3.1 Hz, C^{22}), δ 128.7 (Ar-C), δ 128.5 (Ar-C), δ 128.2 (Ar-C), δ 127.5 (Ar-C), δ 127.4 (Ar-C), δ 125.6 (Ar-C), δ 123.9 (Ar-C), δ 123.8 (Ar-C), δ 122.0 (Ar-C), δ 119.6 (C^{18}), δ 117.6 (sept., $^{3}J_{C\text{-}F}$ = 3.8 Hz, C^{23}), δ 28.8 ($C^{14,16}$), δ 24.4 ($C^{15,17}$), δ 22.8 ($C^{15,17}$), δ 0.3 (C^{19}). ^{31}P {^{1}H} NMR (121 MHz, $CDCl_3$): δ 41.2 (s). ESI-MS (+.ve, m/z): 666.1315 $[M\text{-}MeCN]^+$. ESI-MS (-.ve, m/z): 863.0765 $[B(Ar)_4]^-$. *Anal. Calc.* for $C_{71}H_{51}BClF_{24}N_2PPd \bullet 0.5CH_2Cl_2$: C, 53.20; H, 3.25; N, 1.74. *Found:* C, 53.29; H, 3.77; N, 1.14.

3.5.3.3 [Pd(PPh$_3$)(MeCN)(2-Br-C$_6$H$_3$)CH=N{2,6-^{i}Pr$_2$-C$_6$H$_3$}]$^+$ [B(Ar)$_4$]$^-$ (C33)

The cationic palladacycle **C33** was isolated as an off-white powder (0.15 g, 87 %) using the same synthetic procedure as outlined above for **C11**. The neutral palladacycle **C28** was used as the corresponding reactant. Melting point: 140 - 143°C (decomposes without melting). FT-IR *ν*(C=N) 1616 cm^{-1}; *ν*(C-F) 1353; 1275; 1117 cm^{-1}. ^{13}C {^{1}H} NMR (151 MHz, $CDCl_3$, numbering as per **Figure 3.2a**): δ 179.1 (d, $^{3}J_{C\text{-}P}$ = 4.4 Hz, C^7), δ 161.9 (q, $^{1}J_{C\text{-}B}$ = 49.7 Hz, C^{20}), δ 155.5 (Ar-C), δ 146.2 (Ar-C), δ 144.1 (Ar-C), δ 140.5 (Ar-C), δ 138.1 (Ar-C), δ 138.0 (Ar-C), δ 134.9 (br, C^{21}), δ 134.8 (Ar-C), δ 134.7

(Ar-C), δ 134.0 (d, $J_{C\text{-}P}$ = 6.1, Ar-C), δ 132.6 (Ar-C), δ 130.8 (Ar-C), δ 129.4 (Ar-C), δ 129.3 (Ar-C), δ 129.1 (qq, $^{2}J_{C\text{-}F}$ = 31.5, $^{3}J_{C\text{-}B}$ = 3.5 Hz, C^{22}), δ 128.7 (Ar-C), δ 128.5 (Ar-C), δ 128.2 (Ar-C), δ 127.4 (Ar-C), δ 125.6 (Ar-C), δ 124.0 (Ar-C), δ 123.8 (Ar-C), δ 123.7 (Ar-C), δ 122.0 (Ar-C), δ 119.6 (C^{18}), δ 117.6 (sept., $^{3}J_{C\text{-}F}$ = 3.7 Hz, C^{23}), δ 28.9 ($C^{14,16}$), δ 24.4 ($C^{15,17}$), δ 22.8 ($C^{15,17}$), δ 0.3 (C^{19}). ^{31}P {^{1}H} NMR (121 MHz, $CDCl_3$): δ 41.0 (s). ESI-MS (+.ve, m/z): 712.0791 $[M\text{-}MeCN]^+$. *Anal. Calc.* for $C_{71}H_{51}BBrF_{24}N_2PPd{\bullet}0.5CH_2Cl_2$: C, 51.77; H, 3.16; N, 1.69. *Found:* C, 51.39; H, 2.90; N, 0.94.

3.5.3.4 $[Pd(PPh_3)(MeCN)(2\text{-}F\text{-}C_6H_3)CH{=}N\{2,6\text{-}^{i}Pr_2\text{-}C_6H_3\}]^+ [B(Ar)_4]^-$ (C34)

The cationic palladacycle **C34** was isolated as an off-white powder (0.17 g, 91 %) using the same synthetic procedure as outlined above for **C11**. The neutral palladacycle **C29** was used as the corresponding reactant. Melting point: 134 - 137°C (decomposes without melting). FT-IR *v*(C=N) 1612 cm^{-1}; *v*(C-F) 1353; 1274; 1119 cm^{-1}. ^{13}C {^{1}H} NMR (151 MHz, $CDCl_3$, numbering as per **Figure 3.2a**): δ 173.1 (d, $^{3}J_{C\text{-}P}$ = 4.2 Hz, C^7), δ 162.2 (Ar-C), δ 161.9 (q, $^{1}J_{C\text{-}B}$ = 49.8 Hz, C^{20}), δ 160.4 (Ar-C), δ 155.0 (Ar-C), δ 144.1 (Ar-C), δ 140.6 (Ar-C), δ 134.9 (br, C^{21}), δ 134.8 (Ar-C), δ 134.7 (Ar-C), δ 132.5 (Ar-C), δ 129.4 (Ar-C), δ 129.3 (Ar-C), δ 129.0 (qq, $^{2}J_{C\text{-}F}$ = 31.6, $^{3}J_{C\text{-}B}$ = 2.4 Hz, C^{22}), δ 128.7 (Ar-C), δ 128.6 (Ar-C), δ 128.2 (Ar-C), δ 127.4 (Ar-C), δ 125.6 (Ar-C), δ 123.9 (Ar-C), δ 123.8 (Ar-C), δ 122.0 (Ar-C), δ 119.6 (C^{18}), δ 117.6 (sept., $^{3}J_{C\text{-}F}$ = 4.1 Hz, C^{23}), δ 113.7 (Ar-C), δ 113.5 (Ar-C), δ 28.8 ($C^{14,16}$), δ 24.3 ($C^{15,17}$), δ 22.8 ($C^{15,17}$), δ 0.3 (C^{19}). ^{31}P {^{1}H} NMR (121 MHz, $CDCl_3$): δ 41.2 (s). ESI-MS (+.ve, m/z): 650.1610 $[M\text{-}MeCN]^+$. ESI-MS (-.ve, m/z): 863.0735 $[B(Ar)_4]^-$. *Anal. Calc.* for $C_{71}H_{51}BF_{25}N_2PPd{\bullet}0.5CH_2Cl_2$: C, 53.75; H, 3.28; N, 1.75. *Found:* C, 53.59; H, 3.41; N, 1.23.

3.5.3.5 $[Pd(PPh_3)(MeCN)(2\text{-}OMe\text{-}C_6H_3)CH{=}N\{2,6\text{-}^{i}Pr_2\text{-}C_6H_3\}]^+ [B(Ar)_4]^-$ (C35)

The cationic palladacycle **C35** was isolated as an off-white powder (0.16 g, 88 %) using the same synthetic procedure as outlined above for **C11**. The neutral palladacycle **C30** was used as the corresponding reactant. Melting point: 158 - 160°C (decomposes without melting). FT-IR *v*(C=N) 1604 cm^{-1}; *v*(C-F) 1353; 1274; 1118 cm^{-1}. ^{13}C {^{1}H} NMR (151 MHz, $CDCl_3$, numbering as per **Figure 3.2a**): δ 175.1 (d, $^{3}J_{C\text{-}P}$ = 4.5 Hz, C^7), δ 161.9 (q, $^{1}J_{C\text{-}B}$ = 50.2 Hz, C^{20}), δ 160.2 (Ar-C), δ 156.0 (Ar-C), δ 144.6

(Ar-C), δ 140.9 (Ar-C), δ 135.6 (Ar-C), δ 134.9 (br, C^{21}), δ 134.9 (Ar-C), δ 134.8 (Ar-C), δ 134.7 (Ar-C), δ 132.3 (d, J_{C-P} = 6.6, Ar-C), δ 131.4 (Ar-C), δ 131.3 (Ar-C), δ 129.3 (Ar-C), δ 129.2 (Ar-C), δ 129.1 (Ar-C), δ 129.0 (qq, $^{2}J_{C-F}$ = 32.5, $^{3}J_{C-B}$ = 2.9 Hz, C^{22}), δ 128.8 (Ar-C), δ 128.2 (Ar-C), δ 127.4 (Ar-C), δ 125.6 (Ar-C), δ 123.8 (Ar-C), δ 123.7 (Ar-C), δ 122.0 (Ar-C), δ 119.3 (C^{18}), δ 117.6 (sept., $^{3}J_{C-F}$ = 3.9 Hz, C^{23}), δ 109.0 (Ar-C), δ 55.8 (*o*-methoxy Me), δ 28.7 ($C^{14,16}$), δ 24.3 ($C^{15,17}$), δ 22.8 ($C^{15,17}$), δ 0.3 (C^{19}). ^{31}P {^{1}H} NMR (162 MHz, $CDCl_3$): δ 41.1 (s). ESI-MS (+.ve, m/z): 662.1820 $[M\text{-}MeCN]^+$. *Anal. Calc.* for $C_{72}H_{54}BF_{24}N_2OPPd \bullet 0.5CH_2Cl_2$: C, 54.09; H, 3.44; N, 1.74. *Found:* C, 53.89; H, 3.20; N, 1.48.

3.6 References

1 S. D. Ittel, L. K. Johnson and M. Brookhart, *Chem. Rev.*, 2000, **100**, 1169.

2 S. Mecking, *Coord. Chem. Rev.*, 2000, **203**, 325.

3 L. K. Johnson, C. M. Killian and M. Brookhart, *J. Am. Chem. Soc.*, 1995, **117**, 6414.

4 L. K. Johnson, S. Mecking and M. Brookhart, *J. Am. Chem. Soc.*, 1996, **118**, 267.

5 A. C. Gottfried and M. Brookhart, *Macromolecules*, 2003, **36**, 3085.

6 W. Liu and M. Brookhart, *Organometallics*, 2004, **23**, 6099.

7 W. Beck and K. Sunkel, *Chem. Rev.*, 1988, **88**, 1405.

8 S. H. Strauss, *Chem. Rev.*, 1993, **93**, 927.

9 H. Nishida, N. Takada, M. Yoshimura, T. Sonoda and H. Kobayashi, *Bull. Chem. Soc. Jpn.*, 1984, **57**, 2600.

10 N. Mungwe, A. J. Swarts, S. F. Mapolie and G. Westman, *J. Organomet. Chem.*, 2011, **696**, 3527.

11 W. Zawartka, A. Gniewek, A. M. Trzeciak, J. J. Ziółkowski and J. Pernak, *J. Mol. Catal. A Chem.*, 2009, **304**, 8.

12 F. Antolasic, *Mol. Weight Calc.*, 2005, www.wsearch.com.au.

13 K. J. Keuseman, I. P. Smoliakova and V. V Dunina, *Organometallics*, 2005, **24**, 4159.

14 F. R. Hartley, S. G. Murray and C. A. Mcauliffe, *Inorg. Chem.*, 1979, **18**, 1394.

15 Apex2, *Data Collect. software*, Bruker AXS, 2010.

16 SAINT, *Data Reduct. Software*, Bruker AXS, 2003.

17 R. H. Blessing, *Acta Crystallogr. A.*, 1995, **51 (Pt 1)**, 33.

18 SADABS, *Version 2.05*, Bruker AXS, 2002.

19 G. M. Sheldrick, *Acta Crystallogr. Sect. A Found. Crystallogr.*, 2007, **64**, 112.

20 L. J. Barbour, *J. Supramol. Chem.*, 2001, **1**, 189.

21 POV-Ray, *Version 3.6*, Williamstown, Australia, Persistence of vision ray.

Chapter 4

Reactivity of Cationic Palladacycle Complexes in the Oligomerization and Polymerization of Phenylacetylene

4.1 Introduction

The polymerization of substituted acetylenes has attracted increasing attention over the last three decades or so. With their unique π-conjugated backbones, these polymers offer the potential of having useful properties such as gas permeability,[1,2] magnetic[3] and optical-nonlinear susceptibility,[4] electrical- [5] and photoconductivity.[6,7] Of particular interest are polyphenylacetylenes (PPAs) which exhibit excellent stability in air and show high solubility in most organic solvents. In terms of stability, PPA's are unlike polyacetylenes which readily absorb oxygen from the atmosphere at room temperature leading to polymer decomposition.[8] PPA has versatile physical- and chemical properties which are attributed to its stereoregularity, configuration and helical conformation.[9] This polymer is an insulator when undoped, however it becomes a semiconductor in nature when doped with acceptors or donors materials. [10,11]

4.1.1 Polymerization of phenylacetylene catalysed by transition metals

The first reports regarding the polymerization of phenylacetylene date back to 1955 when Natta *et. al.*[12] employed Ziegler-Natta type catalysts ($ZnEt_2/TiCl_3$, $AlEt_3/TiCl_3$, $AlEt_3/Ti(OC_3H_7)_4$) which were found to be active and produced high molecular weight PPA.[13] By varying the Al/Ti ratio of the catalyst system, linear polymers or cyclic trimers are produced. Two decades later, Masuda and Higashimura developed even more active catalysts derived from group 6 metals which could polymerize phenylacetylene with molecular weights up to 15 000 Da, higher than those obtained with Ziegler-Natta

catalysts.[14] No cyclic trimers of phenylacetylene were obtained. Since then, there has been a large body of research devoted to phenylacetylene polymerization employing group 6 transition metals. Amongst the catalyst systems explored are tungsten and molybdenum-based catalysts[15,16] which produce *trans*-rich and *cis*-rich PPA by varying the reaction conditions such as temperature and catalyst loading.

The drawback of early transition metals as catalysts for olefin transformations is their sensitivity towards air and moisture and therefore the need to be handled under dry and inert atmosphere. Most of these catalysts are binary- or ternary-component systems and the preparation thereof can be challenging. This has led to the development of late transition metal catalysts for olefin transformations especially those in group 9 and 10 since these metals have a low intrinsic oxophilicity and are far less sensitive than their early transition metal analogues. Although the polymerization of phenylacetylene can be achieved by employing Ziegler-Natta catalysts,[12] metathesis catalysts [14] or using radical-[17] and cationic polymerization,[18] rhodium complexes still remain the most widely studied catalysts for this process due to their high reactivity towards alkynes [19] and their stability in polar solvents. Rhodium phenylacetylene polymerization catalysts in general are known for their high selectivity towards *cis*-transoidal PPA structures.

There are a few examples of nickel complexes also capable of polymerizing phenylacetylene. A nickel catalyst system, $Ni(COD)_2$-CF_3COO(allyl), reported by Tsuchihara[20] was found to polymerize phenylacetylene giving polymers with a molecular weight of 12 000 Da. The polymers isolated consist of a mixture of both *cis* and *trans* conformations. Douglas *et. al.*[21,22] successfully polymerized phenylacetylene under solvent-free conditions at 115 °C using cyclopentadienylnickel complexes as catalysts, which afforded a mixture of cyclotrimers, oligo- and polyphenylacetylene. However low molecular weight products ranging from 1600 to 3000 Da were isolated. Palladium complexes have also been found to be efficient catalysts for phenylacetylene polymerization. Li *et. al.*[23] developed diphosphinopalladium catalysts and performed polymerization reactions in a 1:1 CH_2Cl_2:MeCN mixture which produced *cis*-transoidal PPA with a molecular weight of 12 000 Da. Even higher

molecular weight polymers with M_w as high as 27 000 Da were obtained when cationic bis(pyrazole) palladium catalysts were employed. In this case predominantly *trans*-cisoidal PPA is produced.[24]

4.1.2 Stereochemistry of polyphenylacetylene

In terms of the conformation around the C-C single bond and C=C double bond of the polymer backbone, PPA can adopt four different types of stereoregular structures as shown in **Figure 4.1**. The nature of the stereoisomers formed is highly dependent on the reaction conditions, reaction work-up procedures and type of catalyst employed. For example, the benzene soluble fractions of PPA obtained when $AlH(i\text{-}Bu)_2/Fe(acac)_3$ was employed as catalyst consist mainly of a *cis*-transoidal stereoregular structure, however when $AlEt_3/TiCl_3$ or $AlEt_3/Fe(dmg)_2{\bullet}2Py$ (dmg = dimethylglyoxime) were employed, the benzene insoluble fractions had a *cis*-cisoidal stereoregular structure.[12] When Ziegler-Natta catalysts of the type $AlEt_3/M(acac)_n$ were employed, *trans*-PPA was produced.[12,25] Since phenylacetylene is an unsymmetrically substituted monomer, chain growth can occur in three different ways as shown in **Figure 4.2**. The different constitutional stereoisomers can be characterised by IR and NMR spectroscopy since the obtained IR spectra show unique absorption bands as well as characteristic proton- and carbon resonances in their NMR spectra.

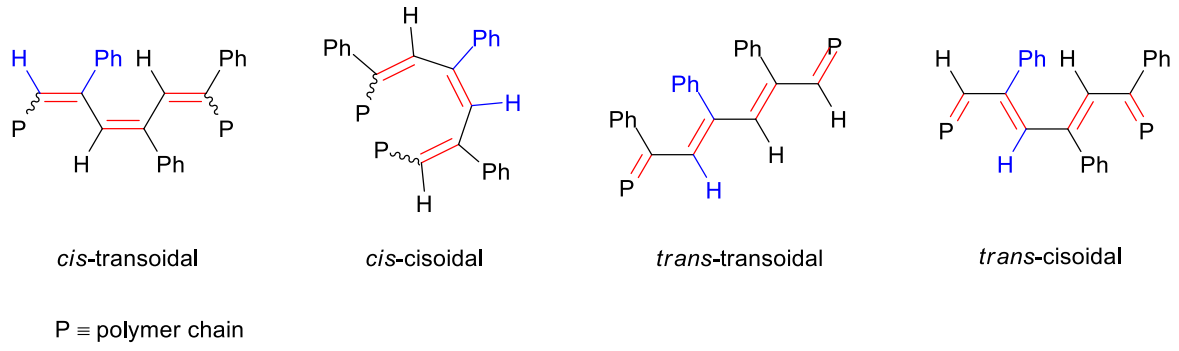

Figure 4.1: Four different constitutional stereoisomers of PPA.[9] The groups highlighted in blue belong to the same phenylacetylene monomer.

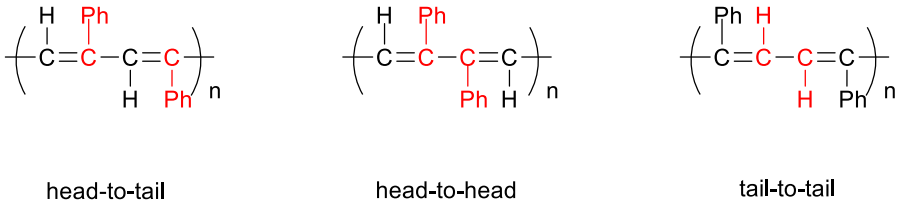

Figure 4.2: Regioselectivity of monomer addition.

4.1.3 Common propagation mechanisms for phenylacetylene

The two most common propagation mechanisms for the polymerization of acetylene and its derivatives catalysed by transition metals are the insertion mechanism[26,27] and the metathesis mechanism.[28,29] In the insertion mechanism, the triple bond of the monomer inserts directly into a metal-carbon single bond (**Scheme 4.1**) resulting in the C-C triple bond changing to a C-C double bond. In the case of the metathesis mechanism, the metal-carbene double bond undergoes metathesis with the triple bond of the monomer leading to a metallacyclobutene intermediate followed by a ring-opening process to complete the chain propagation (**Scheme 4.2**). A new metal-carbene double bond forms and the triple bond of the monomer becomes a single bond in the main polymer chain.

To determine the polymerization mechanism, nutation NMR spectroscopy is a useful technique which can easily distinguish between the two possible mechanisms. Clarke *et. al.*[30] monitored the ^{13}C-^{13}C bond distance in the polymerization of acetylene synthesized from ^{13}C-labeled acetylene. Based on the bond lengths, they could determine whether the ^{13}C-^{13}C bond was a single- or double bond and hence deduce which mechanism was operative. In general, polymerization of phenylacetylene employing group 9 and group 10 transition metal catalysts is believed to proceed *via* an insertion mechanism.

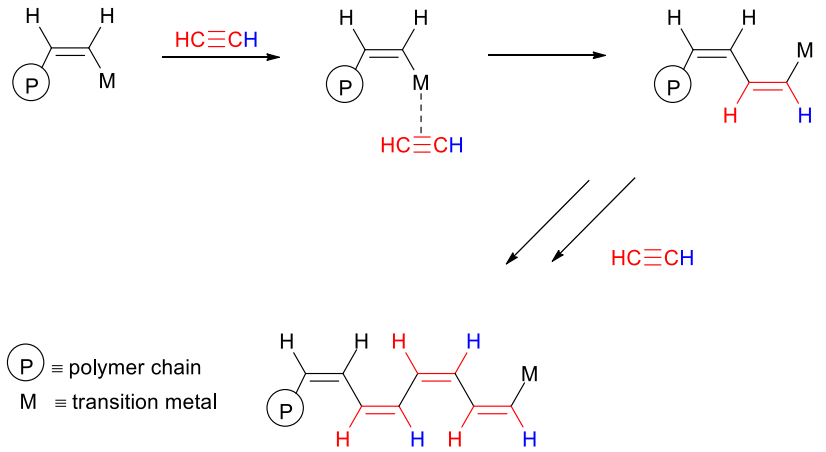

Scheme 4.1: Insertion mechanism. [26,27]

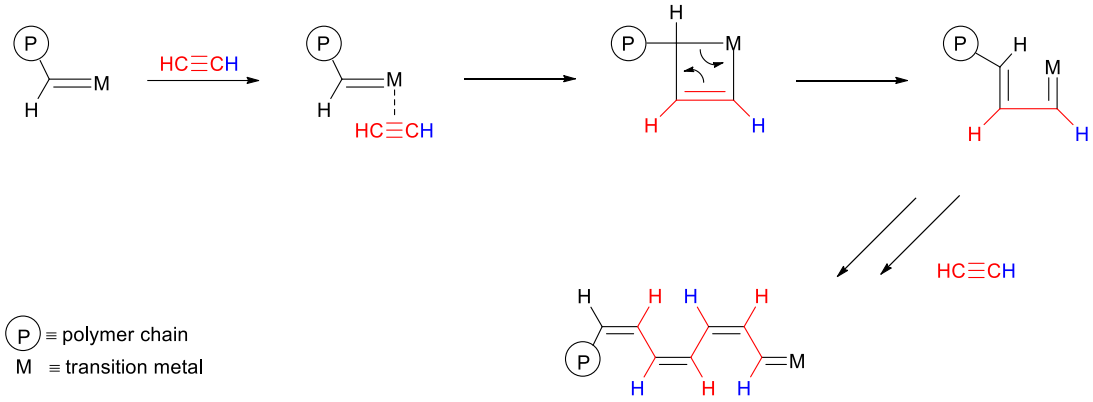

Scheme 4.2: Metathesis mechanism. [28,29]

Palladacycles have been widely studied for various organic transformations, however there are almost no reports on the polymerization of phenylacetylene. As highlighted in **Chapter 3**, cationic palladacycles have gained increasing attention in the field of catalysis. One of the key factors that determine their catalytic ability is the highly electrophilic metal centre. The presence of a weakly coordinating solvent is necessary to stabilize the active catalyst yet the coordination has to be weak enough to allow the monomer access to the active centre of the catalysts in order to initiate the polymerization. In the next section, the application of cationic palladacycle complexes as catalysts in the polymerization of phenylacetylene is reported on.

4.2 Results and Discussion

4.2.1 Cationic palladacycle complexes employed as catalysts in the oligomerization/ polymerization of phenylacetylene.

The cationic palladacycles were evaluated as catalysts in the polymerization of phenylacetylene as shown in **Scheme 4.3**. These complexes differ from each other in terms of the type of ortho-substituents (red circles) on the cyclometallated ring as well as the type of the auxiliary phosphine ligand coordinated to the metal (blue circles) with the latter having different basicities and steric properties (**Figure 4.3**). Incorporating all of these characteristics into the architecture of the complex offers the potential to fine-tune the metal's electrophilicity and to influence steric control around the metal centre.

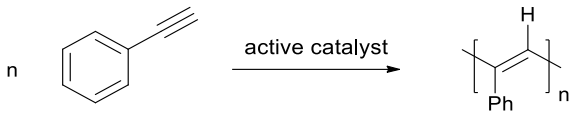

Scheme 4.3: A general scheme for the polymerization of phenylacetylene.

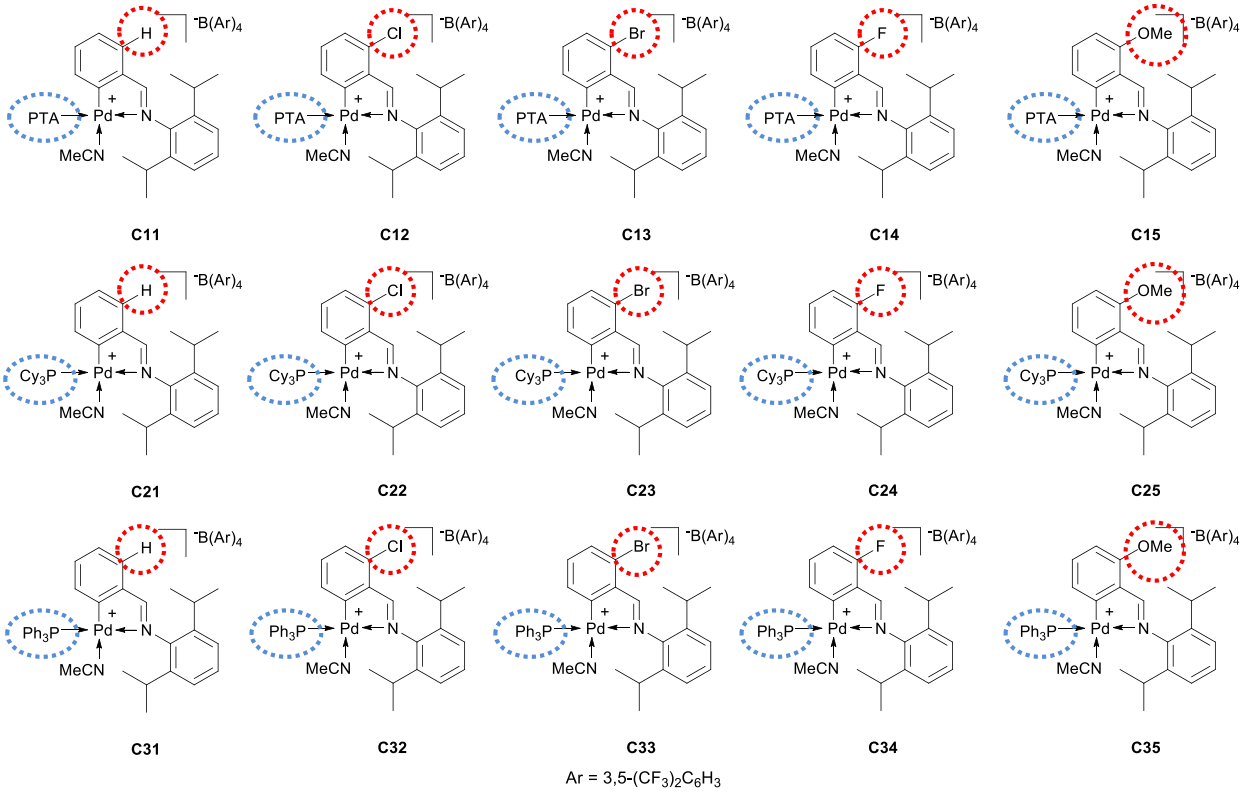

Figure 4.3: Cationic palladacycle complexes bearing different *ortho*-substituents (red circle) and phosphine ligands (blue circle).

The complexes shown in **Figure 4.3** were employed as catalyst precursors without the addition of any co-catalyst or activator. The effect of the nature of the catalyst precursor, solvent, temperature, monomer to catalyst ratio and the reaction time on the efficiency of the polymerization process were studied in detail. Polymers were separated from oligomeric material *via* precipitation by adding methanol to dichloromethane solutions of the product. To distinguish whether the materials isolated were oligomeric or polymeric, gel permeation chromatography analyses were performed to determine the molecular weight. The oligomers and polymers isolated for a specific catalytic reaction showed the same stereochemistry, however they differ in the molecular weight. By definition, PPA is regarded as a polymer if the average molecular weight is greater than 1000 Da, while oligomers have molecular weights less than 1000 Da.[31,32] The *cis* content of the *cis*-transoidal PPA formed in the polymerization reaction was determined following a literature method which uses ^{1}H NMR spectroscopy. [12] In general, the colour of the polymers and oligomers isolated varied from dark-brown to yellow-orange in nature.

4.2.1.1 Effect of catalyst precursors on the polymerization of phenylacetylene

The reaction conditions employed were modified from a previously reported procedure in which polymerization reactions were performed in CH_2Cl_2 using a 50:1 monomer to catalyst ratio at both 25 °C and 60 °C.[33] Under these conditions, the palladacycles were found to be efficient catalysts in the polymerization of phenylacetylene. The graph in **Figure 4.4** shows the behaviour of all the fifteen catalyst precursors in the polymerization of phenylacetylene. The catalyst activities are summarized in terms of the influence of the ortho-substituents on the cyclometallated ring as well as the nature of the phosphine ligand *viz*. PTA, PCy_3 and PPh_3.

In general, under the optimized conditions employed, PTA-based palladacycles gave high conversions with the highest conversion of 95 % observed for **C14**, the PTA based complex with fluorine as the ortho-substituent. **C13**, another PTA based complex but with the bromo ortho-substituent does not conform to the expected trend in that it showed the lowest conversion (56%).

Turnover-numbers (TON) for reactions conducted with the various catalysts in the catalytic polymerization are shown in **Table 4.1**, and range between 2800-4900 g product/mol Pd with the highest TON of 4850 g product/mol Pd observed for **C14**. The catalytic activity of the PTA based catalysts in order of decreasing activity was:

C14 (F) > C12 (Cl) > C11 (H) > C15 (OMe) > C13 (Br)

NB: The ortho-substituent is given in brackets.

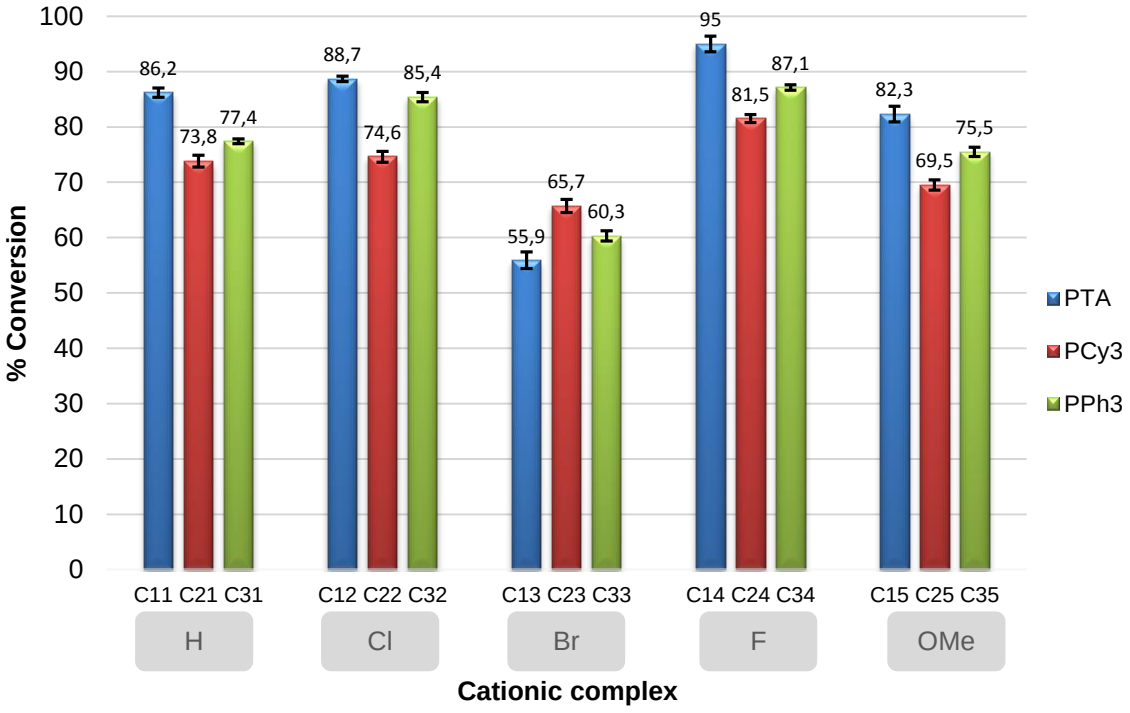

Figure 4.4: Effect of palladacycles bearing different ortho-substituents and auxiliary phosphine ligands on the conversion. Reaction conditions: PA:Pd = 50:1; [Pd] = 3mM; 60 °C; 48 hours; THF (10 mL). Conversions were determined by the total mass of the crude product as a percentage of the monomer used.

Table 4.1: TON and GPC analysis pertaining to the cationic palladacycle complexes. [a]

Entry	Catalyst	TON [b]	M_w [c]	PDI
1	**C11**	4400	2440	1.18
2	**C12**	4533	2515	1.23
3	**C13**	2853	2362	1.16
4	**C14**	4850	2656	1.20
5	**C15**	4203	2557	1.16
6	**C21**	3770	4157	1.16
7	**C22**	3810	3957	1.25
8	**C23**	3353	3934	1.38
9	**C24**	4160	4410	1.19
10	**C25**	3547	4041	1.22
11	**C31**	3953	2710	1.26
12	**C32**	4360	2797	1.35
13	**C33**	3080	2341	1.28
14	**C34**	4447	2875	1.19
15	**C35**	3857	2465	1.31

[a] Reaction conditions: PA:Pd = 50:1; [Pd] = 3mM; 60 °C; 48 hours; THF (10 mL). [b] Turnover number (TON) = g product/mol Pd. [c] Weight average molecular weight of methanol insoluble product. GPC analysis performed at room temperature and measured against polystyrene standards.

The results for the PTA based catalysts highlight the effect of the different ortho-substituents on the catalytic activity. Higher activities were observed when electron withdrawing groups were incorporated into the architecture of the catalyst. The exception to this trend being **C13**, which although containing a bromo substituent shows the lowest activity even lower than **C15**, a complex containing an electron donating methoxy substituent. This general behaviour can be attributed to the fact that electron-withdrawing substituents enhance the electrophilicity of the metal centre, hence promoting monomer coordination. Masuda *et. al.*[34] studied the polymerization of phenylacetylene using rhodium zwitterionic complexes containing tetrafluorobenzobarrelene (tfb) ligands. They found that the electron donating methyl groups on the tetrafluorobenzobarrelene ultimately increases electron density on metal centre which subsequently reduce the ability of the monomer to coordinate which is in agreement with what we observe for our complex with a methoxy-substituent. As stated earlier, the bromo analogue (**C13**) gave the lowest conversion which does not follow the general trend. One would have expected that this catalyst would show similar activity to that of the chloro analogue **C12** since both the bromo and chloro substituents have very similar electronegativities. A further observation regarding these two

precursors was made during the catalytic reactions, namely that the induction period for the polymerization reaction was longer for **C13** since the colour of the reaction mixture in this case was still light brown after 4 hours compared to the dark brown reaction mixtures for the other catalytic reactions. It is however still unclear what is the cause of this discrepancy in which **C13** deviates from the expected trend. We postulate that in the case of the bromo species, **C13**, steric effects dominate electronic effects since it is the catalyst with the largest halide ortho-substituent tested in this study.

Coincidentally, the same substituent effect was noted for the other catalyst systems in this study in which the PTA was replaced by PCy_3 and PPh_3. The order of the catalytic activities for the PCy_3 and PPh_3 analogues respectively were found to be as follows:

C24 (F) > C22 (Cl) > C21 (H) > C25 (OMe) > C23 (Br)

and

C34 (F) > C32 (Cl) > C31 (H) > C35 (OMe) > C33 (Br)

NB: The ortho-substituent is given in brackets.

Moderate to high conversions were obtained for both the above series of catalysts with the highest conversion observed for **C24** and **C34**. However once again the catalysts with the bromo substituent (**C23** and **C33**) in both series gave the lowest conversion.

The nature of the tertiary phosphine ligand also seems to have a marked effect on the efficiency of the catalyst. As discussed in **Chapter 2**, the basicities of the tertiary phosphine ligands may be arranged in decreasing order as follows: **PCy_3 > PPh_3 > PTA**. The catalysts containing the more basic phosphine ligand PCy_3 (**C21-C25**) gave the lowest conversion when compared to their PPh_3 and PTA analogues, with the exception of the catalysts containing the bromo substituent (**Figure 4.4**). The observed trend with regards to the phosphine ligand was attributed to the fact that the more basic phosphine ligand donates more electron density to the metal centre, decreasing the electrophilicity of the metal which

subsequently reduces the rate of monomer coordination. This ultimately impacts on the overall rate of phenylacetylene polymerization.

In addition to controlling the activity of the catalysts, the nature of the phosphine was also influenced the molecular weight of the polymers produced. As mentioned before in **Chapter 2**, PCy_3, PPh_3 and PTA have cone angles of 170°, 145° and 103° respectively. Catalysts containing the more sterically hindered phosphine PCy_3 (**C21-C25**) produced higher molecular weight polymers (**entries 6-10, Table 4.1**) relative to the catalysts with less sterically hindered phosphines (**entries 1-5, 11-15**) under the same reaction conditions. Incorporating steric bulk into the catalyst design is a well-established property and has previously been shown to promote chain propagation in phenylacetylene polymerization reactions using late transition metal complexes as catalysts.[24]

Regardless of the catalyst precursor used, reactions performed at 60 °C selectively produced *trans*-cisoidal PPA which was confirmed by FT-IR- and ^{1}H NMR spectroscopy. The selective formation of the *trans*-cisoidal PPA stereoisomer at elevated temperatures has also been observed previously using other catalytic systems.[35]

4.2.1.2 Polymerization of phenylacetylene using single solvents and a mixture of CH_2Cl_2 and MeCN.

The polymerization of phenylacetylene was performed at both 25 °C and 60 °C in different solvents to investigate the effect of temperature and solvent on the polymerization (**Table 4.2**). The PTA based fluoro complex, **C14**, which was found to be the most active catalyst, was employed as a model catalyst to further explore the above mentioned reaction conditions. At 25 °C, a mixture (66-80 % *cis* content) of both *cis*-transoidal and *trans*-cisoidal PPA (**Figure 4.1**) with moderate molecular weight and narrow polydispersity indices were produced (**entries 1-4**, **Table 4.2**). The stereochemistry of the PPA produced was unambiguously determined and characterized by IR- and ^{1}H NMR spectroscopy. The IR spectrum of the polymer isolated from a catalytic reaction conducted at 25 °C (**Figure 4.5**) showed three absorption bands at 1597 cm^{-1}, 1492 cm^{-1} and 1443 cm^{-1} which are

characteristic of a typical polymer with polyconjugated C=C bonds.[36,37] The material isolated also showed absorption bands at 895 cm^{-1} and 742 cm^{-1} which are indicative of a polymer with a *cis* configuration around the C=C bonds. [37] Furthermore, a the strong absorption band at 694 cm^{-1} corresponding to the C-H out-of-plane bending of the mono-substituted phenyl rings is also observed in the IR spectrum.[38] Polymers which consist of the *trans* configuration were also isolated as shown by the characteristic IR absorption band at 1278 cm^{-1}.[33] This absorption band was more intense for polymers produced during catalytic reactions performed at 60 °C, indicating polymers with a higher content of material with the *trans* configuration in the reaction mixture. The ^{1}H NMR spectra of the PPA produced during reactions conducted at 25 °C (**Figure 4.6, a**) typically showed a sharp, well defined proton resonance at δ 5.84 ppm which is characteristic of the vinylic protons in the polymer backbone. In addition, two sets of broad resonances resonating at δ 6.64 ppm (ortho) and δ 6.95 ppm (meta and para) which integrate for a total of two and three protons respectively are attributed to the phenyl protons in the polymer. The proton resonances at those specific chemical shifts are associated with the regular head-to-tail structure of *cis*-transoidal PPA (**Figure 4.1 – 4.2**), which agrees with the observation made by Li *et.al.*[23] when employing diphosphinopalladium (II) complexes as catalyst for phenylacetylene polymerization.

Table 4.2: Catalytic data pertaining to cationic palladacycle **C14**. [a]

Entry	T (°C)	Solvent	Conversion (%)	TON [b]	M_w [c]	PDI
1	25	THF	44,7	3016	4175	1,03
2	25	CH_2Cl_2	24,3	2183	3615	1,22
3 [d]	25	9:1	38,0	2450	5944	1,02
4 [d]	25	7:1	35,8	2390	6879	1,03
5	60	THF	95,0	4850	2656	1,20
6	60	CH_2Cl_2	62,3	3180	1133	1,47
7	60	PhMe	48,6	2480	1046	1,51
8	60	MeCN	40,2	2050	1249	1,35
9 [d]	60	9:1	76,4	3883	4190	1,46
10 [d]	60	7:1	69,5	3550	4429	1,55

[a] Reaction conditions: PA:Pd = 50:1; [Pd] = 3mM; 48 hours; 10 mL solvent. Conversions were determined by the total mass of the crude product as a percentage of the monomer used. [b] Turnover number (TON) = g product/mol Pd. [c] Weight average molecular weight of methanol insoluble product. GPC analysis performed at room temperature and measured against polystyrene standards. [d] Solvent mixture CH_2Cl_2:MeCN.

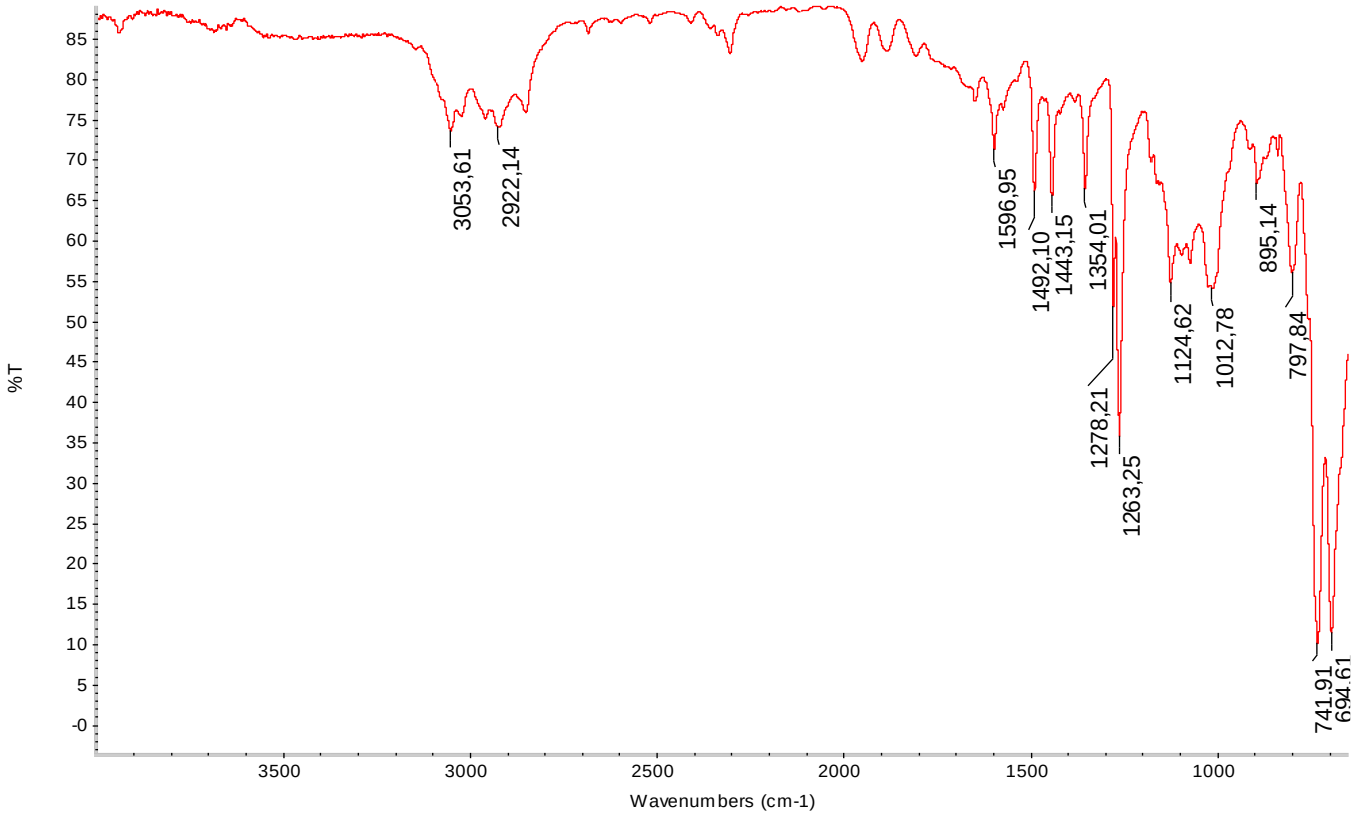

Figure 4.5: IR spectrum of a polymer isolated from a catalytic reaction performed at 25 °C with a monomer to catalyst ratio of 50:1 employing catalyst **C14**.

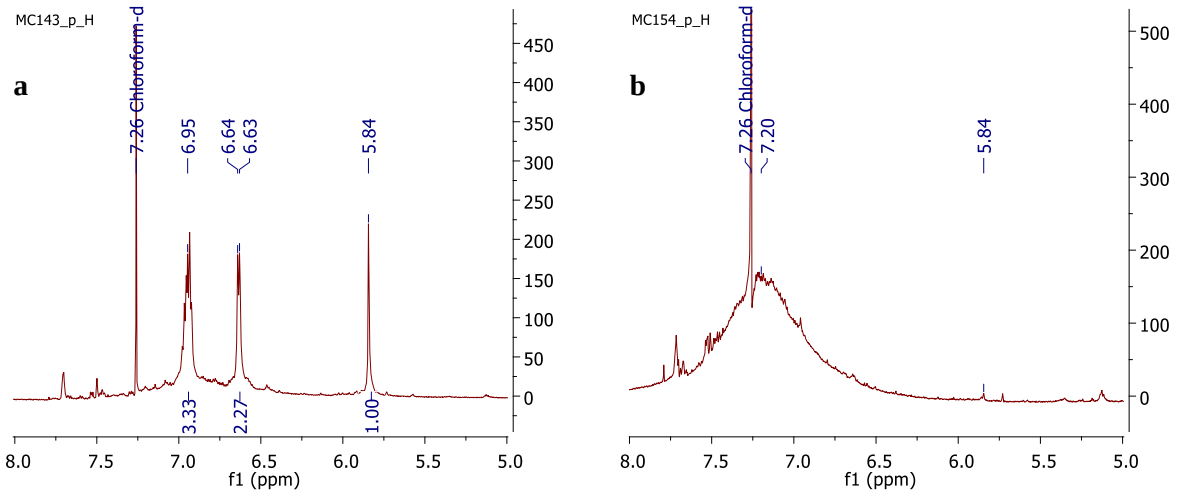

Figure 4.6: ^{1}H NMR spectrum of PPA isolated from (**a**) a catalytic reaction performed at 25 °C (**b**) a catalytic reaction performed at 60 °C showing proton resonances in the region δ 8.00-5.00 ppm. Complex **C14** was employed as precatalyst.

When the polymerization reactions were performed at an elevated temperature of 60 °C (**entries 6-10**), there was a substantial increase in the % conversion with the selective formation of *trans*-cisoidal PPA (**Figure 4.1**). The stereochemistry of this polymer was also characterized by a broad resonance centred at δ 7.20 ppm and the disappearance of the characteristic *cis*-transoidal vinylic proton resonance at δ 5.84 ppm in the ^{1}H NMR spectrum shown in **Figure 4.6 b**.[24,37] The broad resonance centred at δ 7.20 ppm was assigned to the aromatic protons of the polymer backbone. The PPA produced at the higher temperature had slightly lower molecular weights and exhibited higher polydispersity indices than those polymers obtained at 25 °C. This may be attributed to an increase in the rate of chain termination relative to chain propagation at elevated temperatures. The same trend was observed when diphosphinopalladium complexes were employed as catalysts for phenylacetylene polymerization at elevated temperatures.[23] In addition, a larger quantity of methanol insoluble products was isolated at elevated temperatures indicating that more polymeric material than oligomers was formed at the higher temperature.

Polymerization with catalyst **C14** performed in a mixture of 9:1 and 7:1 CH_2Cl_2:MeCN respectively at 25 °C resulted in low conversion but high molecular weight polymers with narrow polydispersity indices (**entries 1-2**). Increasing the proportion of MeCN in the solvent mixture led to a slightly lower conversion, however the molecular weight of the polymers increased by almost a 1000 Da. These results suggest that increasing the concentration of MeCN leads to increased competition between the phenylacetylene monomer and the MeCN solvent for the vacant site on the metal centre. This results in a lower rate of polymerization. However the catalyst lifetime is improved due to the higher stability of the solvated species which promotes polymer chain growth resulting in higher molecular weight polymers. When reactions were performed at 60 °C using the mixed solvent system (**entries 9-10**), a significant increase in conversion was observed with slightly lower molecular weight polymers with higher polydispersity indices when compared to the reactions at 25 °C. It is well established that polymerization reactions are normally faster at elevated temperatures leading to low molecular weight polymers with high polydispersity indices. [23,24] The low molecular weights are a result

of chain termination processes being favoured at high temperatures. When single solvents were used in the polymerization reaction at 60 °C, THF (**entry 5**) was found to give the highest conversion (95 %) followed by CH_2Cl_2 with a more moderate conversion of 62.3% (**entry 6**). The catalyst activity in PhMe and MeCN were however low (**entries 7-8**). The presence of a coordinating solvent (MeCN and THF) is crucial in stabilizing the catalytic intermediate by occupying the catalyst vacant site on the metal which could lead to an increase in the catalyst's lifetime. THF is however more labile than MeCN and can thus be more easily displaced by the incoming monomer than in the case for MeCN. A high concentration of MeCN would reduce monomer coordination since it will compete with phenylacetylene for the vacant site on the metal. The solubility of catalyst **C14** in PhMe was poor and the complex is also not stable in this solvent showing gradual decomposition over time. In general, polymerization in single solvents produces lower molecular weight polymers with higher polydispersity indices in comparison to those obtained when conducting the polymerizations in solvent mixtures.

4.2.1.3 Investigating the effect of different monomer to catalyst ratios and reaction time on the polymerization of phenylacetylene

The effect of different monomer to catalyst ratios was briefly investigated at 60 °C in THF using catalyst **C14** (**Table 4.3**). Relatively high concentrations of phenylacetylene have an adverse effect on the polymerization reaction. A conversion of around 54 % was observed when a monomer to catalyst ratio of 100:1 was employed (**entry 2**) while at the lower ratio of 50:1 almost quantitative conversion was observed (**entry 3**). However when a monomer to catalyst ratio of 500:1 was employed, a conversion of only 12.0 % was registered (**entry 1**). Thus is clear that the reaction is more efficient at lower catalyst to monomer ratio which is similar to what was observed in literature.[24]

Time dependent polymerization experiments were also performed (**Table 4.3**). In general, reaction time is known to have a substantial effect on the catalyst activity due to changes in the stability of the active species in solution over time. At 3 hours, very low molecular weight polymers were obtained

with a polydispersity index of 1.80 (**entry 7**). Increasing the reaction time led to a significant increase in conversion as well as the molecular weight of the polymers (**entries 3-7**) with a further improvement in the polydispersity index under the same reaction conditions (**entries 3-6**).

Table 4.3: Catalytic data pertaining to cationic palladacycle **C14.**[a]

Entry	Time (h)	PA:cat	Conversion (%)	M_w [b]	PDI
1	48	500	12.0	1116	1.25
2	48	100	54.1	1732	1.26
3	48	50	95.0	2656	1.20
4	24	50	72.1	2392	1.22
5	12	50	46.7	1581	1.25
6	6	50	16.2	1095	1.43
7	3	50	5.3	993	1.80

[a] Reaction conditions: Temperature = 60 °C; [Pd] = 3mM; THF (10 mL). [b] Weight average molecular weight of methanol insoluble product. GPC analysis performed at room temperature and measured against polystyrene standards.

Although low molecular weight polymers were produced using cationic palladacycles, the catalysts described here have comparable catalytic activities to those reported in literature. [23,24,37]

4.2.1.4 Possible mechanism for phenylacetylene employing cationic palladacycles.

There are several mechanisms proposed in literature for the polymerization of phenylacetylene.[9,26,39,40] One of the possible mechanisms for chain propagation is the so called insertion mechanism where the alkyne monomer inserts into a Pd-C bond. Although we still need to explore this experimentally, it was thought that in the case of our catalytic system based on palladacycles that this mechanism could likely be operative given that such a mechanism has been proposed for other palladium catalysts. The steps involved in this are shown in **Scheme 4.4**. As mentioned above, mechanistic studies still need to be performed to confirm this however due to time constrains, these experiments could not be completed and are not reported here.

In **Scheme 4.4** the actives species (**A**) could be generated from the neutral complexes discussed in **Chapter 2** by the abstraction of the chloride ligand using a halide abstractor such as sodium tetrakis [3,5-*bis*(trifluoromethyl)phenyl]borate in the presence of acetonitrile which serves to stabilize the catalyst vacant site. The weakly coordinating solvent can easily be replaced by the incoming phenylacetylene forming π-adduct **C**, which undergoes rearrangement via a three-centred intermediate (**D**) to form the metal hydride-phenylethynyl species **E**, a type of species which was first proposed by Noyori *et. al.* in the case of rhodium complexes employed in phenylacetylene polymerization.[26] It has been demonstrated that nickel,[20] palladium[23] and rhodium-based [39] phenylacetylene polymerization catalysts proceeded via the insertion mechanism whereas the metathesis mechanism is more common for molybdenum and tungsten-based catalysts.[41] The next step in the catalytic cycle is the coordination of a second monomer molecule which it is assumed occurs upon dissociation of the imine moiety from the palladium centre (**F**) and this is subsequently followed by a 2, 1-insertion of the monomer into the Pd-C bond to form species **G**. This step is repeated several times forming species **F** which then undergoes reductive elimination producing linear polymers. The molecular weight of the polymers is dependent on the degree of chain propagation which in turn depends on the extent of monomer insertion. For example, if the termination step occurs early in the process, then only short chain oligomers are formed. Following reductive elimination the catalyst is stabilized by a weakly coordinating solvent molecule regenerating the active species **A**.

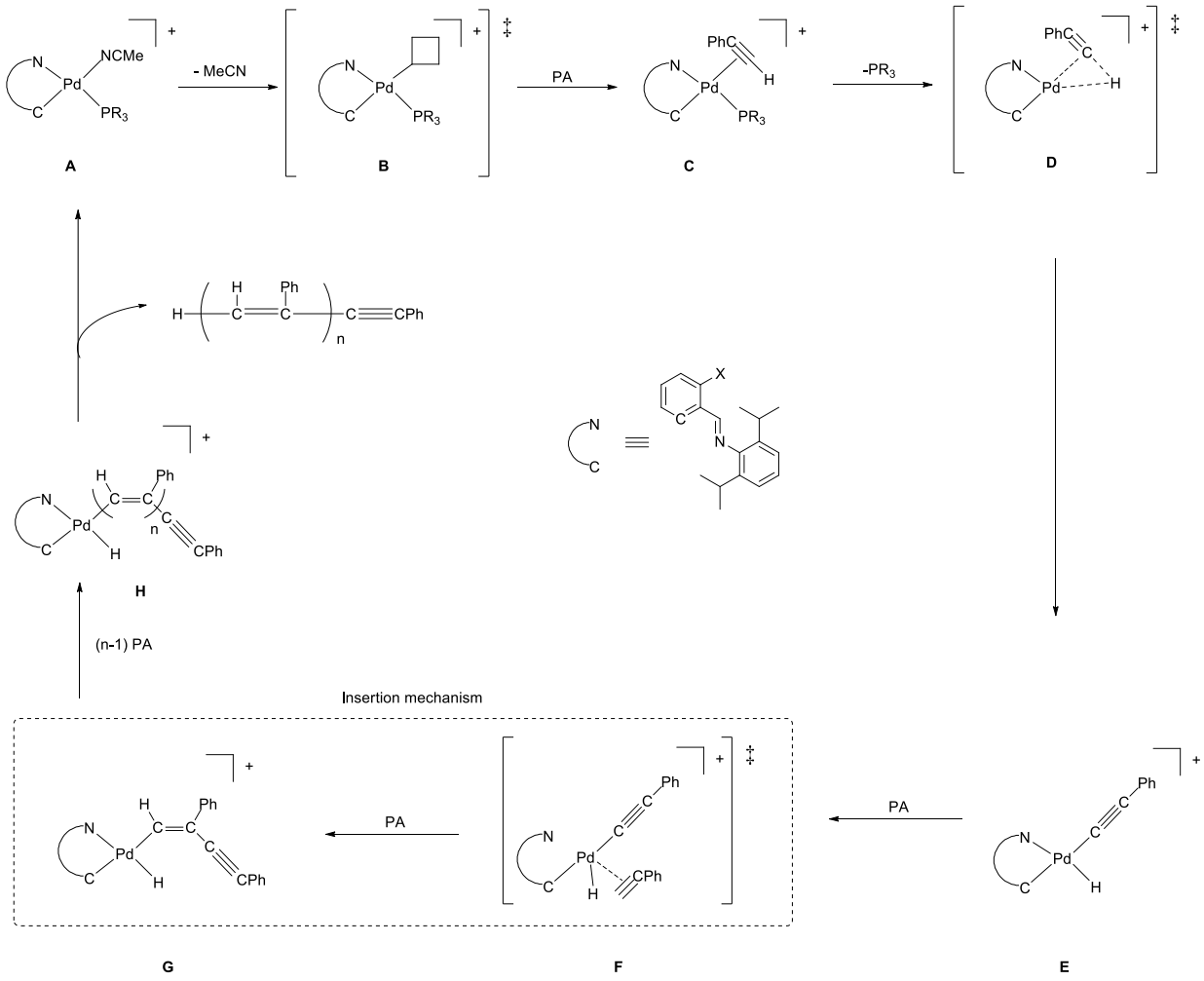

Scheme 4.4: Possible catalytic cycle for the polymerization of phenylacetylene catalyzed by cationic species.

4.3 Conclusion

In this chapter, a series of cationic palladacycle complexes bearing different ortho-substituents and phosphine ligands with different basicities were employed as catalysts in the polymerization of phenylacetylene. A mixture of both *cis*-transoidal and *trans*-cisoidal PPA were produced at room temperature with moderate molecular weights while the *trans*-cisoidal PPA can selectively be produced when the reactions are performed at slightly higher temperatures (60 °C). The ortho-substituent was found to have a marked effect on the catalyst efficiency in that catalysts which contained an electron withdrawing-group were the most active, the exception being the bromo-substituent. In the case of the

latter it is proposed that steric factors may trump electronic effects. Similarly, an increase in the steric bulk of the phosphine ligand leads to higher molecular weight PPA being produced.

4.4 Experimental Section

4.4.1 General remarks and instrumentation

All transformations were carried out under an inert atmosphere of dry nitrogen using a dual vacuum/nitrogen line and standard Schlenk techniques. Phenylacetylene was acquired from Sigma-Aldrich and used without further purification. Solvents were obtained from Merck and Kimix and purified using a Pure Solv^{TM} micro solvent purifier fitted with activated alumina columns. In the case of methanol, the solvents were dried by distillation over a mixture of magnesium filings and iodine. Acetonitrile was dried by distillation over phosphorous pentoxide. FT-IR analyses were performed on a Thermo Nicolet AVATAR 330 instrument with a smart ATR performer accessory and recorded as neat samples. ^{1}H and ^{13}C spectra were recorded on Varian VNMRS 300 MHz and Varian Unity Inova 400 and 600 MHz spectrometers. The chemical shifts for proton and carbon spectra are internally referenced to the residual deuterated solvents and externally referenced to tetramethylsilane (TMS). All catalytic reactions were performed using a Radleys 12-stage carrousel parallel reactor equipped with a gas distribution system. The weight-average (M_w) and number-average molecular weights (M_n) as well as the polydispersity indices (M_w/M_n) of the polymer were determined by gel permeation chromatography (THF, 30°C, rate = 1.0 mL/min) on a Waters 600E system controller (run by Breeze Version 3.30 SPA) equipped with a Waters 717 plus auto-sampler, a Waters in-line Degasser AF, Waters 1515 isocratic HPLC pump and a Waters 2414 differential refractometer detector. Two columns (PLgel 5 μm Mixed-C, 300x7.5 mm) and a pre-column (PLgel 5 μm Guard, 50x7.5 mm) were used and calibration was done using narrow molecular weight polystyrene standards ranging from 580 to 2x10^{6} g mol^{-1}.

4.4.2 Phenylacetylene oligomerization and polymerization reactions

The cationic palladacycle complex (30µmol) was dissolved in either a pure solvent or solvent mixture under inert atmosphere using standard Schlenk techniques. Phenylacetylene (50:1, 100:1 or 200:1 PA/Pd) was added to the stirring solution and the reaction mixture was heated to 25 °C or 60 °C. The total reaction volume was 10 mL with a catalyst concentration of 3mM. The reaction was allowed to stir for the required time under a nitrogen atmosphere. A gradual colour change from light yellow to dark yellow to orange then to dark brown was observed. After the allotted time, the solvent and excess phenylacetylene were removed *in vacuo* and the brown residue was redissolved in a minimum amount of CH_2Cl_2. The polymer was precipitated out of solution by adding methanol (15 mL), yielding a yellow-orange solid. The solid was stirred in methanol for 18 hours, filtered and dried under vacuum. The solvent was removed from the filtrate *in vacuo* yielding a brown residue which was dried under vacuum. Both the methanol soluble and methanol insoluble fractions were subjected to GPC analysis. All catalytic reactions were performed in duplicates.

4.5 References

1 Y. Hayakawa, M. Nishida, A. Okumura, M. Matsui and H. Muramatsu, *Polym. Bull.*, 1992, **28**, 293.

2 T. Masuda, E. Isobe and T. Higashimura, *J. Am. Chem. Soc.*, 1983, **105**, 7473.

3 F. Rossitto and P. Lahti, *Macromolecules*, 1993, **26**, 6308.

4 J. Le Moigne, A. Hilberer and C. Strazielle, *Macromolecules*, 1992, **25**, 6705.

5 C. K. Chiang, C. R. Fincher, Y. W. Park, A. J. Heeger, H. Shirakawa, E. J. Louis, S. C. Gau and A. G. MacDiarmid, *Phys. Rev. Lett.*, 1977, **39**, 1098.

6 A. J. Heeger, *Angew. Chem. Int. Ed*, 2001, **40**, 2591.

7 A. G. MacDiarmid, *Angew. Chem. Int. Ed*, 2001, **40**, 2581.

8 F. G. Will and D. W. Mckee, *J. Polym. Sci. Polym. Chem. Ed.*, 1983, **21**, 3479.

9 Z. Ke, S. Abe, T. Ueno and K. Morokuma, *J. Am. Chem. Soc.*, 2011, **133**, 7926.

10 F. Cataldo, M. Pentimalli and P. Ragni, *Polym. Int.*, 2000, **49**, 1343.

11 F. Cataldo, *Polym. Int.*, 1996, **39**, 91.

12 C. I. Simionescu and V. Percec, *Prog. Polym. Sci.*, 1982, **8**, 133.

13 H. Gibson and J. Porchan, *Encycl. Polym. Sci. Eng.*, 1984, **1**, 87.

14 T. Masuda, K. Hasegawa and T. Higashimura, *Macromolecules*, 1974, **7**, 728.

15 P. S. Woon and M. F. Farona, *J. Polym. Sci. Polym. Chem. Ed.*, 1974, **12**, 1749.

16 A. Keller and L. Szterenberg, *J. Mol. Catal.*, 1989, **57**, 207.

17 S. Amdur, A. Cheng, C. Wong, P. Ehrlich and R. Allendoerfer, *J. Polym. Sci. Polym. Chem. Ed.*, 1978, **16**, 407.

18 T. Masuda and T. Higashimura, *Macromolecules*, 1979, **12**, 9.

19 M. Falcon, E. Farnetti and N. Marsich, *J. Organomet. Chem.*, 2001, **629**, 187.

20 K. Tsuchihara, *Polym. Commun.*, 2000, **41**, 2691.

21 W. Douglas and A. Overend, *J. Organomet. Chem.*, 1993, **444**, C62.

22 W. E. Douglas, *Appl. Organomet. Chem.*, 2001, **15**, 23.

23 K. Li, G. Wei, J. Darkwa and S. K. Pollack, *Macromolecules*, 2002, **35**, 4573.

24 K. Li, M. S. Mohlala, T. V. Segapelo, P. M. Shumbula, I. Guzei and J. Darkwa, *Polyhedron*, 2008, **27**, 1017.

25 C. Simionescu and S. Dumwrescu, *Eur. Polym. J.*, 1970, **6**, 635.

26 Y. Kishimoto, P. Eckerle, T. Miyatake, M. Kainosho, A. Ono, T. Ikariya and R. Noyori, *J. Am. Chem. Soc.*, 1999, **121**, 12035.

27 K. Hirao, Y. Ishii and T. Terao, *Macromolecules*, 1998, **31**, 3405.

28 T. Masuda and T. Higashimura, *Adv. Polym. Sci.*, 1986, **81**, 121.

29 C. Han and T. Katz, *Organometallics*, 1985, **4**, 2186.

30 T. Clarke, C. Yannoni and T. Katz, *J. Am. Chem. Soc.*, 1983, **105**, 7787.

31 R. Matusiak and A. Keller, *Polym. Bull.*, 1999, **43**, 199.

32 T. Higashimura, T. Masuda and M. Okada, *Polym. Bull.*, 1983, **10**, 114.

33 N. Mungwe, A. J. Swarts, S. F. Mapolie and G. Westman, *J. Organomet. Chem.*, 2011, **696**, 3527.

34 N. Onishi, M. Shiotsuki, F. Sanda and T. Masuda, *Macromolecules*, 2009, **42**, 4071.

35 M. Marigo, N. Marsich and E. Farnetti, *J. Mol. Catal. A Chem.*, 2002, **187**, 169.

36 J. G. Rodríguez, A. Lafuente and R. Martín-Villamil, *J. Polym. Sci. Part A Polym. Chem.*, 2005, **43**, 1228.

37 J. M. Sibanyoni, G. B. Bagihalli and S. F. Mapolie, *J. Organomet. Chem.*, 2012, **700**, 93.

38 A. Sen and T. Lai, *Organometallics*, 1982, **1**, 415.

39 M. Casado, A. Fazal and L. Oro, *Arab. J. Sci. Eng.*, 2013, **38**, 1631.

40 N. Onishi, *J. Polym. Sci. Part A Polym. Chem.*, 2010, **48**, 5549.

41 Y. Gal, *J. Macromol. Sci. Part A*, 1997, **34**, 377.

Chapter 5

A Summary of the Preceding Chapters and Future Prospects

5.1 Summary and conclusion of preceding chapters

In summary, this thesis investigated the synthesis, characterization and catalytic evaluation of cationic palladacycles. The aim of this study was to produce active catalysts that could polymerize phenylacetylene. More specifically, the employment of various cationic palladacycles bearing different ortho-substituents and containing different auxiliary phosphine ligands could be used in an attempt to rationalise the observed reactivity and selectivity of the cationic palladacycles.

Chapter 1 entails a brief overview of the potential of palladacycles. The historical origin of palladacycles and the different type of architectures were highlighted. The different synthetic methods employed were discussed and examples involving well characterized palladacycles as catalyst precursors in C-C coupling reactions are highlighted.

In **Chapter 2**, a series of mononuclear neutral palladacycles bearing different electronic and steric properties (**C5-C10**, **C16-C20**, **C26-C30**) were prepared from Schiff base imine ligands containing different ortho-substituents ranging from electron withdrawing to electron donating groups. The Schiff base imine ligands (**L1-L5**) allowed for facile electrophilic C_{Ar}-H activation producing *endo*cyclic dinuclear μ-Cl palladacycles (**C1-C5**). Their subsequent cleavage with tertiary phosphine ligands with different steric bulk and basicities produced the corresponding mononuclear neutral palladacycles. Single crystal X-ray diffraction analysis of **C8**, **C9**, **C18** and **C30** reveals that the coordination of the phosphine ligand to the metal centre is *trans* relative to the imine moiety. and that the palladium centre adopts a slightly distorted square planar geometry.

The synthesis and full characterization of cationic palladacycles (**C11-C15, C21-C25, C31-C35**) is described in **Chapter 3**. The abstraction of the chloride ligand from the mononuclear neutral palladacycles using $NaB(Ar)_4$ is a suitable synthetic methodology for the preparation of cationic palladacycles. These complexes are stable and could be isolated without decomposition occurring. The presence of a coordinating solvent is however crucial in stabilizing the vacant site on the metal centre. Spectroscopy data pertaining to the cationic palladacycles reveals that the coordination of the phosphine to the metal centre remains *trans* relative to the imine moiety with the *endocycle* still intact. In the case of complexes **C15** and **C25**, single crystal XRD studies reveal that the metal centre adopts a slightly distorted square planar geometry with the plane of the 2,6-diisopropylaniline moiety almost perpendicular to the plane of the *endocycle* ring.

Chapter 4 involve the application of mononuclear cationic palladacycles as catalysts for phenylacetylene polymerization. All fifteen cationic palladacycles bearing different ortho-substituents and phosphine ligands were efficient catalysts under the optimized reaction conditions with conversions between 56 and 95 %. The optimum reaction conditions established were found to be a reaction temperature of 60 °C and reaction time of 48 hours using a 50:1 PA:Pd ratio in THF. The results obtained in this study showed that the ortho-substituents on the aromatic ring of the imine substituent had a marked effect on the efficiency of the catalysts with the highest conversion registered for the catalyst with the most electron withdrawing substituent (**C14**). Surprisingly, the complexes containing the bromo-substituent (**C13**, **C23** and **C33**) did not follow the observed catalytic trend as we would have expected similar catalytic activities as their chloro-substituent analogues. The nature of the phosphine ligands also seems to have a significant effect on the molecular weight of the polymers produced. The sterically more bulky phosphine ligand produced higher molecular weight polymers relative to those observed for their PTA and PPh_3 analogues. Higher molecular weight polymers were also produced when a mixture of CH_2Cl_2/MeCN was employed, however low monomer conversion was obtained in these cases. The stereoregularity of the PPA produced was determined by IR- and ^{1}H NMR spectroscopy. A mixture of both *cis*-transoidal and *trans*-cisoidal PPA polymers were produced when

reactions were performed at 25 °C. When reactions were performed at 60 °C, only *trans*-cisoidal PPA polymers were produced. This chapter concludes with a possible catalytic mechanism for the polymerization phenylacetylene using these Pd-based catalysts.

Although the initial aims and objectives were met, the current study has generated a number of questions which need to be addressed in the future.

5.2 Future Prospects

The research presented in this study showed promise for further expansion in order to improve our knowledge regarding the catalytic behaviour of these palladacycles. The main concern in this study was to establish whether the observed catalytic trend was due to an inductive effect or steric effect since the catalysts which contain the bromide substituents, did not follow the expected trend. From an inductive point-of-view, the complexes with a bromide substituent were expected to give similar catalytic activities as their chloride analogues since both halides have similar electron negativities. To gain more insight into this matter, both the isopropyl and trifluoromethyl analogues could be synthesized and tested in the phenylacetylene polymerization to understand to what extent the induction effect plays a role in the process. For instance, if it is found that the catalyst with the isopropyl substituent in the ortho position on the cyclometallated ring has a lower catalytic activity than the bromide analogue, then the catalytic trend is due to steric effects of the ortho substituents since the isopropyl substituent is larger in size than the bromide substituent. The trifluoromethyl is also a bulky substituent but is more electron negative than the fluoride substituent. If it is found that this catalyst shows higher catalytic activities than the fluoride analogue, then the observed catalytic trend is driven by an inductive effect.

We should be able to modulate the cationic palladacycle's electronic and steric properties simply by changing the position of the substituent on the cyclometallated ring to position **2**, **3** or **4** (**Figure 5.1**) and incorporate different aniline moieties via a Schiff-base condensation reaction with the appropriate

aldehyde. It is clear that further detailed mechanistic studies, employing both DFT and spectroscopy techniques, will have to be performed in order to unambiguously determine which chain propagation mechanism is operative and the exact nature of the active species. This, in turn, would further help us to rationalise the observed catalytic activities and selectivities.

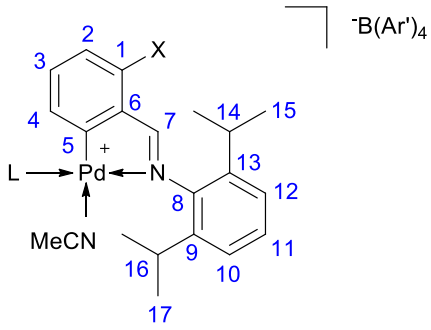

Figure 5.1: Cationic palladacycle with numbering for NMR data. L denotes the different phosphine ligands (L = PTA, PCy_3, PPh_3) and Ar` denotes the 3,5-*bis*(trifluoromethyl)phenyl moiety.